SEQUENCE AND STRUCTURE OF INFLUENZA HEMAGGLUTININ CLEAVAGE SITE MODULATE VIRAL PATHOGENESIS

A Dissertation

Presented to the Faculty of the Graduate School

of Cornell University

In Partial Fulfillment of the Requirements for the Degree of

Doctor of Philosophy

by

Long Ping Victor Tse

January 2014

SEQUENCE AND STRUCTURE OF INFLUENZA HEMAGGLUTININ CLEAVAGE SITE MODULATE VIRAL PATHOGENESIS

Long Ping Victor Tse, Ph. D.

Cornell University 2014

Viruses are obligatory intracellular pathogens requiring host machinery for survival and reproduction. Differing from living organisms, which can grow where nutrients are available, viruses absolutely require hijacking of host machineries to complete their life cycle. Enveloped viruses evolved to have dedicated strategies to passively sense environmental cues to ensure that initiation of infection occurs at the correct moment and place. One general strategy used by enveloped viruses is to precisely control activation of their envelope glycoprotein just prior entry into host cells.

Influenza A virus (AIV) is the causative agent of influenza illness and causes both economical and public health problems globally and annually. As a successful pathogen infecting a wide range of animals, IAV excels in sensing the environment to ensure efficient infection by employing two sequential activating steps during viral entry: proteolytic cleavage for priming of the hemagglutinin (HA) and low-pH-triggered conformational changes allowing release of the fusion peptide.

Proteolytic cleavage of influenza HA controls viral pathogenesis by influencing viral growth rate and viral tropism. The primary sequence and tertiary structure of the HA determine the overall properties of HA activation and hence, viral pathogenesis.

Mutations on the primary sequence of the HA cleavage site affect viral activation in two dimensions, 1) HA activation efficiency and 2) alteration in protease repertoire for HA activation. The former modulates viral growth kinetics and the later

is important for viral tropism. Mutations that modifies HA tertiary structure also play an important role in viral activation, in particular virus growth.

In this thesis, I describe three interrelated studies of mutations on primary and tertiary structure of HA and their consequence on HA cleavage and viral pathogenesis. These mutations also allow influenza virus to interact with prokaryotic pathogens and open up another dimension in virus-bacteria-host interactions and synergy.

BIOGRAPHICAL SKETCH

Long Ping Victor Tse was born in Hong Kong in summer of 1985. He spent his first eighteen years of his life in Hong Kong before moving to Santa Monica, CA in 2003. He attended Santa Monica College, and then University of California, Los Angeles (UCLA), in 2005. He received a Bachelor of Science degree in Microbiology, Immunology and Molecular genetics (MIMG) and also a cum laude graduate of UCLA in Spring of 2007. As an undergraduate research assistant for 1.5 years and staff research associate for 1 year in Dr. Jeffery F. Miller's laboratory in Department of MIMG, Victor participated in two research projects, characterizing the molecular mechanism and developing practical application of diversity-generating retroelement (DGR) in *Bordetella bronchiseptica* phage.

In autumn 2008, Victor arrived in Ithaca, NY and enrolled at Cornell University to obtain a Ph.D. In May 2009, he began his doctoral research with Dr. Gary R. Whittaker in Department of Microbiology and Immunology in College of Veterinary Medicine, Cornell University.

During his pursue of Ph.D., Victor developed a keen interest in the packaging mechanism of segmented viruses and non-coding small RNA biology. Upon completion of his Ph.D., he plans to stay in United State of American as a post-doctoral fellow in laboratories that fit his research interest. He wishes to pursue a career in academia studying the basic life cycle of viruses and developing viruses as tools for practical use and live a happy life.

In memory of my grandfather

Fuk-Num Tse

謝福南

ACKNOWLEDGMENTS

Over the past 5 years at Cornell University, I received tremendous amount of help and support from my family, advisors, colleagues and friends. The care I received from them not only allowed me to develop into a better scientist, but also a more mature person.

I would like to thank my major advisor, Dr. Gary R. Whittaker for his support. He gave me the freedom to explore questions that are not immediately related to my thesis projects and entrust me more as his peer than his student. He also accepted and tolerated my rebellious mind with his unbelievable patience. Under his guidance, I became more mature as a scientist and as a person.

I would also like to thank my committee members, Dr. Colin R. Parrish and Dr. Brian R. Crane for always offering me fresh perspectives on my thesis project. Their input always guided me back on track. I also appreciate the confidence they entrusted in me during my work.

I would not have been living happily without my friends and colleagues, especially in Ithaca. I would like to show my gratitude to all faculty and staff members, especially to Walter A. Iddings, Sachiko Funaba, Shirley A. Cramer and Janna Lamey for their support.

I would like to thank all my friends especially Dr. Jean K. Millet, Dr. Yueting Zhang, Dr. Lu Huang, Dr. Mengqaio Wang and Dr. Yading Ling for making my life more colorful in the snow covering Ithaca. I would also like to thank all the members of the Chinese Dragon Soccer Club (CDSC) for their support, and who are like brothers.

Finally, I would like to acknowledge my parents, Wai-Ling Ng 吳惠玲 and Hou-Lung Tse 謝校龍 and my sister Angela Tse for their love and care for my past

twenty-eight years. My parents' unconditional support both emotionally and financially allowed me to concentrate on my studies. Last but not least, I would like to thank Yian Xu, a girl that supported and understood me during the hardest times in my study.

《如果；巴黎》

如果，今天的巴黎放晴；
請你閉著眼睛，那微熱的溫暖；
是我抱你的証明。

如果，今天的巴黎多雲；
請你仰望天空的列痕，那一絲的曙光；
是我偷看你的烙印。

如果， 今天的巴黎下雨；
請你走近丁香樹， 那晶瑩的水滴；
是我送你的珍珠。

如果，今天的巴黎吹著和緩的風；
請你站在廣場的正中， 那休閒的一刻；
就像在我背上的輕鬆。

我雖不能喚雨呼風，
但讓思念替我們倒數時鐘；
讓我拖著妳的手；
穿越炎夏，走過寒冬。

金槍

二零一一· 三· 十九

TABLE OF CONTENTS

LIST OF FIGURES

CHAPTER 1
INTRODUCTION

1.1 The Influenza Problem

1.1.1 Influenza Infection

Influenza, commonly known as “flu”, is an upper respiratory disease that is caused by influenza viruses. Flu symptoms were first described by the ancient Greek physician, Hippocrates of Cos dating back to 412 BC (1). Presently, influenza viruses are still circulating around the world, infecting and causing disease in vertebrates. Among the three different genera of influenza viruses, influenza A virus (IAV) and Influenza B virus were first isolated in 1933 in the human population (2). IAV originated from waterfowls where it adapted well and causes only asymptomatic infection in its natural hosts (3). IAV becomes pathogenic and causes a range of symptoms after zoonotic transmission to different hosts. IAV becomes widely spread and infects a wide range of vertebrates, from whale to bat (4, 5). Due to the huge diversity of IAV, they are categorized into subtypes which are determined by the two surface viral glycoproteins, hemagglutinin (HA) and neuraminidase (NA) (6, 7). Each subtype has a unique antigenic profile but share rather similar biological properties. Currently, 18 HA and 11 NA subtypes have been identified (8). Although most of them reside in waterfowls (9), two IAV subtypes, H1N1 and H3N2 are continuously infecting the human population and causing seasonal influenza each year.

1.1.2 Seasonal and Pandemic Influenza

Seasonal human IAV infects 3 to 5 million people annually (9). Clinical presentations of influenza infection include fever, cough, sore throat, running nose, muscle pain, headaches, fatigue and sometime diarrhea (10). In normal circumstances, patients infected by IAV typically require 5 to 7 days to recover;

hence, such infections lead to loss in productivity. According to the Centers for Disease Control and Prevention (11), the estimated economical loss in the United States due to influenza related illness is in the range of 27 to 87 billion US Dollars (USD) per year (12, 13). Influenza infections can also lead to death; annual mortality associated with IAV is around 250,000 to 500,000 deaths (9). People with sub-optimal/immature immune system, such as infants, senior citizens and pregnant women or having chronic underlying diseases, such as obesity, diabetes and bacterial infections are particularly of high risk (14, 15). Differing from seasonal influenza, pandemic influenza emerges unpredictably and shows less discrimination between healthy and sub-optimally healthy individuals in terms of disease severity and prevalence (16). In the last century, three pandemic influenza viruses have emerged by gene exchange between two or more influenza viruses through a process called antigenic shift (6). Due to lack of immunity in the human population, pandemic viruses are able to spread across the population in a short period of time. For instance, in 1918, the “Spanish flu” infected up to 40% of the global population and killed more than 50 million people (16, 17). The most recent influenza pandemic in 2009 arose from a triple reassortment event between human, avian and swine influenza viruses (18). Within two months after the first reported case in Mexico, the viruses spread throughout the entire northern hemisphere and the World Health Organization (WHO) announced to the world a phase 6 global pandemic alert (19). Fortunately, catastrophic consequences of that pandemic were avoided thanks to the relatively low virulence of the virus and advancements in the current medical system. However, the 2009 pandemic still cost an estimated 71 to 167 billion USD in economical loss on top of the regular seasonal influenza (20).

1.1.3 Avian Influenza

Avian influenza virus (AIV) was directly involved in three of the pandemic influenza outbreaks and the 1918 pandemic which also has a speculated avian origin (6, 18). Moreover, the increase in incidences of humans infected by AIV is becoming a new public health concern (21, 22). Modern human practices in poultry and livestock industries provided effective ways for influenza viruses to transmit between species. Indeed, people infected by avian influenza viruses are mainly farm workers who are exposed to or in close contact with avian species (21, 23). In 1997, a highly pathogenic avian influenza virus (HPAI) H5N1 emerged in Hong Kong, spread locally and killed 6 people out of 18 infected patients (23, 24). Although the Hong Kong government had been effective in controlling HPAI locally by exterminating all live poultries in the city, it is still a reoccurring public health issue in Southeast Asia (25). Subsequently, HPAI has already infected more than 600 people worldwide with an extremely high fatality rate (~60%) according to the CDC. Despite limited incidences showing HPAI transmission from human to human in nature, recent reports have shown that HPAI could transmit between humans efficiently. Two separate research groups were able to show that after serial passages (>10) of HPAI in ferrets, the virus was able to transmit between animals via aerosol. Mapping of the viral mutations revealed that HPAI only requires 2 mutations from PB1 and NP, 4 mutation on HA and 1 mutation on PB2 to acquire such phenotype (26, 27). Ferrets serve as the best model animal for influenza infection due to the similarity of its upper respiratory system and clinical presentation with the human ones (28). These reports not only demonstrate the possibility of a “humanized” HPAI but also raise the concern of a potential escape of the “humanized” HPAI from laboratories. Open access of the protocol for humanizing HPAI also raised alarm for the potential misuse of such viruses by bioterrorist (29).

1.1.4 Influenza Vaccine and Therapeutic Drugs

Protective vaccines are formulated every year to protect the human population from seasonal influenza prior to the influenza season, which spans from November to April in the northern hemisphere. However, due to the unpredictability of pandemic influenza, it is impossible to have a vaccine ready for an unknown pathogen. A universal vaccine eliciting neutralizing antibodies to a broad range of influenza viruses by targeting a conserved region, such as the matrix protein 2 (M2) or the stalk domain of HA, would constitute the holy grail of influenza vaccine development (30-32). However, a recent report has shown antibody dependent enhancement (5) after administration of a broadly neutralizing vaccine in a swine model, questioning the safety and feasibility of such a vaccine (33, 34). Furthermore, influenza viruses mutate rapidly to change epitopes over time, limiting such vaccine strategy for long term usage. Therapeutic drugs are available for treating influenza infections. Two groups of drugs exist: the NA inhibitors, zanamivir (Relenza) (35) and oseltamivir (Tamiflu) (36); and the ion channel blockers, amantadine (Symmetrel) and rimantadine (Flumadine) are currently used to combat influenza infection (37). The M2 ion channel inhibitors are effective only when administrated in the early stage of infection, which limits its actual use as a prophylactic drug (38). Furthermore, as predicted, many influenza viruses are gaining resistance to the drugs due to influenza's high mutation rate, for instance, R292K, N294S or H273Y mutation in NA gave rise to virus resistance to oseltamivir (39, 40). Therefore, a better understanding of influenza life cycle is important for developing new strategies or combination therapy to combat the virus.

1.2 The Influenza Particle

1.2.1 Influenza Virion

Influenza A viruses are enveloped negative-strand segmented RNA viruses belonging to Orthomyxoviridae family. The size of IAV genome is 13.5 kb length that is separated into eight viral RNA (vRNA) segments. By alternative splicing, the genome encodes for up to 11 to 14 viral proteins (41). Influenza virions are pleiomorphic but mainly can be classified into two morphological groups, either spherical or filamentous. Spherical virions are usually found in laboratory adapted (possibly by embryonic chicken egg (ECE) and tissue cultures) viruses which are around 100 nm in diameter. Filamentous virions are found in clinical samples from natural infections and have similar width as spherical virions but can be up to 20 μm in length (42, 43). Multiple determinants, such as the Ala41 in matrix protein 1 (M1) and the M2 amphipathic helix located in the first 17 amino acid of the cytoplasmic tail have been reported to be associated with filamentous morphology *in vitro* (44, 45). A recent study has shown that serial passages of spherical virus, PR8 in guinea pig change the virus' morphology from spherical to filamentous. In contrast, passaging filamentous virus, A/Udorn/72/H3N2 (Udorn) in tissue culture converts the virus into spherical morphology (46). Although clinical samples are always associated with filamentous morphology, which argues its importance in *in vivo* infections, the functional aspects of filamentous influenza are uncertain (47, 48). A recent study shows that filamentous virus grows slower and has decreased cell-to-cell spread compared to spherical virus *in vitro* (49). The underlying mechanism of how filamentous viruses are produced is still largely unknown.

Inside each influenza virus is a genome set in the form of ribonucleoproteins (RNPs), a combination of vRNA segments and proteins. Each vRNA segment is coated with nucleoproteins (NP) with each individual NP binding around ~24 RNA nucleotides (50). At the 3' end of each segment is the heterotrimeric RNA dependent

RNA polymerase (RdRP) composed of polymerase acidic (PA), polymerase basic 1 (PB1) and polymerase basic 2 (PB2), all together, they form the viral RNP (vRNP). Viral RNPs are surrounded by the M1 and wrapped by host derived lipid envelope that is obtained from plasma membrane lipid rafts which are enriched in cholesterol and sphingolipids (SPs) (51). On the virion, M2 has a ratio of 1:10 to 1:100 compared to HA and forms proton channels between within lipid envelopes that are essential for releasing the vRNPs into the cytoplasm after membrane fusion (52). Two surface glycoproteins are found on the surface of the virus membrane, HA and NA for viral entry and egress. There are about 500 molecules of HA homotrimer on the surface and they are found as clustered islands on each virus (53). HA is responsible for receptor binding and membrane fusion of the virus during the entry step. NA is a tetrameric sialidase which hydrolyzes terminal sialic acids and releases the virion during viral egress. There are about 120 NA molecules on each influenza virion which are mainly located at the budding end of the virus (53). Some trace amounts of host derived proteins are found on the surface of flu particles, that are incorporated either by active or passive mechanisms, including cytoskeletal proteins, annexins, glycolytic enzymes and tetraspanins (54). Some of these have been shown to be involved in the viral life cycle or pathogenesis. For instance, annexin A2 was shown to recruit plasminogen (Plg) for HA activation during influenza entry, and actin was shown to be essential for influenza entry in polarized cells (55, 56).

1.3 Influenza Proteins

1.3.1 The Influenza RNA-dependent RNA polymerase (RdRP)

Influenza requires its own RdRP for transcription of (+) mRNA and replication of (-) vRNA inside host cells. The influenza RdRp is a 250 kDa heterotrimer composed of three subunits: PB1, PB2 and PA. The C-terminus and N-terminus of

PB1 binds to PB2 and PA respectively (57, 58). PB1 is the core of the RdRP as it is responsible for elongation during RNA replication and transcription and its active site resembles the typical RdRP motif with Ser-Asp-Asp at position 444 to 446 (59). PB2 is required for the initial step of "cap snatching" (a process in which the 5' m^7GTP cap is stolen from cellular mRNAs and used as a primer for viral RNA transcription) and initiates RNA replication as it binds to cellular mRNA 5' m^7GTP cap. The binding of PB2 and mRNAs involves two aromatic amino acids, 357 His and 404 Phe that sandwiches the m^7GTP cap by stacking interactions (60). PA is a member of the Pro-Asp-Asp/Glu-X-Lys family of endonucleases with two Mn^{2+} ions at its active site (61). Its primary function is to cleave off the m^7GTP cap from the 5' end of cellular mRNAs. PA also has proteolytic function involving two residues: S624 and T157, however, the function of such activity is unknown but essential, as mutation of those residues affects RNA replication (62). As human cells do not have RdRP, it is an attractive drug target for treatment of influenza infection. Indeed, the influenza RdRP inhibitor T-705 is currently being developed and is under a phase II clinical trial.

Figure 1.1. Influenza Virion

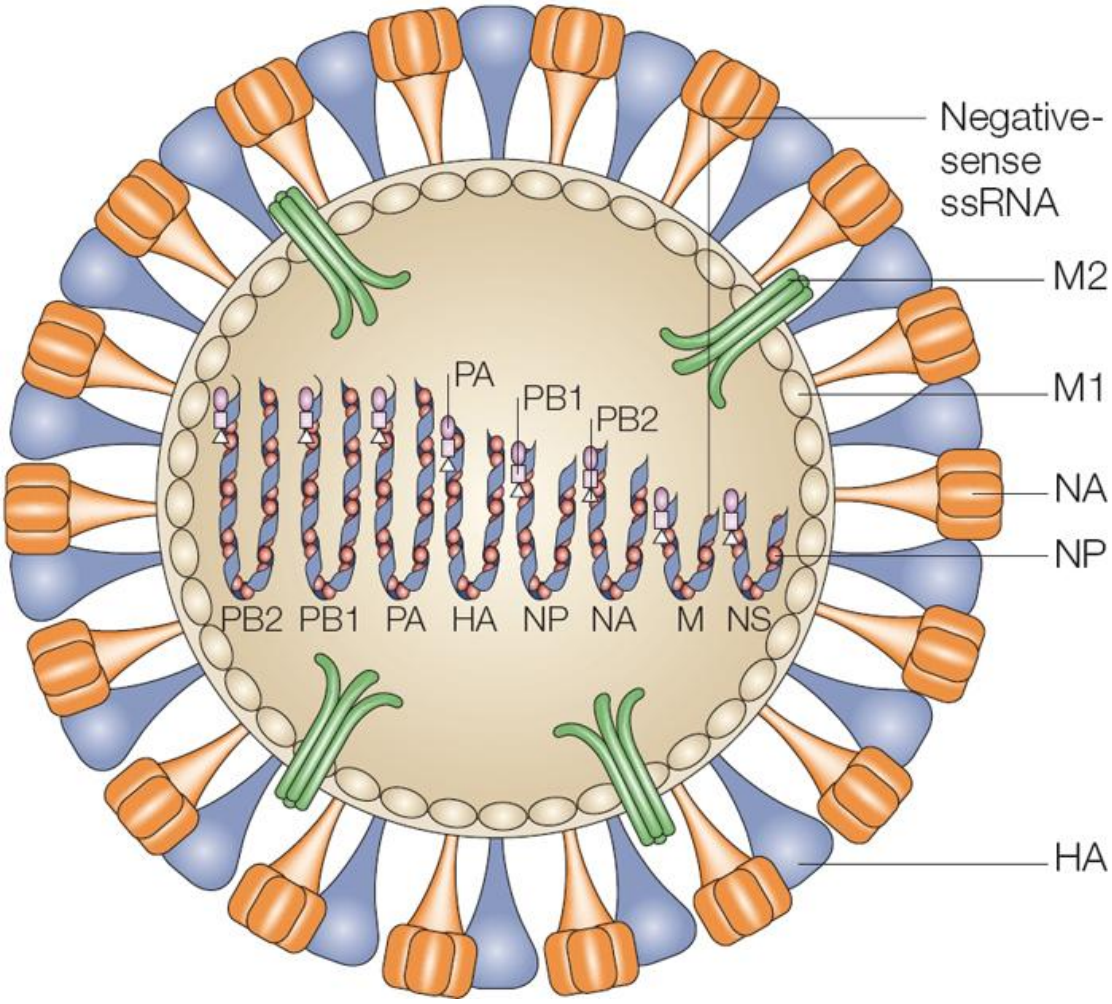

Adapted from Horimoto T. and Kawaoka Y, Nature Review Microbiology 3, 591 (2005) (63)

1.3.2 Hemagglutinin (HA)

HA is a monomeric rod-shaped molecule with the C-terminus residing in the cytoplasm (Type I transmembrane protein) and assembles into a trimer which projects out as a “spike” from the viral membrane (41). HA trimers are also prototypes of class I fusion protein, which form extensive α-helices. Also, as a class I fusion protein, they need to be proteolytically cleaved to expose the protein’s fusion peptide (64). A typical HA trimer is about 180 to 240 kDa, 135 Å tall and is held together in a coiled-coil structure by hydrophobic interactions. HA monomers are produced as a single molecule, HA_0, which contains two functional domains, HA_1 and HA_2. Before HA activation, HA_1 and HA_2 are covalently linked together; after activation, the two domains are held together by di-sulfide bonds (65). HA_1 is the “crown” of HA which is responsible for receptor binding; depending on the host range of the virus, it can bind to two differentially linked sialic acids, SAα2,6Gal and/or SAα2,3Gal (65). Experiments using fluorescent lectins, *Sambucus nigra* agglutinin (SNA) which binds SAα2,6Gal and *Maackia amurensis* agglutinin (MAA) which binds SAα2,3Gal, reveal that the human upper respiratory tract contains mainly SAα2,6Gal whereas deeper in the respiratory tract, in bronchioles and alveoli, both SAα2,6Gal and SAα2,3Gal are found (66, 67). On the other hand, avian respiratory and intestinal tracts mainly contain SAα2,3Gal (67). Generally, influenza viruses with HAs that are able to bind to SAα2,6Gal mainly infect humans while viruses with HAs that can bind SAα2,3Gal are more likely to infect avian species. Other host species, such as swine, have both SAα2,6Gal and SAα2,3Gal on their respiratory tract, and are hence susceptible to infecting with virus containing any HAs and could potentially serve as a mixing vessel for avian and human influenza allowing for recombination events to occur and generation of novel virus strains (68, 69). Therefore, the sialic acid binding specificity

of influenza virus is an important determinant for the viral host range. Several mutations have been identified that control the sialic acid binding properties of influenza HA and hence modulate viral tropism. One particular example is the single mutation, HA-190E which is able to switch the HA from binding SAα2,3Gal to SAα2,6Gal (70). The recent advances in glycan array technology allow researchers to test HA binding on more complex glycan structures, and test parameters such as chain length, branching patterns, sulfation and fucosylation.

HA_2 is the "stem" region of HA and is essential for membrane fusion. Before HA activation, HA_2 is covalently linked to the C-terminus of HA_1 and locked in a closed position. Unlike HA_1, HA_2 is highly conserved between subtypes especially in the fusion peptide region which is located at the first 22 N-terminal amino acid of HA_2 (41). Mutational analyses have shown that the HA fusion peptide has very low tolerance for mutations (71). At neutral pH, activated HA_2 is folded under HA_1 and the fusion peptide is buried inside a pocket in the center of the coiled-coil stem, mimicking the closed position of a "Swiss-army knife" (65). The neutral pH conformation of HA_2 is trapped in a metastable state (72). In acidic conditions, HA_2 undergoes loop to helix conformation change that creates a coiled-coil structure that projects the fusion peptide out for 100 Å and allowing insertion into the endosomal membrane (65). After the viral and cellular membranes are bought into close proximity, HA_2 folds back and forms a trimeric hairpin structure that pulls the two membranes towards each other. The inner leaflet of the endosomal membrane and the outer leaflet of the viral envelope fuse together by hydrophobic interactions and reach a metastable hemifusion state. The actual trigger for pore formation is still unknown. Recent biophysical studies using total internal reflection fluorescence (TIRF) microscopy to monitor single particle fusion events support the notion that HA

fusion is a multistep process which likely require three distinct steps (73). Although the exact number of HA molecules required for fusion varies between reports, which is likely due to differences in assumptions and models used, the consensus is that very low amounts of HA molecules (less than 10) are required for successful fusion to occur.

Influenza HA is also the main target for the host immune system and it faces constant pressure from neutralizing antibodies. In particular, five regions on HA_1, Sa, Sb, Ca1, Ca2 and Cb are the most immunogenic among the entire virion (74). HAs are separated into two phylogenetic groups, group 1 (H1, 2, 5, 6, 8, 9, 11, 12, 13 and 16) and group 2 (H3, 4, 7, 10, 14, and 15). Cross-reactive antibodies are more likely to react within the members of the same group as they are more antigenically similar. For instance, the V(H)1-69 antibody has been identified as a broadly neutralizating antibody that neutralizes all group 1 HAs whereas Fab CR8020 was shown to neutralize all group 2 HAs (30, 75). To counteract the pressures from the immune system, HA_1 undergoes constant mutation (antigenic drift); one way the virus evades neutralizing antibodies is the introduction of glycosylation sites on the HA protein. Asn (N)-linked glycosylation have a conserve motif of Asn-X-Ser/Thr where X can be any amino acid except Pro (76). Glycans are bulky sugar molecules that mask the antigenic site from neutralizing antibodies (65). However, adding glycosylation sites could potentially mask the receptor binding domain (RBD) of HA as well (77). Therefore, the number of glycosylation sites on a particular HA is finely tuned to allow for immune evasion and receptor binding affinity (78). It is interesting to note that a tissue culture adapted virus, A/Puerto Rico/8/1934 H1N1 (PR8), has lost most of its glycosylation sites on HA_1. A likely explanation for this is that there is no immune pressure *in vitro* (79).

Figure 1.2. Influenza HA

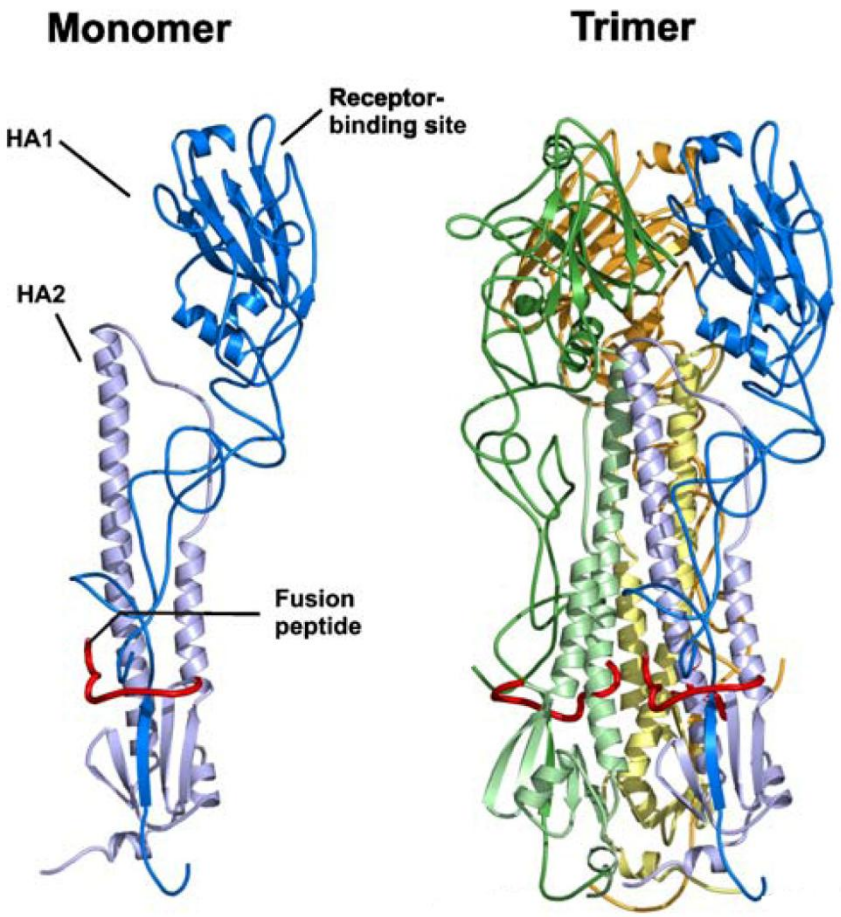

Adapted from Amorij JP et al., Pharm Res 25, 1256 (2008) (80)

1.3.3 Nucleoprotein (NP)

Similarly to all other negative sense RNA viruses, influenza virus encodes the NP to coat its RNA genome to form the ribonucleoprotein (RNP) complex. NP is a 498 amino acid long protein with an overall positive charge and is post-translationally modified with phosphorylation at Ser3 (41). NP is a multi-functional protein involved in many different steps of the viral life cycle including RNA replication, RNP trafficking and packaging (81). NP performs these functions by interacting with viral and cellular proteins. For instance, the nucleus localization signal (NLS) of NP interacts with cellular importin α to allow nuclear import of viral RNPs (82). NP is a co-factor for RNA elongation through an interaction with the RdRP complex. Studies have shown that viral RNA without NP can initiate transcription but fail to continuously elongate (83). NP also controls the viral life cycle by regulating the switch between RNA transcription and RNA replication (84). Although host factors may also be involved, NP is an important factor in this switching process. Later in the viral life cycle, NP interacts with M1 which initiates packaging of RNP into influenza virion (85, 86). NP is also a drug target for treating influenza infection. A recent study showed that administration of drugs that promote oligomerization of NP rescues mice from lethal infection of influenza virus (87).

1.3.4 Neuramindase (NA) and Matrix Protein 2 (M2)

Influenza NA is produced as a 55 - 60 kDa monomer with six β-sheets arranged in a propeller formation and assembles as a tetramer on the virion surface (88). As it names implies, NA is a sialidase which catalyzes hydrolysis of sialic acid. Its primary function is to release influenza virus from sialic acid receptors and mucus during viral egress (89). Influenza C virus does not have NA but instead has a haemagglutinin-esterase (HEF) protein that carries the function of HA and NA on one

protein (90). Similarly to HA, NA is also antigenic and thus, constantly mutating to escape from host immune system selective pressure. Currently, there are 11 NA subtypes known that are separated into two groups based on sequence homology (41). In addition to its role in viral egress, NA is also involved in viral entry. Studies have shown that NA is responsible for removal of non specific viral receptors in mucins and cilia which allows penetration of influenza virus in target cells (91). NA has also been shown to act as a viral receptor binding protein and be involved in binding to the cell surface directly. WSN NA has also been shown to bind plasminogen (Plg) and facilitate HA cleavage during influenza activation (92-94).

M2 is a splice variant encoded on segment 7. M2 is produced as an 11 kDa α-helix monomer with its cytoplasmic tail undergoing palmitoylation and phosphorylation post-translational modification (95, 96). M2 assembles into tetramers on the viral membrane and forms proton channels that are critical for viral uncoating during entry (97). The crystal structure of M2 reveals the H+ conductance mechanism controlled by the His37 and Trp41 amino acid clusters (98). A small portion of the M2 protein is exposed on the viral surface and its sequence is highly conserved and therefore, would constitute a good candidate epitope for generating universally neutralizating antibodies (32). Both NA and M2 are attractive targets for drug development and NA and M2 inhibitors are currently used as therapeutics for treating influenza infection (covered in “1.1.4 Influenza Vaccine and Therapeutic Drugs”).

1.3.5 Matrix Protein 1 (M1) and Nuclear Export Protein (99)

Segment 7 encodes both M1 and M2 proteins by alternative splicing (41). M1 is the most abundant protein in the influenza virion and mainly plays a role in viral assembly. During viral assembly, M1 is translocated into the nucleus and interacts with vRNP and the nucleosome (85). Such interactions are thought to initiate

dissociation of vRNPs from the nuclear matrix and allow export of vRNPs out of the nucleus. M1 also interacts with NEP which mediates nuclear export for the whole vRNP-M1-NEP complex by interacting with the host export machinery Crm1 and nucleoporins (100, 101). NEP is a splice variant of segment 8 and is not incorporated into influenza virions. The N-terminus of NEP contains a Met/Leu rich nuclear export signal and is critical for vRNP export (102). NEP regulates RNP export by binding to the NLS of M1 to prevent it from being imported back to the nucleus (103). M1 protein also plays a role in viral morphogenesis that has been covered in section 1.2 “Influenza Particles”.

1.3.6 Non Structural Protein 1 (NS1)

NS1 is a dimeric nuclear protein which is highly expressed in influenza infected cells but not incorporated inside virions. NS1 is an antagonist of type I interferon (IFN) which is part of the innate immune response for viral infections in eukaryotes (104). NS1 is composed of 2 functional domains: the N-terminal dsRNA binding domain and an effecter domain (104-106). Expression of the dsRNA binding domain is sufficient to block IFN production suggesting its important role for antagonizing IFN in infected cells. NS1 antagonize IFN at transcriptional level by targeting multiple host factors upstream of the IFN signaling cascade. NS1 inhibits transcription factors including Interferon regulatory factor-3 (IRF-3) and nuclear factor κB (NF-κB). NS1 also binds to RIG-I and prevents the downstream signaling for IFN activation (107-109). Furthermore, NS1 also interacts with TRIM25 which is the upstream regulator of RIG-I further preventing IFN induction (110). The Protein Kinase R (PKR) and RNase L pathways are also inhibited by NS1 protein by sequestering viral dsRNA which is the activator for both pathways (111, 112). The effector domain is also important for the viral life cycle as deletion of the effecter

domain attenuates virus infection mice (113). The effector domain blocks host mRNA translation by interacting with the cleavage and polyadenylation specificity factor (CPSF) which halts mRNA nuclear export for translation (114).

1.3.7 Accessory Proteins

Ten core proteins that we were covered previously are expressed among all IAV. Four non-essential proteins, PB1-F2, PB1-N40, PA-X and M42 are expressed in a strain dependent manner and modulate viral pathogenesis without affecting the normal life cycle of influenza virus (115, 116). PB1-F2 is initiated from AUG4 in the +1 open reading frame (ORF) of segment 2 (117). The length of PB1-F2 ranges from 79 to 90 amino acids long depending on the strain (116, 118). PB1-F2 localizes to the mitochondria and is pro-apopototic and pro-inflammatory (117, 119, 120). PB1-F2 has also been shown to be associated with increased virulence in bacterial co-infection setting, suggesting synergistic effects between viruses expressing the protein and bacteria (121). PB1-N40 was first discovered in 2009 and is a truncated version of PB1 that lacks the first 39 amino acid of the N-terminus which is the region critical for interaction with PA (122, 123). Although viruses lacking PB1-N40 have slower growth rates, the function of the protein is still unclear. PA-X is a 252 amino acids long protein encoded in segment 3 via ribosomal frameshifting. Eliminating PA-X production from the 1918 “Spanish flu” virus increases viral pathogenesis and induces a global change in host transcription profile. The function of PA-X is still unclear but is important in modulating host response and viral pathogenesis (124). M42 is the latest non-essential protein discovered in 2012 from a splice variant in segment 7. Its primary function is to compensate the loss of M2 ion channel in tissue culture adapted viruses. The actual function of M42 in natural infection is still unclear (125).

Figure 1.3 Organization and alternative splicing of Influenza genes

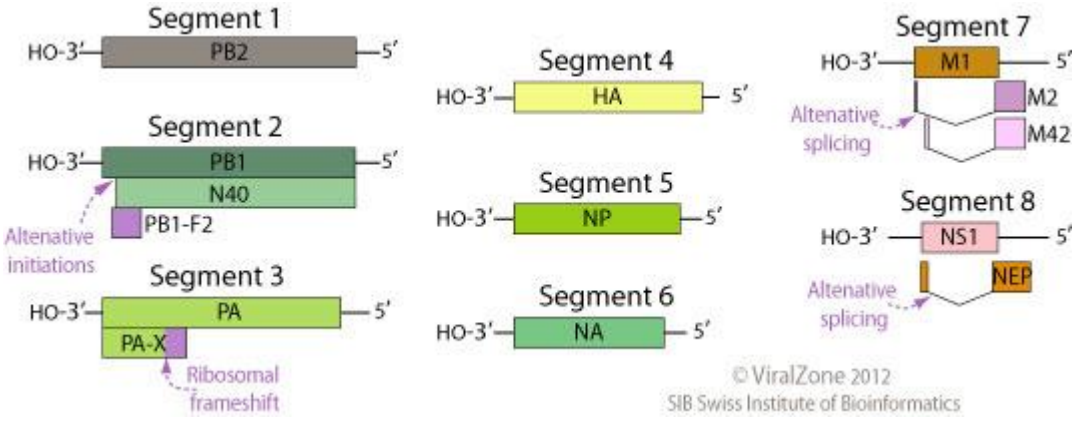

Adapted from ViralZone 2012, SIB Swiss Institute of Bioinformatics

1.4 Influenza Entry

1.4.1 Influenza Attachment and Endocytosis

Human IAV mainly infects non-ciliated epithelial cells from the upper respiratory tract and in a minority of cases, penetrates deep into lungs and infects type I and type II pneumocytes (126). Autopsy analysis of patients that died of H5N1 HPAI infection have shown diffuse alveolar damage indicating infection in the lower respiratory tract whereas type II pneumocytes are the main cell types being infected (99, 127). In avian species, influenza viruses target the epithelial cells of both the respiratory and gastro-intestinal tracts (21). Regardless of the host and tissue, influenza viruses first need to penetrate through physical barriers including the mucus and ciliated cells to reach the surface of target cells. Once have the virus reached the apical side of cell surfaces, human influenza HA binds to N-acetylneuraminic acid linked to the penultimate galactose by a α2,6 linkage (SAα2,6Gal), whereas avian influenza HA binds to the same sugar molecule but with a α2,3 linkage (SAα3,3Gal) (41). The actually trigger for influenza endocytosis is still unknown; however, there is evidence that the multivalent binding between HA and receptor triggers the activation of receptor tyrosine kinase and induces a signal for endocytosis (128, 129). Early electron microscopy and recent stochastic optical reconstruction microscopy (STORM) data reveal that up to 65% of influenza particles are wrapped around by a clathrin coated pit on the surface or are found completely inside clathrin coated lattices (CCL) indicating the involvement of clathrin mediated endocytosis (CME) (129). Biochemical analysis using dominant negative mutants of ezrin1, a membrane-microfilament linker, demonstrated its critical role in influenza CME (130). The other 35% of influenza viruses are found inside non-clathrin coated pit suggesting alternative pathways for influenza entry. STORM and use of chemical inhibitors also

demonstrated that influenza particles use lipid-raft-dependent caveolin mediated endocytosis (129, 131). Interestingly, influenza entry is not affected after blockage of both CME and caveolin mediated endocytosis by various drugs and dominant negative constructs, suggesting a non-clathrin, non-caveolin endocytosis route of entry (132). Recently, a dynamin-independent pathway which resembles some aspects of macropinocytosis has been identified and has been shown as the major entry pathway for filamentous influenza virus (133, 134).

Figure 1.4. Influenza endocytosis

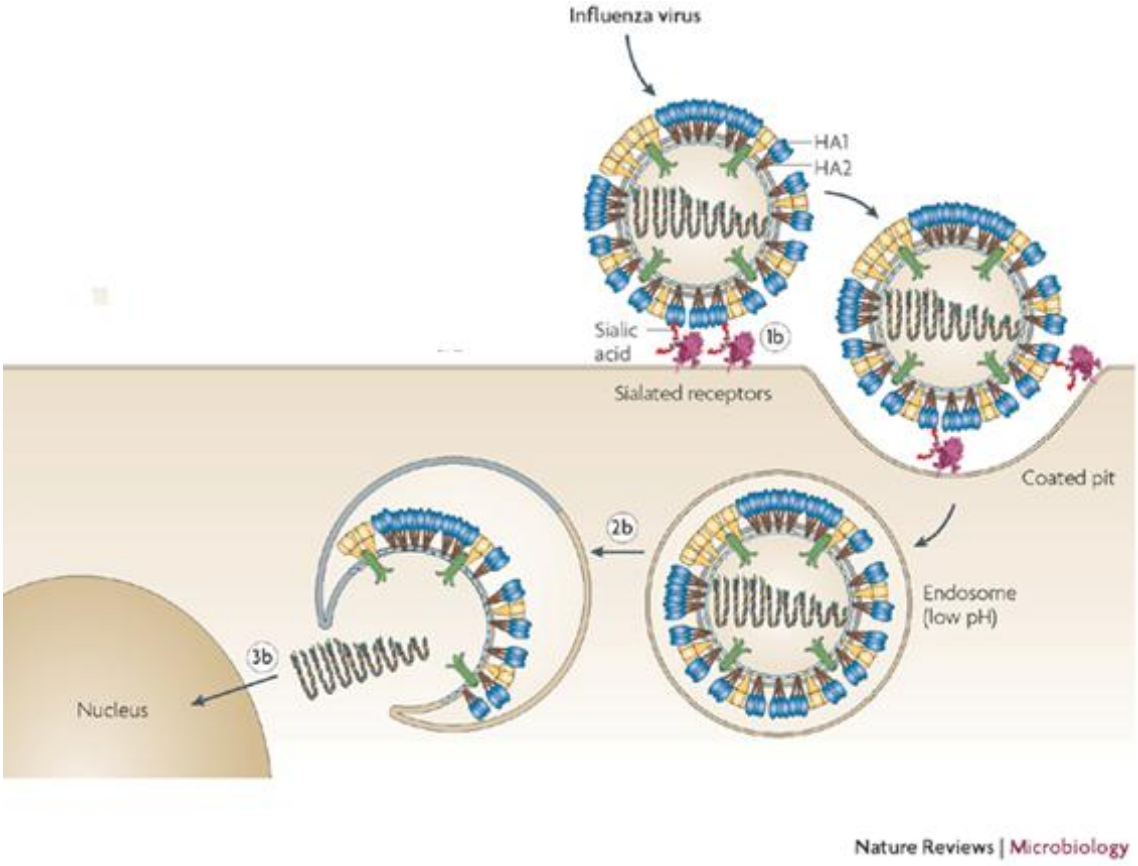

Adapted from Karlsson Hedestam GB et al., Nature Review Microbiology 6, 143 (2008) (135)

1.4.2 Membrane Fusion

After endocytosis, influenza viruses are wrapped inside endosomal vesicles. The endosomal machinery is a system dedicated to intracellular trafficking of macromolecules inside eukaryotic cells (136). Endosomes constantly fuse with other intracellular vesicles during the process of maturation which adds different surface markers as identifiers of their nature and also dictate the destination of the cargos (137). For instance, early endosomes (EE) with Rab5 on their surface mature into late endosome (LE) which are decorated with Rab7 and eventually fuse with the lysosome for cargo degradation. EE can also recycle back to the plasma membrane via the recycling endosome (RE). Large macromolecules, such as influenza virus, are targeted to the lysosome for degradation; therefore, in order to initiate productive infection, influenza viruses need to escape from the endosome. HA mediated membrane fusion and uncoating both require an acidic environment (low pH) as a trigger to release viral contents into the cytoplasm (138). The pH value inside the EE is around 5.0 – 6.0, during maturation, the pH value decreases and reaches the threshold pH (5.0 – 5.7) for HA mediated membrane fusion (139). Low pH triggers a conformation change of the activated HA trimer for membrane fusion (65). Simultaneously, influx of protons (H+) from the endosome via the M2 ion channel acidifies the interior of influenza particles which disrupt protein-protein interactions and release the vRNPs from other viral components (140, 141). This strict pH requirement controls the precise timing for vRNPs release. The released vRNPs are further translocated to the nucleus for replication and transcription to continue the viral life cycle.

Figure 1.5. Influenza mediated membrane fusion

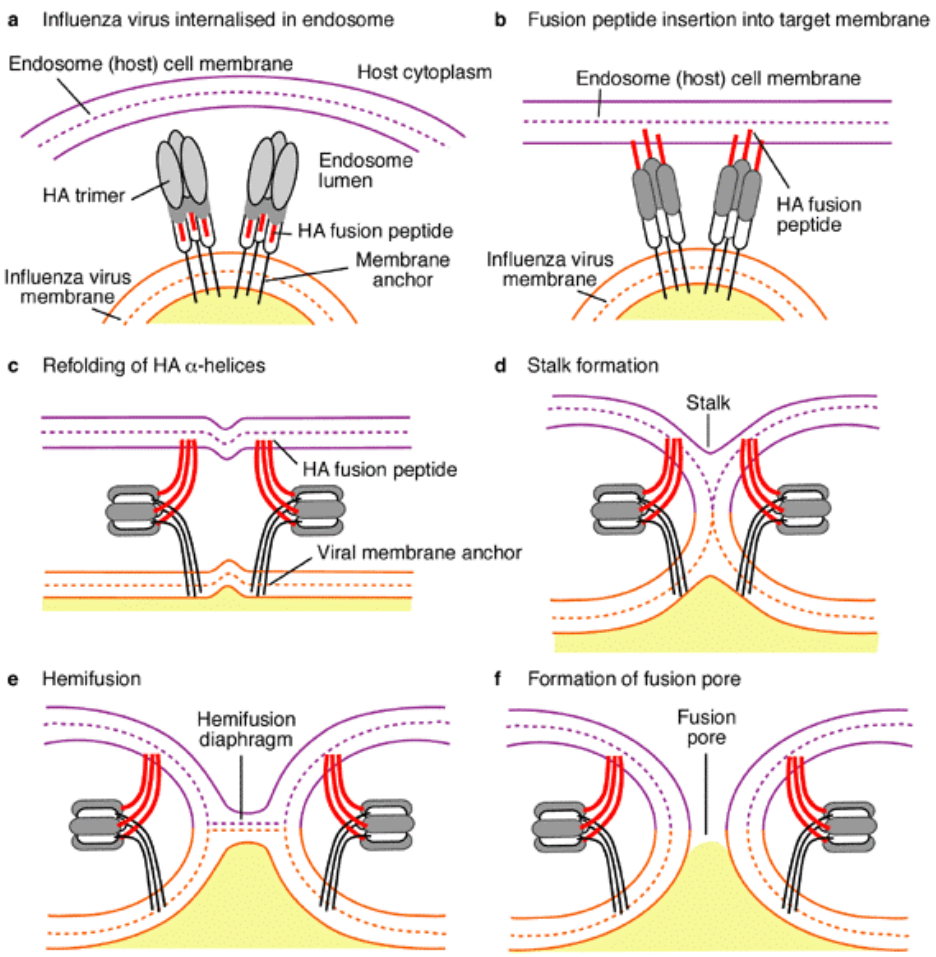

Stalk-pore hypothesis for membrane fusion mediated by influenza haemagglutinin (HA)

Adapted from Cross KJ, Burleigh LM & Steinhauer DA, Expert Reviews in Molecular Medicine,3, 1 (2001) (142)

1.4.3 Hemagglutinin Activation

HA activation is an essential step for influenza infection as it allows release of the fusion peptide from HA and hence, initiates downstream reactions that were covered at section 1.4.2 “membrane fusion”. In most cases, HA activation takes place in the extracellular matrix or on the cell surface, in the case of HPAI, HA activation by furin takes place in the trans-Golgi network (TGN) during viral assembly (143-145). Activation of HA involves a one-step proteolytic cleavage at the HA cleavage site located at the junction between the HA_1 and HA_2 domain by host, and sometimes, bacterial proteases. Although HA cleavage sites vary between subtypes, the P1 position (the first amino acid at the N-terminus of the cleavage site) is conserved with an Arg residue among all subtypes with a few exceptions that include a Lys at P1. A monobasic cleavage site is defined by the presence of single Arg at P1 and is cleaved by trypsin-like serine proteases (146, 147). These proteases are distributed mainly in the respiratory and/or intestinal tracts, and therefore, such cleavage site restricts the tropism of influenza viruses within these tissues. In some rare situations, influenza viruses, such as A/WSN/1933 (H1N1), acquire mutations on the HA cleavage site and the NA to gain the ability to replicate in the brain by using an alternative protease, plasmin (Pm) (92, 148). In extreme cases, highly pathogenic avian influenza (HPAI) viruses gain universal tropism by using ubiquitous proteases for activation (149). For instance, HPAI H5 HA has a polybasic HA cleavage site which contains multiple basic residues Lys or Arg that can be cleaved by ubiquitously expressed furin-like proteases (150, 151). Therefore, the protein sequence at the HA cleavage site determines which protease is used and subsequently, influence influenza tropism and pathogenesis. The sequence variability of the HA cleavage site

between subtypes suggest that influenza viruses use a broad spectrum of proteases for activation. Since the discovery of HA activation in the late 1970s, the field has gained a tremendous amount of knowledge regarding the proteases involved in this critical step.

1.5 Serine Proteases

1.5.1 Serine proteases overview

Serine proteases consist of almost one-third of all proteases that have been identified and a subset of the family of proteins is able to activate influenza HA. The active site of serine proteases consist of a catalytic triad composed of aspartic acid (113), histidine (His) and Ser which act as a nucleophile during hydrolysis of the targeted peptide bond (152). Catalysis of serine proteases involves four steps, 1) A nitrogen on His removes a proton from Ser which initiates the nucleophilic attack on the carbon of the peptide bond and forms a tetrahedral intermediate. 2) The electron from the peptide bond attacks the proton on His and breaks the peptide bond generating the acyl-enzyme intermediate, releasing the N-terminus of the peptide (152). 3) A water molecule acts as a nucleophile and attacks the carbon of acyl-enzyme intermediate, ejecting the C-terminus of the peptide (152, 153). 4) The active site is regenerated by re-protonation of the Ser by a hydrogen ion on His which originated from water (152). Despite of the overall similarity of the catalytic process, substrate specificities of serine proteases are vastly different. Specificity of substrate is measured by the value k_{cat}/K_m whereas k_{cat} is mainly determined by the binding pocket of each serine proteases (152). The substrate specificity determinants can extend from P6 to P3' (P3' being the third amino acid at the C-terminus of the

cleavage site) of the peptide. Furthermore, there is a dynamic selection process between HA cleavage sites and host proteases. Below, we will discuss further some of the typical serine proteases that activate influenza HA.

1.5.2 Trypsin and Factor Xa

Trypsin and factor Xa are the proteases of choice when culturing influenza viruses *in vitro*. Trypsin is the activated form of trypsinogen which is produced in the pancreas and is a very abundant digestive enzyme of the intestinal tract (154). Its broad substrate specificity (only requiring a P1 Arg or Lys, except substrates with P1' Proline, Pro or P) and high efficiency allow it to activate most if not all influenza viruses *in vitro*. However, it is not considered to be relevant for human influenza infection *in vivo* due to its localization in the intestinal tract. Factor Xa is a coagulating factor in blood that preferably cleaves at the carboxyl side of an Arg in the following motif: Ile-(Glu or Asp)-Gly-Arg. It is very abundant in ECE and is responsible for activating influenza viruses during virus cultivation in ECE (155). As for trypsin, it is considered to be irrelevant in *bona fide* infection as influenza virus does not get into the blood stream typically.

1.5.3 Tryptase Clara and Mini-plasmin

Tryptase Clara and mini-plasmin were isolated from the supernatant and the membrane fraction of rat lung tissue respectively and were shown to activate influenza HA (H3N2) (156, 157). Tryptase Clara is a soluble protease secreted by non-ciliated secretory Clara cells found in the bronchial epithelia. Tryptase Clara cleaves at the carboxyl side of Arg found in the protease's preferred cleavage site, Gln-Ala-Arg. Mini-plasmin is found on epithelial cells in the upper divisions of bronchioles (158). Unlike tryptase Clara, it is a hydrophobic protein and is mainly cell

associated. Its preferred substrate is Glu-Lys-Lys which is not typical for most influenza cleavage sites that typically have Arg at the P1 position. Nevertheless, both mini-plasmin and tryptase Clara are considered to play an important role in influenza activation *in vivo*.

1.5.4 Type II transmembrane serine proteases (TTSPs)

Before the establishment of human adenoid epithelial cell (HAEC), studies of HA cleavage *in vitro* mainly relied on permanent cell lines. HAEC demonstrated multiple physiological hallmarks of actual upper respiratory tract cells and is considered to be an adequate model for natural infection. Studies on HAEC shows that HA activation is largely cell associated, suggesting an important role of membrane bound proteases (143). TTSPs are serine protease involved in homeostasis and development, currently, there are seventeen indentified members in humans and four of them, TMPRSS2, TMPRSS4, TMPRSS13 and human airway trypsin like protease (HAT or TMPRSS11D), have been shown to activate HA (159-162). All four of them have been detected on the cell surface along the upper respiratory tract and many other epithelia, suggesting a role in *in vivo* HA activation. TMPRSS2 and HAT are able to activate all HAs that have been tested (H1 – H16) with variable efficiency (161). TMPRSS4 has been shown to cleave the 1918 pandemic HA whereas TMPRSS13 can cleave tetra-basic HA cleavage sites (162). To our knowledge, the biochemical properties of TTSPs have not been systemically studied yet, and substrate specificities of individual members are largely unknown.

1.5.5 Plasmin (Plg) and Plasminogen (Pm)

Plg is produced in the liver as a zymogen by folding in a closed conformation and is very abundant in the plasma (2 μM) (163). Plg is a 81 kDa protein separated into 2 domains: structural kingle domain and the protease domain (164). The cellular function of Pm is to degrade fibrin in blood clot by fibrinolysis. Activation of Plg to Pm requires tissue plasminogen activator (tPA) and/or urokinase plasminogen activator (uPA) (165, 166). Both PAs are serine proteases which cleave between Arg561 and Val562 of Plg and release the protease domain as Pm. Soluble Pm is readily inactivated by α_2-antiplasmin and α_2-macroglobulin which are very abundant in plasmin (167). Functional Pm is the first protease shown to activate influenza HA, with its preference for substrates with an aromatic residue at the P2 position, such as Tyr, Phe and Trp. WSN is a mouse adapted influenza virus with a P2 Tyr at the cleavage site and was shown to use Pm extensively (148). Along with an additional mutation on NA that recruits Plg, WSN is able switch tropism and replicate in the brain in a NA dependent manner (92).

1.5.6 Furin

Furin belongs to the subtilisin type of serine proteases and is a member of proprotein convertase family (PC) (168). Furin is ubiquitous expressed in humans and is mainly located in the trans-golgi network (TGN) inside cells (169). The binding pocket of furin is highly acidic (negatively charged) and thus prefers substrates that are highly basic. As such, the optimal cleavage site for furin is Arg/Lys-X-Lys-Arg/Lys. In normal circumstance, furin does not activate influenza HA; however, it specifically activates the polybasic cleavage site of HPAI and therefore, allows the virus be activated systemically within the body (151).

1.5.7 Miscellaneous Proteases

Other serine proteases have also been identified to have proteolytic activities on influenza HA, including matriptase, kallikrein 5 (KLK5), kallikrein12 (KLK12) (170, 171). Interestingly, some of them show subtype specificity, supporting the idea that each influenza virus might have its own preference for a particular protease. For instance, KLK5 is able to cleave H1 and H3 efficiently, while KLK12 prefers H1 and H2 subtype. Activation of HA is not limited to eukaryotic proteases, some bacterial proteases or co-factors can activate HA directly and indirectly. A 43 kDa protein isolated from *Staphylococcus aureus* supernatants was shown to activated HA directly (172). Streptokinase A (ska) and staphylokinase (sak) from *Streptococcus sp.* and *Staphylococcus sp.* respectively, are able to cleave HA via activation of host Plg (173). The three-way interactions between host, bacteria and virus suggest a novel synergistic mechanism by influenza and bacterial co-infections.

1.6 Bacterial Co-Infections with Influenza

Bacterial co-infections and secondary infections with influenza has been shown to associate with disease complication and death (174). The bacterial agents implicated in disease progression includes *Staphylococcus aureus*, Group A *Streptococcus* (155), *Streptococcus pneumoniae* and *Haemophilus influenza* (174). However, the synergy between bacteria and influenza are multidirectional and multi-faceted and are largely unknown. Although a comprehensive mechanism of the relationship is unclear, current studies provide convincing evidence on different aspects. So far, the hypothesis of bacterial-influenza synergy mainly includes three areas: a) Immune-modulation by the pathogens, b) Influenza priming bacterial infection and c) bacterial enhancement of influenza virus pathogenesis (175).

1.6.1 Immune Modulation

When bacteria or viruses infect a cell, they both elicit similar pro-inflammatory responses by inducing IL1, IL4 and TNF-α production. However, during dual infections, the combined effects result in an elevation of pro and anti-inflammatory responses which lead to dysregulation of the immune system. Accumulation of non-functional neutrophils results in influx of inflammatory cells into the site of infection (176). On the other hand, a pro-apoptotic protein PB1-F2, which is encoded in some strains of influenza, is associated with increased in virulence of the virus in bacterial co-infection setting (177). In a mouse model study, PB1-F2 induces pro-inflammatory cytokines and an influx of neutrophils into the lungs which impairs the host ability to kill bacteria (118).

1.6.2 Influenza Virus Infection as a Primer to Bacterial Infection

Viruses are able to prime host tissue and turn them into a favorable environment for bacterial attachment and colonization. Ciliated cells serve as a physical barrier to prevent easy penetration of pathogens into the respiratory tract by the beating motion of cilia. The beating motion is decreased during influenza infection which facilitate bacterial invasion of the respiratory tract (178). Influenza infection also induces epithelial damage, exposing the basal layer of cells for bacterial attachment and colonization (179). Influenza proteins can also directly modify otherwise non-functional bacterial receptors. In influenza infected MDCK cells, viral NA removes the glycan of an unknown receptor which is otherwise inaccessible to *S. pneumoniae*, therefore enhances the binding of the bacteria to host cells (180). Another pathogen GAS, also attaches to influenza-infected MDCK cells. This attachment relies on the viral HA and the presence of fibronectin (181, 182).

1.6.3 Bacteria Priming Influenza Infection

In a mouse model study, an increase of influenza viral titers is observed in *S. pneumoniae* co-infection. The result suggests that influenza replicates better in the presences of *S. pneumoniae* (183). Other studies have also shown that patients suffering from bacterial-influenza co-infection require a prolonged phase for recovery than patients with a sequential bacterial infection after influenza infection (184). Together, these studies suggest that bacteria enhance and prolong viral infection duration by some unknown mechanisms. One hypothesis is that bacterial co-infection with influenza virus infection allow the virus to access blood circulation and spread systemically within the body. For example, a study shows when *Escherichia coli* is inoculated intratracheally along with H9N2 LPAI, the virus can spread to different parts of the body (185). However, information regarding the systemic spread of influenza virus remains poorly defined. Previous studies have shown that viral RNA was presence in the kidney and liver of MS96 infected farm chicken, suggesting that the virus is able to disseminate to other organs. Bacteria have been shown to directly enhance pathogenesis of influenza virus. Influenza virus requires proteolytic cleavage on its' HA to become infectious. *S. aureus* has been shown to secrete a protease for this activation event (172, 186).

1.7 HA Cleavage and Implications

The HA cleavage site not only determine the activation state of influenza viruses, but also play a significant role in viral tropism and pathogenesis. In 2013, there are approximately 650,000 HA sequences that are found on online databases, for all of the 18 HA subtypes; each subtype has its signature HA cleavage site and there are a myriad of variations for each. Better understanding of the biochemical properties of these cleavage sites will lead to knowledge of viral pathogenesis and better pandemic planning for potentially highly pathogenic influenza viruses infecting

humans. Furthermore, the possibility of uncovering subtype specific proteases would allow for the development of a targeted approach for therapeutics using inhibitors for specific proteases. In this thesis, I will present three interrelated research work projects aiming to dissect the molecular mechanism of this long discovered, yet still overlooked issue, influenza activation.

1.8 Thesis Overview

The object of this thesis is to understand the structure and function relationship of influenza HA cleavage site and its influence on viral pathogenesis. Chapter 2 begins with characterization of a single Ser to Tyr mutation, at the primary amino acid structure level, in the HA cleavage site of the 2009 H1N1 pandemic virus. This chapter further develops a novel mechanism of influenza virus using an alternative protease, Pm for HA activation. The chapter concludes with the finding that bacterial co-infection modulates influenza virulence *in vivo*. Chapter 3 describes how a combination of primary and tertiary structure on influenza HA modulates HA activation. A loss in sugar moiety and a tri-basic cleavage site converts a LPAI H9N2 to gain universal HA activation by furin *in vitro*, a hallmark property of HPAI. The finding in chapter 3 also suggests a different evolutionary pathway of H9 HA that set it apart from H5 and H7. Chapter 4 demonstrates the same Ser to Tyr mutation on AIV which uses a unique mechanism for HA activation. Chapter 5 summarizes the result and discusses future directions on research on HA activation. Chapter 6 is the overall material and method section in this thesis. Appendix 1 and 2 describe the baculovirus expression system and immune plaque assay respectively.

CHAPTER 2

PLASMIN-MEDIATED ACTIVATION OF PANDEMIC H1N1 INFLUENZA VIRUS HEMAGGLUTININ INDEPENDENT OF THE VIRAL NEURAMINIDASE

Abstract

Influenza virus is well recognized to modulate host tropism and pathogenesis based on mutations in the proteolytic cleavage site of the viral hemagglutinin (HA), which activates HA and exposes the fusion peptide for membrane fusion. Instead of the conventional trypsin-mediated cleavage event, modification of the cleavage site allows for extended use of host cell proteases and enhanced spread *in vivo*. For H1N1 influenza viruses, the mouse-adapted A/WSN/33 strain is known to replicate in the brain based on recruitment of plasminogen by the viral neuraminidase (NA), as well as a Ser-Tyr substitution at the P2 position of the HA cleavage site. Here, we show that an equivalent Ser-Tyr substitution has occurred in the HA of naturally occurring human H1N1 influenza viruses. We characterize one of these viruses (A/Beijing/718/2009), as well as the prototype A/California/04/2009 with a Ser-Tyr substitution in the cleavage site, and show that these HAs are preferentially cleaved by plasmin. Importantly, cleavage-activation by plasmin/plasminogen was independent of the viral NA, suggesting a novel mechanism for HA cleavage activation. We show that the viral HA itself can recruit plasminogen for HA cleavage. We further show that cellular factors, as well as streptokinase from bacteria commonly co-infecting the respiratory tract of influenza patients, can be a source of activated plasminogen for plasmin-mediated cleavage of influenza HAs that contain a Ser-Tyr substitution in the cleavage site.

2.1 Introduction

Influenza virus remains a major cause of morbidity and mortality in the human population (187), with the ever-present risk of new pandemics arising—especially as emerging viruses from zoonotic transmission events. The influenza virus hemagglutinin (HA) mediates both receptor binding and membrane fusion during virus entry (188). A key step in activation of HA is its cleavage by host cell proteases (147, 150, 189), where proteolytic cleavage activation is directly related to exposure of the fusion peptide (190). Low pathogenicity influenza virus strains contain a HA cleavage site with a single arginine residue, and are thus described as having monobasic cleavage sites. These viruses can utilize trypsin (or other trypsin-like serine proteases) for activation, with the tissue distribution of the activating protease typically restricting infection to the respiratory and/or intestinal organs (149). In the case of highly pathogenic avian influenza viruses (HPAIs) such as H5N1 and H7N7, it is well established that mutations in the region of the HA cleavage site lead to an insertion of several arginine or lysine residues in addition to the cleavage site arginine. Such HAs can be recognized by furin or related intracellular serine proteases found in many cell types, allowing a widening of the cell tropism of the virus (151). The presence of a polybasic cleavage site is critical for the systemic spread and increased virulence associated with HPAI.

Influenza A viruses exist as many different subtypes (H1-H17), with H1 and H3 viruses currently infecting humans and H1N1 viruses responsible for the 2009 influenza pandemic (187, 191). With the exception of the 1918 influenza virus, H1 viruses are considered to have low pathogenicity and as such have a monobasic cleavage site. However, two H1 isolates A/WSN/33 (WSN) and A/NWS/33 (NWS) have been selected to propagate in mouse brain, and are thus considered to be

highly pathogenic, neurovirulent viruses in mice (192, 193). The A/WSN/33 virus in particular has been used extensively for studies on influenza replication and pathogenesis, in part because this virus forms plaques in the absence of trypsin and serves as a model of highly pathogenic influenza virus. The HA of the A/WSN/33 virus was originally shown to be cleaved by plasmin, following activation of serum plasminogen in MDBK cells (194). The virulence properties of A/WSN/33 were subsequently linked to the neuraminidase (NA) gene (195) and the absence of a glycosylation site at position 130 of NA (94). In addition, the presence of a C-terminal lysine on NA was shown to be critical for the virulence properties of A/WSN/33, with the viral NA binding and sequestering plasminogen on the cell surface, leading to increased cleavage of HA (92, 196). Nayak and colleagues originally suggested that plasmin-mediated cleavage of A/WSN/33 HA may be influenced by residues neighboring the HA cleavage site arginine (197), and we have recently determined that a mutation in the HA cleavage site of A/WSN/33 is important for plasmin-mediated cleavage and neurovirulence (148). This is a Ser-Tyr substitution at the P2 cleavage site position, adjacent to the P1 cleavage site Arg. HA cleavage data is consistent with biochemical data showing that bulky hydrophobic residues in the P2 position of substrates strongly promote their plasmin-mediated cleavage (198-200).

While A/WSN/33 represents a specific and highly-laboratory adapted form of influenza virus, ongoing influenza surveillance studies have shown that an equivalent Ser-Tyr substitution in the P2 cleavage site position of HA has also occurred in certain naturally occurring influenza viruses. Here, we studied the cleavage activation of the HA of one of these naturally occurring influenza viruses (A/Beijing/718/09), as well as the prototype A/California/04/09 H1N1 virus with a Ser-Tyr substitution in the P2 cleavage site position of HA. We show that the presence of a P2 Tyr markedly

enhances plasmin-mediated cleavage of naturally occurring influenza viruses. Significantly, plasmin-mediated cleavage activation occurs independent of the viral neuraminidase, and so represents a distinct mechanism for enhanced cleavage activation of HA *in vivo*.

2.2 Results

2.2.1 Bioinformatics analysis of the influenza virus H1 cleavage site

A multiple sequence alignment of the HA genes of representative H1 influenza viruses reveals an invariant Arg at position 329 (numbering based on H3 subtype virus A/Aichi/2/68), which comprises the P1 position of the proteolytic cleavage site (Fig. 2.1A). In addition to the invariant Arg at the cleavage site, H1 influenza viruses usually contain a highly conserved Ser at position 328 (the P2 cleavage position). A/WSN/33 is an exception to the consensus cleavage site, containing Tyr at position 328. The HAs of A/Beijing/718/2009 (NCBI accession # ACZ98546) and A/Beijing/720/2009 (NCBI accession # ACZ98560) also represent exceptions to the consensus cleavage site, as they also contain a Tyr at position 328. A/Beijing/718/2009 and A/Beijing/720/2009 were sequenced from human nasal swabs, as part of an outbreak of pandemic influenza in Beijing, China in November 2009. No other information on these viruses is currently available. Additional viruses also contain an equivalent substitution (see Discussion) (Fig. 2.1B)

Figure 2.1. Multiple sequence alignment of the influenza H1 HA cleavage site and fusion peptide. (A) A total of 4325 H1N1 HA amino acid (aa) sequences of H1N1 from the NCBI Influenza Virus Resource (http://www.ncbi.nlm.nih.gov/genomes/FLU/FLU.html) were aligned using muscle v3.8.31, and the aligned sequences of representative viruses at the HA cleavage site are shown, along with the consensus sequence. Dots represent identical residues, P6 – P1' positions of the cleavage site and the location of the fusion peptide are shown. The representative strains selected are the following: A/ South Carolina/1/1918 (accession number AAD17229), A/Puerto Rico/8/1934 (ABO21709), A/Wilson-Smith/1933 (ABD77796), A/New Caledonia/20/1999 (ABF21272), A/California/04/2009 (ACP41105), A/WSN/33 (AAA43209), A/Beijing/718/2009 (ACZ98546) and A/Beijing/720/2009 (ACZ98560). (B) List of H1 viruses with serine (S) to tyrosine (Y) mutation at the P2 position of the cleavage site, along with the information on subtype, accession number and species of isolation.

A

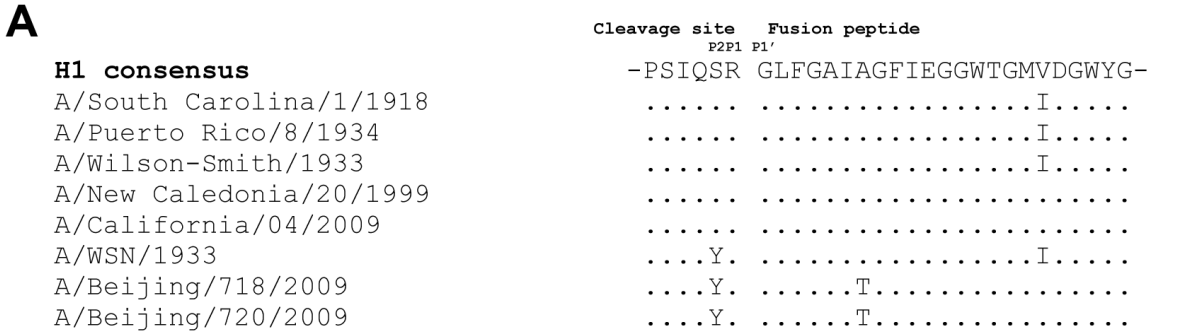

B

Strain	Subtype	Accession number	Speices	Cleavage site P6 - P6'
A/Beijing/718/2009	H1N1	ACZ98546	Human	PSIQYR GLFGAI
A/Beijing/720/2009	H1N1	ACZ98560	Human	PSIQYR GLFGAI
A/Wilson-Smith/1933	H1N1	ABF21278	Human	PSIQYR GLFGAI
A/WSN/1933	H1N1	ACF54598	Mouse Adapted	PSIQYR GLFGAI
A/WSN/1933 TS61	H1N1	ABF47955	Mouse Adapted	PSIQYR GLFGAI
A/WSN/1933	H1N1	AAA43209	Mouse Adapted	PSIQYR GLFGAI
A/swine/Shaanxi/s1/2011	H1N1	AFU92407	Swine	PSIQYR GLFGAI
A/swine/Tainan/46-4/2005	H1N2	ACO07051	Swine	PSIQYR GLFGAI
A/swine/Shaanxi/sf/2011	H1N1	AFU92387	Swine	PSIQYR GLFGAI
A/swine/Shaanxi/sw/2011	H1N1	AFV77705	Swine	PSIQYR GLFGAI
A/swine/Shaanxi/s3/2012	H1N1	AFV77715	Swine	PSIQYR GLFGAI

2.2.2 Cleavage activation of A/Beijing/718/2009 HA by plasmin

Based on the prediction that the presence of a Tyr at the P2 cleavage site position would increase HA cleavability by plasmin, we examined HA cleavage for the A/Beijing/718/2009 HA. An influenza A/Beijing/718/2009 HA gene was synthesized based on the database sequence. We compared this HA to a consensus A/California/04/09 HA, as well as the A/Beijing/718/2009 HA with a mutation of Tyr-Ser to match the H1N1 consensus. HAs were expressed in 293T cells and surface biotinylation was performed. Cells were then treated with human plasmin and HA detected by Western blot to assess the efficiency of plasmin-mediated cleavage. Around 32% of the wild type A/Beijing/718/2009 HA was cleaved by plasmin after 60 min (Fig. 2.2). In contrast, A/Beijing/718/2009 (Y328S) HA showed approximately four times less cleavage by plasmin (Fig. 2.2).

As a control, we also mutated the A/California/04/09 HA, to replace the P2 Ser to Tyr. Similar to Beijing/718/2009 HA, the Ser-Tyr mutation at the P2 position of A/California/04/09 HA significantly increased HA cleavage by plasmin (Fig. 2.3). The higher level of HA cleavage in A/Beijing/718/2009 (codon optimized) than A/California/04/09 (non-codon-optimized) likely correlates to the differences in expression level.

Figure 2.2. Cleavage of the HA of A/Beijing/718/2009 influenza HAs by human plasmin. (A) Human plasmin-dependent HA cleavage of A/Beijing/718/2009 (Bei718) HA and Bei718 HA-328S. Surface biotinylation was performed on 293T cell expressing each HA. Transfected cells were treated with human plasmin (100 mU/ml) at the indicated time and cleavage product(s) were detected by western blot using anti-HA antibody. (B) Quantification of the time-dependent human plasmin mediated HA cleavage efficiency of Bei718 HA and Bei718 HA-328S. The error bars represent the standard deviation of three independent experiments. Statistics were performed using a Student's t-test (unpaired, one-tail) by GraphPad Prism, comparing each individual treatment time (* $p<0.05$, ** $p<0.005$, *** $p<0.0001$).

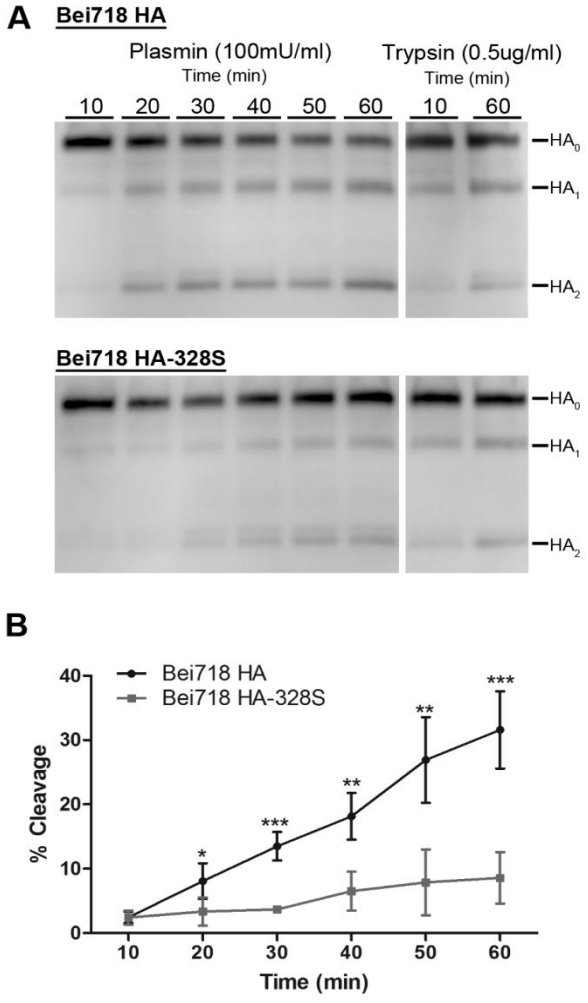
A
Bei718 HA
Plasmin (100mU/ml)
Time (min)
Trypsin (0.5ug/ml)
Time (min)
10 20 30 40 50 60 10 60
HA0
HA1
HA2
Bei718 HA-328S
HA0
HA1
HA2
B
Bei718 HA
Bei718 HA-328S
% Cleavage
40
30
20
10
0
*
***
**
**
***
10 20 30 40 50 60
Time (min)

Figure 2.3. Cleavage of the HA of A/California/04/2009 influenza HAs by human plasmin. (A) Human plasmin-dependent HA cleavage of A/California/04/09 (CA0409) HA and CA0409 HA-328Y. Surface biotinylation was performed on 293T cell expressing each HA. Transfected cells were treated with human plasmin (100 mU/ml) at the indicated time and cleavage product(s) were detected by western blot using anti-HA antibody. (B) Quantification of the time-dependent human plasmin mediated HA cleavage efficiency of CA0409 HA and CA0409 HA-328Y. The error bars represent the standard deviation of three independent experiments. Statistics were performed using a Student's t-test (unpaired, one-tail) by GraphPad Prism, comparing each individual treatment time (* $p<0.05$, ** $p<0.005$, *** $p<0.0001$).

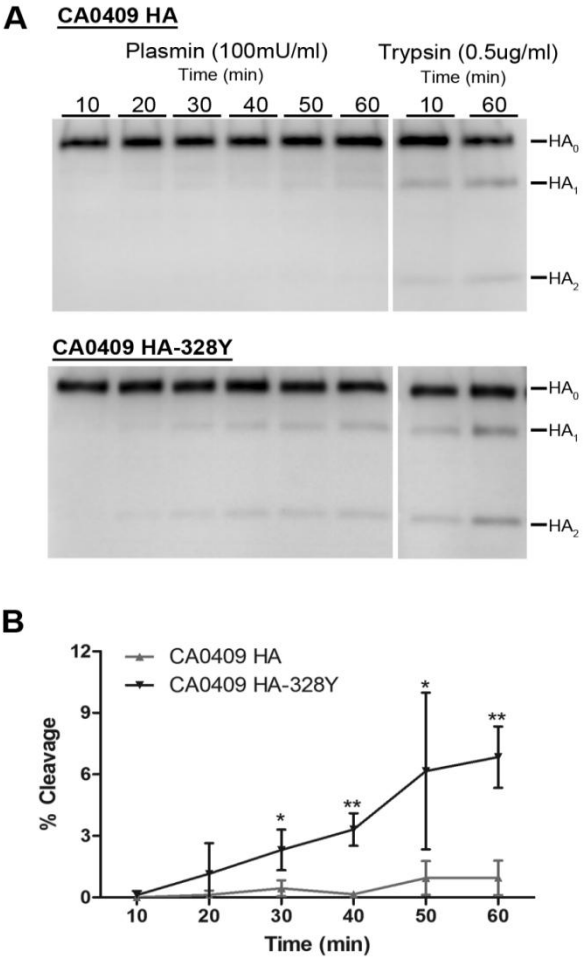
A
CA0409 HA
Plasmin (100mU/ml)
Time (min)
Trypsin (0.5ug/ml)
Time (min)
10 20 30 40 50 60 10 60
HA0
HA1
HA2
CA0409 HA-328Y
HA0
HA1
HA2
B
CA0409 HA
CA0409 HA-328Y
% Cleavage
12
9
6
3
0
10 20 30 40 50 60
Time (min)
*
**
*
**

2.2.3 Rescue of plasmin-activation H1N1 infection by introduction of Tyr at the P2 cleavage site position

To determine whether the presence of Tyr at the P2 cleavage site position can rescue plasmin-mediated infection of pandemic H1N1 influenza, we introduced a S328Y mutation into the A/California/04/09 HA and rescued both wild type and mutant recombinant viruses by reverse genetics and growth in embryonated chicken eggs. Despite efforts, rescue of the intact A/Beijing/718/2009 HA on a A/California/04/09 background was unsuccessful. The introduction of the S328Y mutation into the A/California/04/09 HA resulted in increasing levels of plasmin-mediated cleavage as for A/Beijing/718/2009 (Fig 3). Whereas the wild type A/California/04/09 formed plaques on MDCK cells after addition of exogenous trypsin, addition of plasmin failed to rescue plaque formation (Fig. 2.4A). In contrast, the A/California/04/09 HA S328Y mutant readily formed plaques in the presence of plasmin, as well as with trypsin (Fig. 2.4A). Plasmin-dependent plaque formation, but not trypsin-dependent plaque formation, was inhibited by the plasmin inhibitor 6-aminohexanoic acid (6-AHA). Interestingly, addition of serum alone did not rescue plaque formation for A/California/04/09 HA-S328Y, in contrast to the situation with A/WSN/33 (92, 196) (not shown). In addition to rescuing efficient plaque formation, the majority of plaques formed in the presence of plasmin were significantly bigger for the Y328 mutant, compared to wild type A/California/04/09 (Fig. 2.4B).

Figure 2.4. Plaque forming properties of recombinant virus on MDCK cells. Representative picture of immuno-plaque assay of A/California/04/2009 (rCA0409) (A) and rCA0409 HA-328Y (B) virus on MDCK cells. Plaque assays were performed by inoculating 30–40 pfu virus on MDCK cells in the presence of TPCK-trypsin (1 μg/ml), human plasmin (h-Pm) (3 mU/ml), 5% FBS or mock treated with or without addition of 6-AHA (5 mg/ml) for 3 days. Cells were fixed and viral NP were stained with mouse α-NP Ab. Secondary α-mouse Ab conjugated with Alkaline phosphotase (AP) was used to detect virally infected cell clumps visually. Images were taken using an Alpha DigiDoc™ AD-1200 imager. At least three individual experiments were performed for each condition.

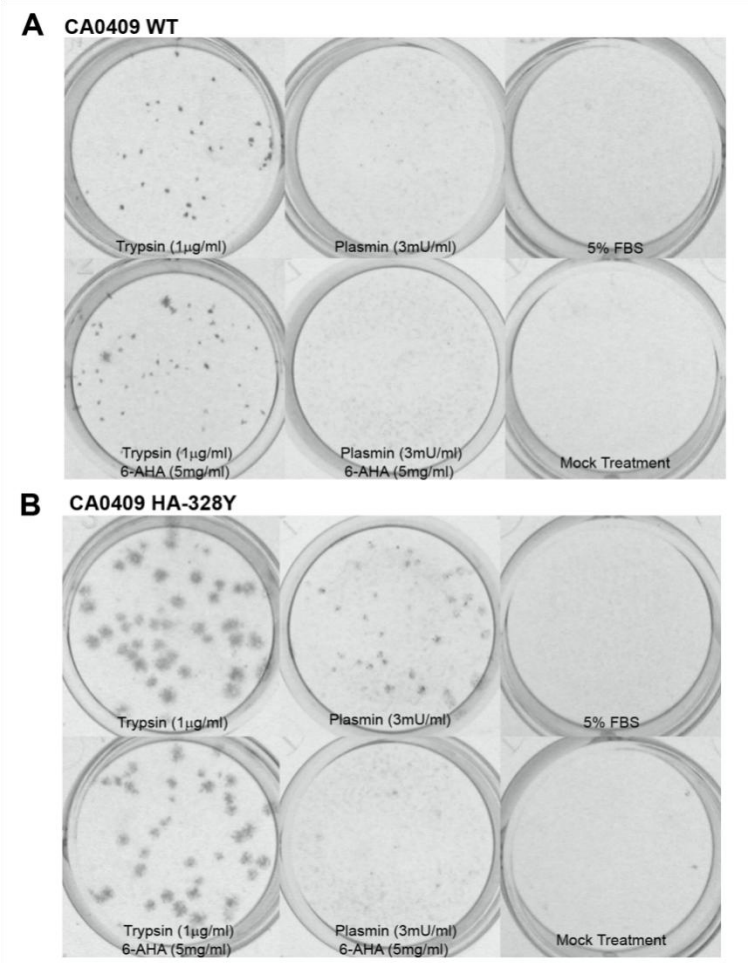

2.2.4 Effects of introduction of Tyr at the P2 cleavage site position in a mouse model of H1N1 influenza

To investigate the effects of introducing a Tyr at the P2 cleavage site position of HA, we challenged mice with the A/California/04/09 and the A/California/04/09 HA-S328Y mutant via both intra-nasal and intra-cranial routes of inoculation. Mice were first challenged intranasally, and samples of lung, trachea, kidney, spleen and brain taken at 3 or 6 days post infection. Tissue samples were then assayed for the presence of virus by plaque assay in MDCK cells. Both A/California/04/09 and A/California/04/09 HA-S328Y replicated well in the lung, and to a limited extent in the trachea, with no discernible differences between the wild type and mutant viruses (Fig. 2.5A). There was no evidence for spread to the kidney, spleen and brain in either case (Fig. 2.5A). Mice inoculated with viruses lost about 15% of weight at the end of experiment with no mortality observed, indicated limited pathogenesis in mouse. However, there is no difference on weight loss between the A/California/04/09 and A/California/04/09 HA-328Y (Fig. 2.5B).

We also challenged mice intracranially, with brain samples taken at 3 days post infection, and assayed for the presence of virus by plaque assay in MDCK cells. A/WSN/33 was included as a control for these experiments. While A/WSN/33 replicated in the brain, there was no evidence for replication of either A/California/04/09 or A/California/04/09 HA-S328Y after intracranial inoculation (Fig. 2.5A). Only A/WSN/33 infected mice showed limited sign of infection with 5% of weight loss at the end of experiment. In contrast, A/California/04/09 and A/California/04/09 HA-328Y showed no sign of infection and no weight loss as the ASCF control (Fig. 2.5C).

Figure 2.5. Mouse model of viral pathogenesis following intranasal and intracranial inoculation. (A) Summary of viral titer after 3 days or 6 days post-intranasal inoculation and 3 days post-intracranial inoculation. Values inside the parentheses indicate the portion of positive samples for viral detection in each group. Average titers were calculated based on positive samples and were represented as $\log_{10}$ pfu/g of tissue. The sign, <, represents viral titer below the detection limit (i.e. 20 pfu/ml). (B) Percentage of initial weight loss of mice. Mouse body weights were measured every 24 hr for intranasal inoculation or (C) every 12 hr for intracranial inoculation. Body weights were normalized to the initial body weight prior to viral inoculation.

A **Intranasal Inoculation**

			Titer (pfu/g) $\log_{10}$		
Day 3	Brain	Spleen	Kidney	Lung	Trachea
rCA0409 WT	<	<	<	5.64 ± 0.353 (4/4)	4.465 (2/4)
rCA0409 HA328Y	<	<	<	5.11 ± 0.206 (4/4)	4.60 (1/4)

			Titer (pfu/g) $\log_{10}$		
Day 6	Brain	Spleen	Kidney	Lung	Trachea
rCA0409 WT	<	<	<	4.75 ± 0.415 (4/4)	4.79 ± 0.360 (3/4)
rCA0409 HA328Y	<	<	<	4.28 ± 0.223 (4/4)	4.67 ± 0.381 (4/4)

Intracranial Inoculation

	Titer (pfu/g) $\log_{10}$
Day3	Brain
rCA0409 WT	<
rCA0409 HA328Y	<
rWSN WT	3.40 ± 0.430 (3/3)

B

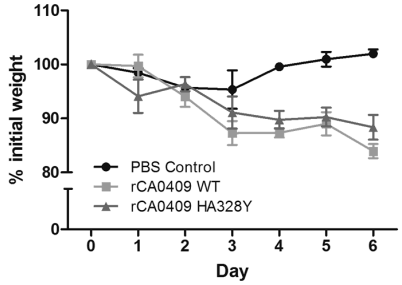

C

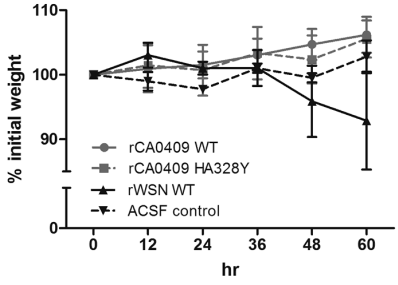

2.2.5 Role of the viral neuraminidase on cleavage activation of A/Beijing/718/2009 HA

It is well established for the neurotropic mouse-adapted influenza virus A/WSN/33 that the viral neuraminidase (NA) plays a major role in recruiting the plasminogen needed for plasmin-mediated HA activation. To assess the role of the NA in the context of A/Beijing/718/2009, we examined the effect of co-expression of A/California/04/2009 NA on HA cleavage. A/California/04/2009 NA was chosen because of its high sequence identity to A/Beijing/718/2009 NA (2 mutations, V106I and N248D, corresponding to N2 subtype). The mutations were not predicted to have any effect on plasmingoen recruitment. The NA from A/WSN/33 was used as a positive control. These experiments were performed in the presence of plasminogen, the inactive precursor of plasmin. As expected, A/WSN/33 NA co-expression resulted in a greatly enhanced cleavage of A/Beijing/718/2009 HA (Fig. 2.6). In contrast, co-expression of A/California/04/2009 NA resulted in very limited cleavage of its cognate HA (Fig. 2.6) and was at a level equivalent to that in the absence of any NA expression.

While short term (1h) exposure to plasminogen allowed only minimal or no HA cleavage in the presence of A/California/04/2009 NA or vector control, longer-term treatment (6h) did result in some degree of HA cleavage. To investigate this further, we used conditioned medium from MDCK cells to determine if endogenous plasmin activators were present. Media recovered from MDCK cells after 24h of cell growth allowed HA cleavage activation in the presence of plasminogen, equivalent to the level of cleavage with activated plasmin (Fig. 2.7). It is likely that MDCK cells release cellular factors such as tissue plasminogen activator (tPA) or urokinase, that would account for the low level of plasminogen-mediated HA activation seen in Fig. 2.6.

Figure 2.6. HA cleavage by human plasminogen independent from its cognate neuraminidase. (A) Time-dependent human plasminogen mediated cleavage of A/Beijing/718/2009 (Bei718) HA and Bei718 HA-328S. Surface biotinylation was performed as in Fig. 2.2 by co-transfecting Bei718 HA with vector control, WSN NA or CA0409 NA and treated with human plasminogen (6 μg/ml) as indicated duration. (B) Quantification of three individual experiments. The error bars represent the standard deviation of three independent experiments, and statistics were performed as for Fig. 2.2.

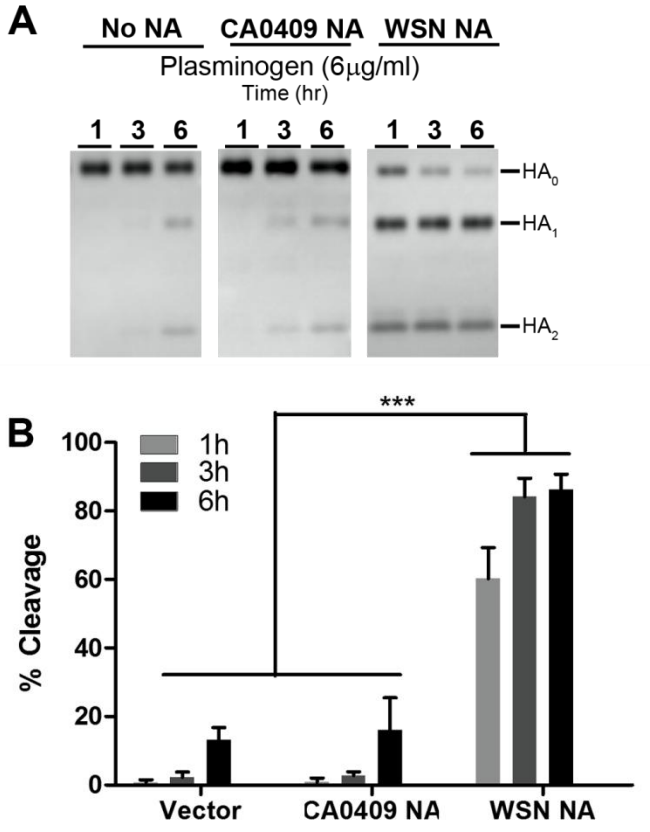

Figure 2.7. HA cleavage by conditioned medium from MDCK cells. (A) HA cleavage of A/Beijing/718/2009 HA. Plg-MDCK conditioned medium was prepared by incubating human plasmin (h-Plg) (5 μg/ml) on MDCK cells for 18h. The conditioned medium was used to treat HA transfected cell for 30 min. Human plasmin (100 mU/ml) was used as positive control and MDCK medium alone as negative control. (B) Quantification of plasminogen (Plg)-MDCK conditioned medium mediated HA cleavage. Relative cleavage efficiencies were calculated for Fig. 2.2. The error bars represent the standard deviation of three independent experiments, and statistics were performed as for Fig. 2.2.

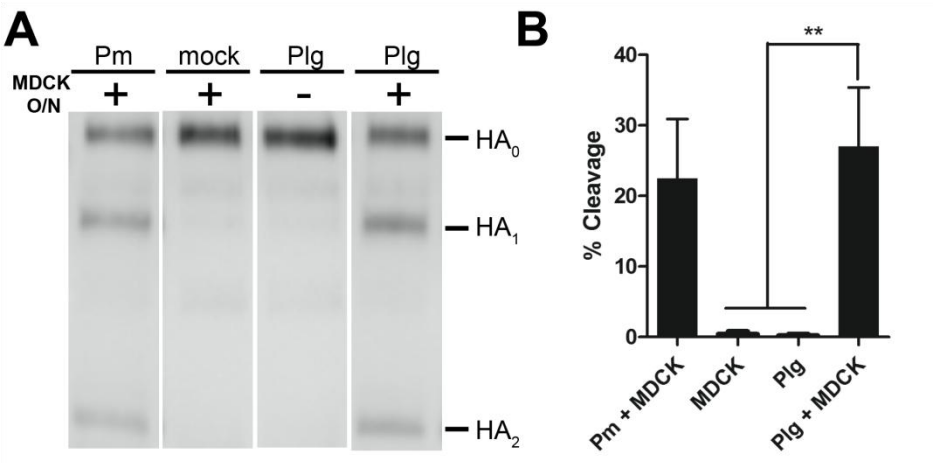

2.2.6 Recruitment of plasminogen by influenza hemagglutinin

Unlike the situation with A/WSN/33, our data show that H1N1 viruses can undergo cleavage activation by the plasmin/plasminogen system in an NA-independent manner. A similar situation has been reported for the 1918 influenza virus, where the viral HA facilitated robust plasminogen binding (159). To determine whether an equivalent situation exists for other influenza H1N1 viruses, including A/Beijing/718/2009 HA, we tested plasminogen binding of HA using flow cytometry. As with A/South Carolina/1/18 HA, the A/Beijing/718/2009 HA bound plasminogen (Fig. 2.8). In fact, plasminogen binding was a common property all the HAs tested. A/PR/8/34 and A/California/04/09 HA showed the most robust binding (Fig. 2.8), with HAs such as A/NWS/33 and A/WS/33 showing less efficient binding. In agreement with the findings in Fig. 2.6, A/California/04/2009 NA transfected cells failed to recruit any plasminogen as shown by FACS. In these studies, we also included A/WSN/33 NA, which served as a positive control for plasminogen binding, as well as a mutated version of A/WSN/33 NA (R146N, ΔK470; corresponding to N2 subtype), as a negative control. Combined, these mutations were shown to abolish plasminogen binding (93, 94).

Figure 2.8. Plasminogen binding on HA and NA transfected cells by flow cytometry. (A) Percentage of human plasminogen binding cell. A/WSN/33 (WSN) NA was used as a positive control, pEF4 was used as background binding and WSN NA R146N, ΔK470 was used as negative control. CA0409 NA, and eight different H1 HAs; WSN, A/South Carolina/1/1918 (1918), CA0409, Bei178, A/NWS/1934 (NWS), A/Wilson-Smith/1933 (WS), A/Puerto Rico/8/1934 (PR8), A/New Caledonia/20/1999 (New Caledonia) and one H9 HA (not shown) were tested. The error bars represent the standard deviation of three independent experiments. Statistics were performed as for Fig. 2.2 by comparing each sample to the negative control. (B) Representative FACS traces are shown. Plots were all overlaid with the background control (pEF4 empty vector) to illustrate the peak shift on x-axis (APC, staining for plasminogen). The Y-axis represents the percentage of cell normalized to the maximum cell number in a single channel within the plot.

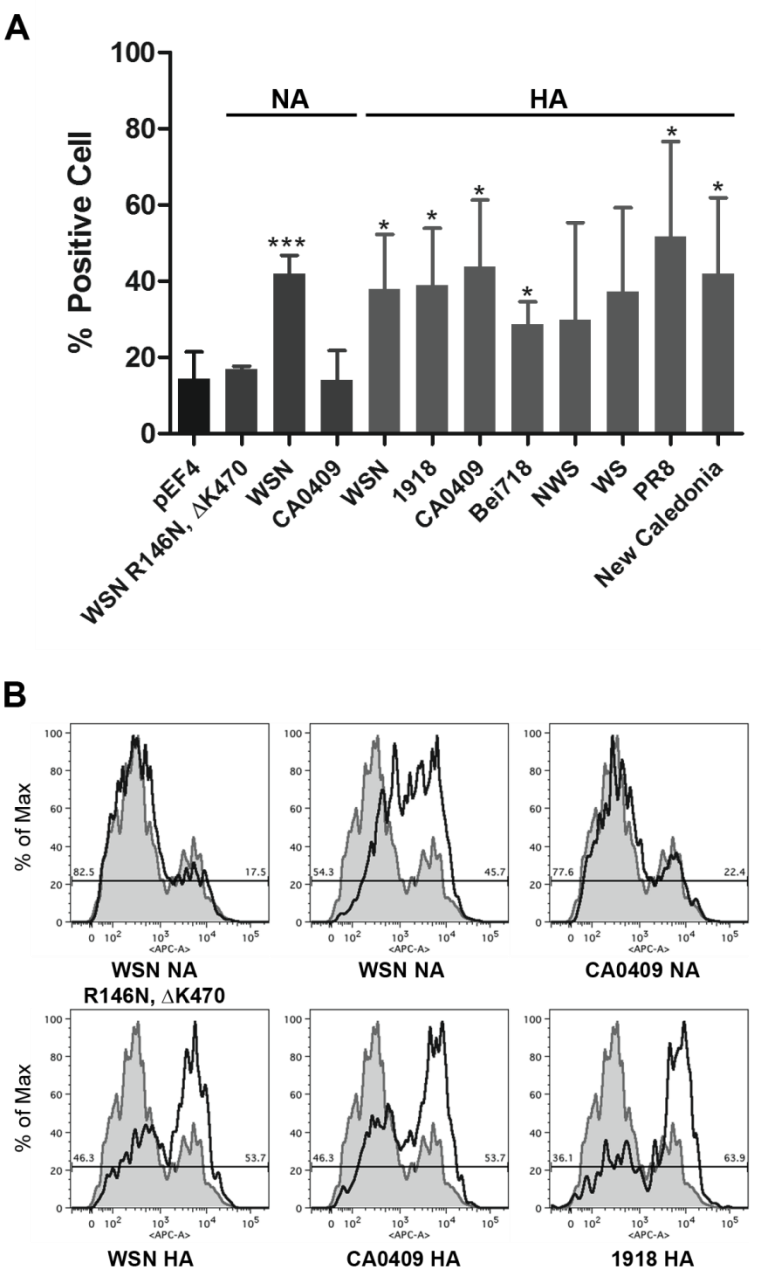
A
% Positive Cell
100
80
60
40
20
0
NA
HA
***
*
pEF4
WSN R146N, ΔK470
WSN
CA0409
WSN
1918
CA0409
Bei718
NWS
WS
PR8
New Caledonia
B
% of Max
82.5
17.5
54.3
45.7
77.6
22.4
WSN NA
R146N, ΔK470
WSN NA
CA0409 NA
46.3
53.7
46.3
53.7
36.1
63.9
WSN HA
CA0409 HA
1918 HA

2.2.7 Bacterial streptokinase can recruit plasminogen for cleavage activation of A/Beijing/718/2009 HA

As our data clearly indicated that A/Beijing/718/2009 HA was preferentially activated by plasmin in an NA-independent manner, we also examined other ways that plasminogen could be recruited and activated for HA cleavage. One likely possibility is via bacterial virulence factors. Bacterial co-infections are common in more severe cases of influenza, with *S.aureus*, *S. pneumoniae*, *S. pyogenes* and *H. influenzae* commonly co-infecting the respiratory tract and contributing to the pneumonia often associated with influenza morbidity and mortality (11, 201). Many of these bacterial species express virulence factors that can recruit and activate plasminogen, including streptokinase and staphylokinase (173). As an example virulence factor, we tested the effects of streptokinase from *S. pyogenes* (202). A/Beijing/718/2009 HA, or the Y328S mutant, was expressed on the surface of cells and biotinylated. Cells were then exposed to inactive plasminogen (5 μg/ml)), bacterial streptokinase (5 μg/ml), or a combination of both inactive plasminogen and bacterial streptokinase, and the cleavability of HA was determined. Cells were exposed to trypsin as a positive control, and with media only as a negative control. Exposure to a combination of both inactive plasminogen and bacterial streptokinase led to significant increases in the cleavage of HA for A/Beijing/718/2009 HA (Fig. 2.9). In contrast, treatment with plasminogen and streptokinase led to a much-reduced level of HA activation for the Y328S mutant (Fig. 2.9).

Figure 2.9. HA cleavage by bacterial streptokinase-activated human plasminogen. (A) Surface biotinylation was performed as mentioned above. 293T cells transfected with A/Beijing/718/2009 (Bei718) HA or HA-328S mutant were treated with different proteases as indicated for 1h. Cleavage products were detected by western blot using anti HA antibody. (B) Quantification of the streptokinase/plasminogen (Skc-Plg)-dependent HA cleavage efficiency. Cleavage efficiencies were calculated. The error bars represent the standard deviation of three independent experiments, and statistics were performed as in Fig. 2.2.

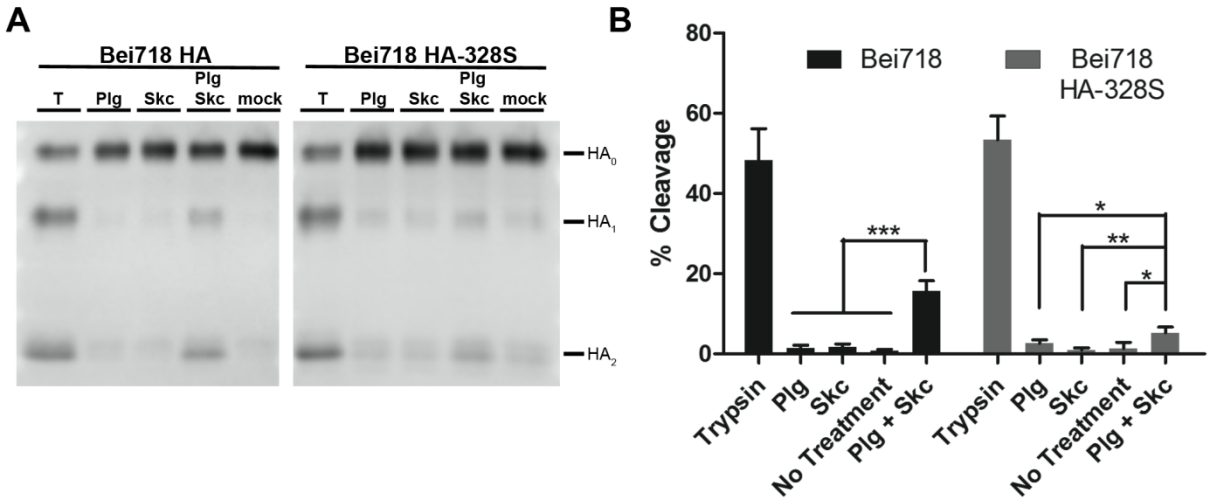

2.2.8 Secondary infection by *Streptococcus pyogenes* (NZ131) increase weight loss of A/California/04/2009 HA-328Y infected mice

To test the synergistic effect of CA0409 HA328Y and *Streptococcus pyogenes in vivo*, we developed a mouse model for bacterial secondary infection. Wild type CA0409 and CA0409 HA-328Y were inoculated intranasally in mice followed by NZ131 inoculation on Day 3 PI. Regardless of NZ131 secondary infection, CA0409 infected mice show the same magnitude of weight loss (Fig. 2.10a). In contrast, CA0409 HA-328Y infection followed by NZ131 secondary infection shows significant weight loss in mice whereas CA0409 HA-328Y and NZ131 infection alone did not cause any phenotype (Fig. 2.10b). At day 7 post infection, lung, kidney, brain, spleen were harvested from each mouse. However, none of the tissue shows presences of viruses or bacteria. (Data not shown)

Figure 2.10. Body weight loss of mice followed by *Streptococcus pyogenes* (NZ131) secondary infection. (A) Schematic of experimental design. Mice were infected on Day 0 with $1x10^5$ pfu intranasally followed by $1x10^6$ cfu of NZ131 on Day 3. Body weight were measured every 24 hr for 7 days. Tissues, including lung, kidney, spleen and brain were harvested on Day 7 PI. (B) Percentage of initial weight of mice after intranasal infection with, CA0409, NZ131 and CA0409 + NZ131. (C) Percentage of initial weight of mice after intranasal infection with CA0409 HA328Y, NZ131 and CA0409 HA-328Y + NZ131.

A

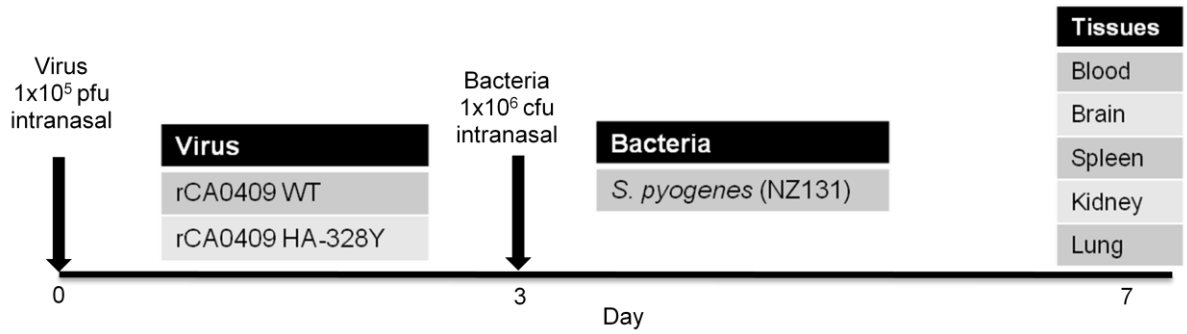

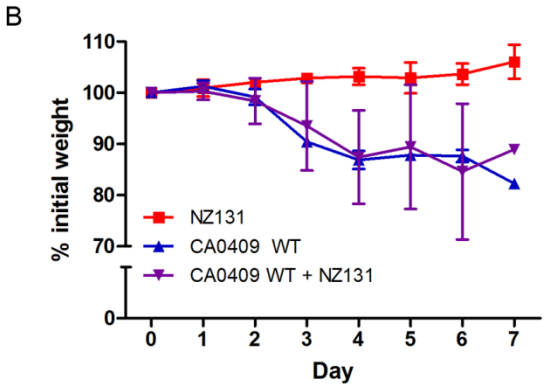

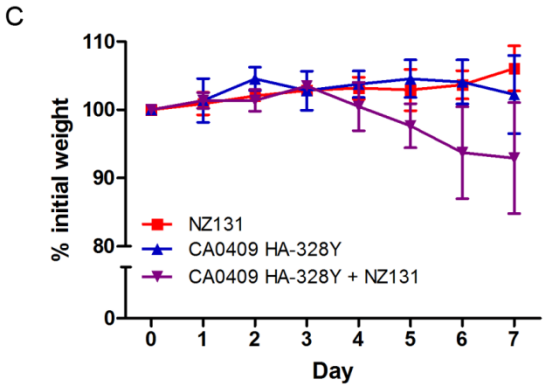

2.3 Discussion

We show here that plasmin-plasminogen mediated activation of influenza HA can be influenced by mutations in the HA cleavage site of circulating virus strains. While cleavage activation of influenza mediated by plasmin-plasminogen has been established for some time, its importance for virus infection has been restricted to the highly laboratory adapted A/WSN/33 strain, which is known to specifically recruit plasminogen via the viral NA protein, with a Ser-Tyr mutation in the P2 position of the HA cleavage site contributing to efficient HA cleavage and enhanced viral pathogenesis. Here we show that an equivalent Ser-Tyr mutation in the HA of a circulating human H1N1 strain also contributes to enhanced cleavage by plasmin-plasminogen, but without recruitment of plasminogen by NA.

Our study focused on one pandemic H1N1 virus, A/Beijing/718/2009, however it should be noted that this is likely not an isolated example of a virus that is preferentially activated by plasmin. In addition to the A/Beijing/720/2009 virus from the same surveillance site as A/Beijing/718/2009, a pandemic H1N1 virus with a cleavage P2 Ser-Tyr substitution was also isolated in a separate surveillance study in humans – A/Taiwan/97196/2009 (203), as well as for several H1 viruses in swine (see Fig. 2.1B). As with A/Beijing/718/2009, no clinical information is available for these viruses.

In addition to A/WSN/33, a role for plasmin-plasminogen has been reported for other influenza strains, with plasminogen activation mediated by the host cellular protein annexin II, which is incorporated into the virus particles (56). A role for plasmin-plasminogen has also been proposed for the 1918 influenza virus via direct binding to the viral HA (159). Our data show that sequestration of plasminogen by HA is a common property of distinct viral strains. However, in general, plasminogen

binding by HA was less efficient than for the A/WSN/33 NA (not shown). HA-mediated binding of plasminogen likely works in concert with cellular factors such as annexin II, tPA or urokinase and mutations in the HA cleavage site to promote HA cleavage activation.

One possible cell type where plasminogen is known to be highly active is endothelial cells, which are suggested to be important in the “cytokine storms” associated with highly pathogenic influenza viruses (204). Both A/California/04/09 and the Ser-Tyr mutant were able to infect blood microvascular endothelial cells (HMVEC-LBI, Lonza), as detected by immuno-fluorescence assays for viral HA and NP (not shown). However, experiments to address any increased virus replication in endothelial cells based on a Ser-Tyr cleavage site mutation or use of plasmin-plasminogen failed to show any productive rounds of virus infection as compared to A/WSN/33, which appeared to replicate to a limited degree (not shown).

Although *in vitro* data shows enhanced usage of plasmin for HA activation with Ser-Tyr substitutions at the P2 cleavage site position, data from the mouse model shows no discernible differences between A/California/04/09 and A/California/04/09 HA-328Y. The situation in humans remains unresolved, with the lack of effect in the mouse possibly due to differences in the activating protease. This discrepancy could be addressed in cell culture models of the human respiratory epithelium. The data from intracranial inoculation showing that A/California/04/09 HA-328Y is unable to replicate in brain indicates that additional mutations in HA are required for neurotropism. Given that bacterial co-infections are common with influenza, and based on the data reported here on the role of bacterial streptokinase, one possible outcome is that P2 Ser-Tyr substitution is important in the context of a bacterial co-infection, e.g. with plasminogen-activating *S. aureus* or *S. pyogenes*. One possibility

is that a Ser-Try mutant can be selected in the respiratory tract of a patient with ongoing influenza-bacterial co-infection, which would allow extended use of proteases such as plasmin. In the absence of clinical data from humans, it will be interesting to test this in mouse models of influenza-bacterial co-infections.

Despite extensive efforts regarding influenza surveillance, and the large amount of sequence information in the database, molecular characterization of clinically relevant viruses identified in surveillance studies is still lacking. The combination of bioinformatics analysis and experimental virology plays an important role is translating the sequence information to a real understanding of the heterogeneous viral population. Here, we provide an example of a distinct variant human pandemic virus with discrete biological properties, and describe its molecular properties both *in vitro* and *in vivo*. Such studies can provide important information for pandemic planning.

2.4 Acknowledgments

The authors thank Yueting Zhang, Jean K. Millet, Alice M. Hamilton, Tamar Friling and all the members in the Whittaker Lab for helpful discussions. We also thank Lu Huang for helpful discussion on flow cytometry. We would also like to thank Toru Takimoto for provision of the recombinant virus system. These studies were funded by the United States Department of Health and Human Services contract HHSN266200700008C (NIAID Centers of Excellence for Influenza Research and Surveillance). Work in the author's laboratory is also supported by a research grant from the National Institutes of Health (R01 AI48678).

CHAPTER 3

ACTIVATION OF AVIAN INFLUENZA VIRUS H9N2 BY FURIN

Abstract

Avian influenza H9N2 is prevalent in waterfowl worldwide and has become endemic in poultry in Asia and the Middle East. H9N2 influenza viruses have served as a reservoir of internal genes for other influenza viruses that infect humans, and several cases of human infections by H9N2 influenza viruses have indicated its threat to the human population and pandemic potential. Fortunately, an extensive surveillance program enables close monitoring of H9N2 influenza viruses worldwide and has generated a large repository of virus sequences and phylogenetic information. Despite the large quantity of sequences in different databases, very little is known about specific virus isolates and their pathogenesis. Here, we characterize a low pathogenicity avian influenza virus (LPAI), A/chicken/Israel/810/2001 (H9N2) (Israel810), which is representative of influenza virus strains that have caused severe morbidity and mortality in poultry farms. We show that under certain circumstances, the Israel810 virus can be activated by furin, a hallmark of highly pathogenic avian influenza virus (HPAI). We demonstrate that Israel810 HA can be cleaved in cells with high levels of furin expression, and that a mutation that eliminates a glycosylation site in HA1 allows the Israel810 HA to gain universal cleavage in cell culture. Pseudoparticles generated from Israel810 HA, or the glycosylation mutant, transduce cells efficiently. In contrast introduction of a polybasic site into H9 HA lead to pseudoviruses that are comprised for transduction. Our data indicate a mechanism for an H9N2 evolutionary pathway that may allows it to gain virulence in a distinct manner from H5 and H7 influenza viruses.

3.1 Introduction

Influenza A virus H9N2 was first isolated in the United States in 1966 in turkeys (205), and was subsequently found to be prevalent among waterfowl and able to spread to poultry worldwide (206-208). H9N2 avian influenza viruses have now become endemic in China and the Middle East (207, 209, 210). The impact of H9N2 influenza is not restricted to the poultry industry and avian species; sporadic cases of humans infected by H9N2 have also been reported (21, 211). H9N2 influenza is different from H5 and H7 influenzas, where some strains are defined as highly pathogenic by the World Organization for Animal Health (212) based in part by the presence of multiple basic amino acids in the hemagglutinin (HA) cleavage site (212). All of the isolated strains of H9N2 are of low pathogenicity according to the OIE classification. Despite this, several outbreaks of H9N2 virus infections have caused serious disease, and in some cases a high mortality rate, in domestic poultry farms (213-215). Several known reassortment events of H9N2 with H5N1 mean that H9N2 influenza viruses have the potential to be the donor or acceptor for more virulent influenza viruses (22, 216, 217). Furthermore, some H9N2 viruses have similar receptor specificity as human influenza (218). Due to the lack of immunity of the global human population to H9 viruses, these viruses are of some concern from the perspective of pandemic potential for the human population (22, 219).

The influenza hemagglutinin (HA) is an important pathogenesis determinant of the virus and plays a crucial role for infection (65). Influenza HA needs to be proteolytically cleaved at a defined cleavage site to enable exposure of the fusion peptide during viral entry, which initiates successful infection (190). In most cases, influenza HAs have monobasic cleavage site that contains a single arginine (Arg or

R) at the P1 cleavage position. Such cleavage sites are typically activated by trypsin-like serine proteases (150). This requirement restricts the tropism of influenza viruses to the types of tissues that express the proteases for activation. In some situations, highly pathogenic avian influenza (HPAI) viruses of the H5 and H7 subtypes have gained the ability to systemically infect the host by facilitating the activation of their HAs. HPAI H5 HAs are mutated to have multiple insertions of basic residues (Arg, R or Lys, K) at the cleavage site, to gain a polybasic cleavage site, and to make use of more ubiquitously expressed furin-like proteases (150, 151).

Furin is a member of the proprotein convertase family that is ubiquitously expressed (169). Although furin is expressed universally, expression levels vary and can be quite low depending on tissue types (220). Under specific conditions including co-infections with other pathogens, furin expression is elevated (221-223). Substrates of furin are mostly basic in nature, as determined biochemically by fluorescence resonance energy transfer (FRET)-based peptide assays (224). The minimum sequence requirement of furin is R-X-X-R, which consists of two paired arginine residues at the P1 (cleavage) and P4 position, where X can be any amino acid. However the presence of a basic residue at P2 enhances furin cleavage markedly (168). Interestingly, the consensus cleavage site of H9N2 influenza virus is predicted to be capable of cleavage by furin, with the sequence of R-S-S-R (serine, Ser or S). Furthermore, a subset of H9N2 viruses have a mutated cleavage site (R-S-K-R or R-S-R-R) that is predicted to be more optimized for furin cleavage (225). However, several studies have shown that such HA sequences are not efficiently cleaved by furin (226, 227). The inconsistency of the biochemical prediction and the actual biological data suggests that other factors may play a role in HA cleavage.

Influenza HA is a complex protein, folded in a tertiary structure. In this situation, accessibility of the cleavage site to proteases becomes as important as the primary sequence itself. A notable example of this is the influenza A/chicken/Pennsylvania/83 (H5N2) (H5 Penn/83) isolate, which becomes more pathogenic after a single mutation at the bottom of the stalk of HA (228).This mutation eliminates a glycosylation site, which is in very close proximity to the cleavage site. The loss of the bulky sugar moieties is thought to reduce the steric hindrance of the protease to the cleavage site; thus, indirectly increasing the accessibility of the cleavage site. In addition to the polybasic cleavage site, HPAI H7 HAs contain a peptide insert upstream of the HA cleavage site to increase the accessibility of the cleavage site to proteases (229). In other situations (most notably with equine H7N7 viruses) the addition of 11 amino acids adjacent to the cleavage site allowed increased cleavage and fusion activation (171, 230), presumably by repositioning and increasing accessibility of the cleavage site motif. The impact of these types of modifications for H9 influenza has not been evaluated.

Here, we use a prototype H9N2 virus with an R-S-K-R cleavage site, and which is associated with high mortality in poultry (A/chicken/Israel/810/2001 [Israel810]). We characterize the possibility of HA activation by furin under different expression conditions, and in the context of addition of peptide inserts in the HA cleavage site and removal of glycosylation at the base of the HA stalk. In this study, we find that furin expression level is directly proportional to the efficiency of HA cleavage, with implications for viral spread in the host. We also find that removal of glycosylation site 13, a mutation already present in certain H9N2 field strains, leads to the efficient activation of A/chicken/Israel/810/2001 by endogenous furin, showing the

potential for a defined constellation of mutations that impact HA activation. Our studies allow better understanding of the virus at the biological level in the context of influenza surveillance data and pandemic preparation.

3.2 Results

3.2.1 Minimum furin cleavage site in H9 HA

Based on multiple sequence alignment analysis of a total of 2801 sequences of H9N2 HA from the Influenza Research Database (FluDB), the consensus sequence of the H9N2 cleavage site was determined to be R-S-S-R (Fig. 3.1). However, the HA cleavage site of H9 influenza viruses is somewhat variable particularly at the P2 position, which has predominant substitutions of lysine (K), arginine (R), asparagine (N) and glycine (G). While R-S-S-R constitutes a minimal furin cleavage site, it is notable that a substantial number of isolates, (29/2801, or 1%) have a single Lys (K) substitution at the P2 position of their cleavage site, S321K (based on H3 numbering, A/Hong Kong/1968) that is predicted to be a more optimized substrate for furin (227). Predictive scores for furin cleavage are shown in Fig. 3.1, based on the Pitou 2.0 furin cleavage prediction algorithm (231). Pitou 2.0 accurately predicts furin cleavage sites by taking into account solvent accessibility and binding strength of residues of protein sequences. A sequence with a negative score is considered to be unfavorable for furin recognition and cleavage, while a positive score is predictive of furin cleavage with higher values being more processive.

Israel810 HA (with R-S-K-R cleavage site) is predicted to be cleaved by furin, with the highest score of +9.14 among all the H9 sequences. In comparison, HPAI A/Chicken/Hong Kong/220/1997 (H5N1) has a score of +13.59 (Not shown). Wisconsin1966 (V-S-S-R) has a negative score, which indicates it is not able to be cleaved by furin, and the consensus sequence (R-S-S-R) has a score of +3.72. Viruses containing the S321K mutation are clustered in Middle East and are

responsible for several outbreaks in local poultry farms infecting a wide range of avian species (Fig. 3.1B) (232) . The full list of strains containing the 321K substitution, along with their accession numbers, are shown in Fig. 1B. A/Israel/810/2003 (H9N2) was selected as a prototype virus representing H9 viruses with the 321K substitution within the Middle East.

Figure 3.1. Multiple sequence alignment of H9 HA. (A) A total of 2801 sequences obtained from NCBI Influenza Database (http://www.ncbi.nlm.nih.gov/genomes/FLU/FLU.html) were aligned by MUSCLE alignment program. HA cleavage site from P6 to P1 and fusion peptide are shown. H9HA consensus sequence is shown in bold font, underneath it are representative strains where sequence differences from the consensus H9HA are indicated as single letter amino acid code. Representative strains and their accession number are as follow: A/Duck/Hong Kong/W213/1997 (BAG72217), A/Chicken/Hong Kong/G9/1997 (AAF00701), A/Turkey/Wisconsin/1/1966 (BAA14335), A/Turkey/Israel/810/2001 (ABS50802), A/Ostrich/Eshkol/1436/2003(AAW29080), A/Quail/Shantou/2061/2000 (ABM46232), A/Chicken/Israel/786/2001 (ABS50800), A/Turkey/Israel/747/2005 (ABS50799). Pitou furin prediction score of the representative strains, positive value indicates favorable cleavage by furin where the value is proportional to the predicted efficiency of cleavage of a given site. (B) Summary of strains harbors the same mutation as Israel810. This information was up-to-date during the preparation of the manuscript (August 2013).

A

	Cleavage site P2P1	Fusion peptide P1′	PiTou-Score
H9 consensus	-PARSSR	GLFGAIAGFIEGGWSGLVAGWYG-	
A/Turkey/Wisconsin/1/1966	..V...	..............P........	-27.00
A/Duck/Hong Kong/W213/1997	......	.....	+3.72
A/Chicken/Hong Kong/G9/1997	......	.....	+3.72
A/Quail/Shantou/2061/2000	....R.	..............P........	+8.97
A/Chicken/Israel/786/2001	....N.	..............P........	-22.27
A/Turkey/Israel/810/2001	....K.	..............P........	+9.14
A/Ostrich/Eshkol/1436/2003	....K.	..............P........	+9.14
A/Turkey/Israel/747/2005	....G.	..............P........	+2.84

B

Accession #	Strain Name
ABP48866	A/turkey/Avigdor/1209/03
AAZ14983.1	A/turkey/Avigdor/1215/03
AAZ14991	A/turkey/Givat Haim/622/02
AAS48376.1	A/turkey/Givat Haim/810/01
AAZ15000.1	A/turkey/Givat Haim/868/02
AAW29076	A/turkey/Givat Haim/965/02
AAZ14988	A/turkey/Kfar Vitkin/615/02
AAZ14989	A/turkey/Kfar Vitkin/616/02
AAZ14984.1	A/turkey/Kfar Warburg/1224/03
ABS50798	A/turkey/Israel/619/02
ABS50802	A/turkey/Israel/810/01
ABS50806	A/turkey/Israel/1013/02
ABS50807	A/turkey/Israel/1209/03
AAZ14992.1	A/turkey/Yedidia/625/02
AAZ14977	A/turkey/Yedidia/911/02

Accession #	Strain Name
AAZ14979	A/turkey/Avichail/1075/02
AAZ15002.1	A/Turkey/Beit HaLevi/1009/02
ABP48870	A/turkey/Brosh/1276/03
AAZ14980.1	A/turkey/Ein Tzurim/1172/02
ABP48864	A/turkey/Hod Ezyon/699/02
AAZ14990	A/turkey/Mishmar Hasharon/619/02
ABP48865	A/turkey/Naharia/1013/02
ABP48867	A/turkey/Qevuzat Yavne/1242/03
AAZ14981.1	A/turkey/Sapir/1199/02
AAW29080	A/ostrich/Eshkol/1436/03
ABP48863	A/chicken/Kfar Monash/636/02
AAZ14997	A/chicken/Tel Adashim/812/01
AAZ14999	A/geese/Tel Adashim/830/01
AAZ14998	A/geese/Tel Adashim/829/01

3.2.2 Israel810 HA can be cleaved by furin, but cleavage depends on furin expression level

To examine the effect of the 321K substitution in Israel810 HA, a revertant HA (321S) with the cleavage site R-S-S-R was generated by site-directed mutagenesis. This HA was examined by western blot, along with the WT HA, following cell surface biotinylation of 293T cells. Neither HAs were cleaved by an endogenous protease, predicted to be furin, in 293T cells (Fig. 3.2A). We hypothesized that endogenous levels of furin may be very low in 293T cells, and so not enough for efficient HA cleavage. To test this, plasmids containing HA and either human furin (h-furin) or chicken furin (ch-furin) were co-transfected in 293T cells. Western blot analysis showed that, WT HA was able to be efficiently cleaved by either human or chicken furin, whereas the 321S revertant was not (Figs. 3.2B, 3.2C). Israel810 (WT) HA showed 40% and 52% HA cleavage by h-furin and ch-furin respectively.

3.2.3 Chicken furin has higher processivity than human furin on Israel810 HA

The above data suggested that chicken furin has a higher processivity than human furin in cleaving H9N2 avian influenza HA (Figs. 3.2B, 3.2C). To test this observation in a more systematic way, we constructed two tunable expression plasmids for ch-furin and h-furin using the ProteoTuner^{TM} Shield Systems (Clontech). By fusing the destabilization domain (DD) from the immunophilin FK506-binding protein (FKBP) protein to the C-terminus of each furin, overexpressed furin-DD will be degraded by default in proteasomes. Furin-DD can be protected by adding Shield 1, a stabilizing ligand that binds to the DD and prevent it from degradation. Therefore, furin-DD stability can be fine-tuned by addition of different amounts of Shield 1 into the transfection mix - as the concentration of Shield 1 will be directly proportional to

the level of overexpressed furin in the cell. Furin-DD and Israel810 (WT) HA were co-transfected into 293T cells supplemented with different concentration of Shield 1 as described in materials and methods. Biotinylation and western blot analysis showed that HA cleavage is proportional to the concentrations of Shield 1 for both ch-furin and h-furin, where ch-furin showed a higher percentage of HA cleavage than h-furin (Fig. 3.2D). Quantification of the HA cleavage showed that ch-furin has a higher processivity than h-furin on WT HA and was statistically significant at > 500 nM Shield 1 added (Fig. 3.2E).

Figure 3.2. Cleavage of Israel810HA and Israel810HA-321S by endogenous proteases, human furin (h-furin) and chicken furin (ch-furin). (A) Representative western blot image of HA cleavage by cell surface biotinylation of Israel810HA-WT (WT) and Israel810HA-321S (321S) in 293T cells. HA_0 and HA_2 bands were labeled as indicated. Quantification and statistical analysis of HA cleavage from the blot is shown on the right. Error bars represent 1 standard deviation (S.D.) from at least 3 independent experiments. Data were analyzed by one-tailed Student's t-test where * indicate $p<0.05$, ** $p<0.01$ and *** $p<0.005$. (B) Representative western blots and quantification of WT and 321S HA cleavage by transiently co-transfecting HAs and plasmids expressing h-furin and (C) cf-furin into 293T cells. Error bars represent 1 S.D. from at least 3 independent experiments. Statistical analysis and notations were same as above. (D) Representative western blot image of surface biotinylation of WT HA cleavage by tunable furin expression system in 293T cells. Concentrations of Shield 1 were indicated on top of each lane and HA_0 and HA_2 bands were labeled as above. (E) Quantification of HA cleavage of Fig. 3.2D. A curve is fit with each set of data with the equation $y=10^{mlogx} + c$ where m is slope and c is y-intercept. Data are analyzed by one-tailed Student's t-test as mentioned above.

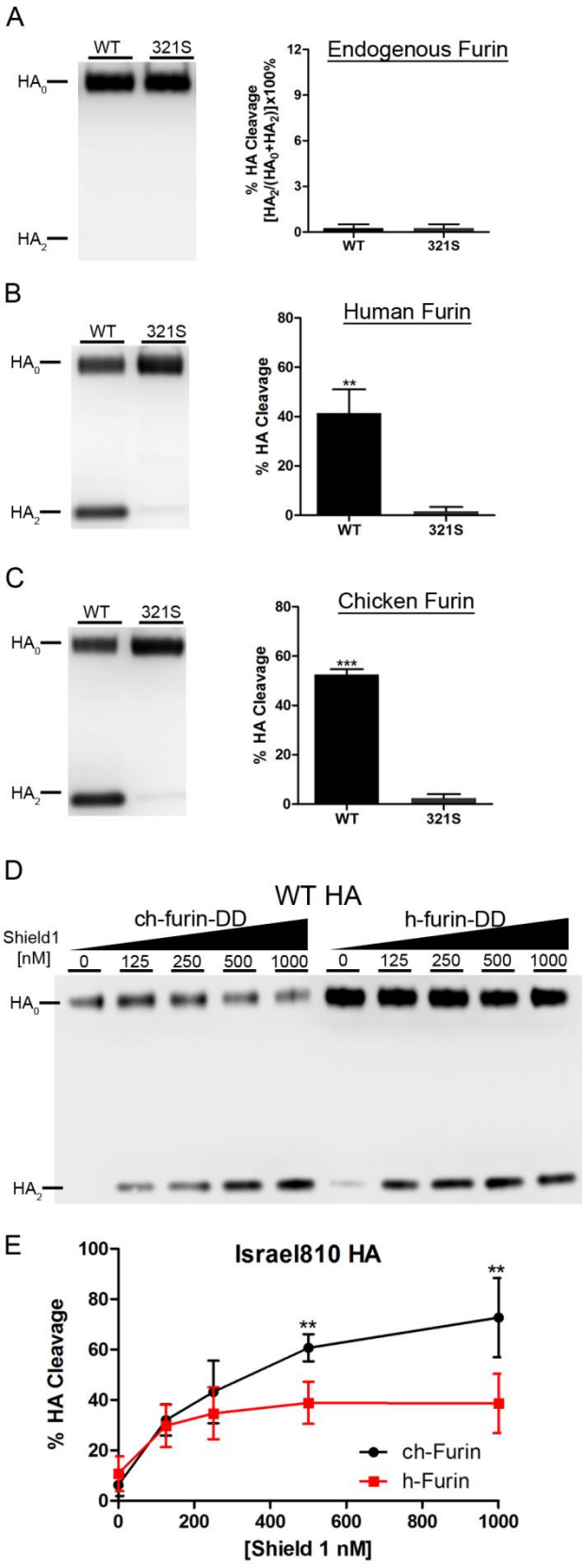
A
WT
321S
HA0
HA2
Endogenous Furin
% HA Cleavage
[HA2/(HA0+HA2)]x100%
12
9
6
3
0
WT
321S
B
WT
321S
HA0
HA2
Human Furin
% HA Cleavage
80
60
40
20
0
**
WT
321S
C
WT
321S
HA0
HA2
Chicken Furin
% HA Cleavage
80
60
40
20
0
***
WT
321S
D
WT HA
ch-furin-DD
h-furin-DD
Shield1
[nM]
0
125
250
500
1000
0
125
250
500
1000
HA0
HA2
E
Israel810 HA
% HA Cleavage
100
80
60
40
20
0
**
**
ch-Furin
h-Furin
0
200
400
600
800
1000
[Shield 1 nM]

3.2.4 Analysis of glycosylation sites close to the cleavage site of H9N2 HA

As furin-mediated cleavage of Israel810 HA was shown to occur, we examined possible ways for this process to be more efficient. We first assessed likely scenarios for increased cleavage site accessibility via loss of glycosylation. Three H9N2 isolates have mutations at the bottom of the stalk region of HA1, which accordingly eliminates the consensus, N-X-S/T motif for N-linked glycosylation (Fig. 3.3A). According to a homology model of Israel810HA generated by Swiss-Model (233, 234) and Glyprot (http://www.glycosciences.de/modeling/glyprot/php/main.php), and based on the crystal structure of A/Swine/Hong Kong/9/1998 H9N2 (PDB# 1JSD), Glycan 13 is very close to the HA cleavage site (Fig. 3.3B). Due to such close proximity, this particular glycosylation is likely to affect HA activation by sterically hindering protease accessibility to the HA cleavage site. An equivalent mutation was found on A/chicken/Pennsylvania/83 (H5N2), and was associated with increasing HA activation and thus, pathogenesis of the virus (171, 230). A similar mechanism has also been found on mouse-adapted influenza virus, with an increase in virulence of the virus (235). To further characterize this mutation in the context of H9 HA, we chose to characterize the T15P mutation that was found in two natural isolates, A/chicken/Iran/THLBM865/2007 and A/chicken/Guangdong/11/1999.

3.2.5 HA cleavage of Israel810HA ΔGlyco13 in 293T cells by endogenous protease(s)

From the previous data, the Israel810 R-S-K-R cleavage site is not able to cleave by endogenous furin (see Fig. 3.2A). We predicted that the loss of glycosylation site 13 (ΔGlyco13) would likely to enhance HA cleavage. To test the hypothesis, two constructs were made and tested following cell surface biotinylation of 293T cells. Western blot analysis showed that "Israel810HA Δ glycosylation 13" (WT ΔGlyco13) can be cleaved by endogenous protease(s) in 293T cells, with ca. 10% of its HA being cleaved which supported our hypothesis. In contrast 321S ΔGlyco13 remains intact in its uncleaved form in 293T cells (Fig. 3.3C). Cleavages of both ΔGlyco13 HAs are furin dependent, as over-expression of human or chicken furin increase the percentage of HA cleavage. WT ΔGlyco13 showed 80% and 90% HA cleavage by h-furin and ch-furin respectively, whereas 321S ΔGlyco13 showed 38% and 50% HA cleavage by h-furin and ch-furin respectively (Fig. 3.3D). In general, ch-furin showed slightly higher cleavage efficiency than h-furin on all the HAs tested (Figs.3- 2B, 3.2C, 3.3D).

Figure 3.3. Glycosylation site 13 affects HA cleavage in Israel810 HA. (A) Multiple sequence analysis of H9 HA. Sequence alignment and analysis were done as mentioned in Fig. 1A, amino acid 10 – 18 containing an N-linked glycosylation site (198) was shown. H9 HA consensus sequence is shown in bold font, underneath are three strains where a single mutation eliminate the potential glycosylation site. Strain names and their accession number are as follow: A/Chicken/Iran/THLBM865/2007 (ACY25800), A/Chicken/Guangdong/11/1999 (ACH95446) and A/Pheasant/Shantou/4709/2003(ABV48004). (B) Homology modeling of Israel810 HA by Swiss-Model based on A/Swine/Hong Kong/9/1998 H9N2 (PDB# 1JSD). Bottom of the stem region of HA monomer is illustrated in cartoon form, where HA_1 in green, HA_2 in cyan and fusion peptide in red. The P4 position of HA cleavage site (Arg319) is labeled in magenta and glycan (Glyco13) is illustrated as stick in standard CPK colors. The closest distance between Arg322 and Glycan13 is determined by PyMol as 5.4A. (C) HA cleavage of Israel810HA and Israel810HA-321S with a constellation of mutations T15P (∆Glyco13) by endogenous proteases in 293T cells. Representative western blot image of HA cleavage by surface biotinylation of Israel810HA-T15P (∆Glyco13) and Israel810HA-T15P-K321S (321S ∆Glyco13) in 293T cells. HA_0 and HA_2 bands were labeled as indicated. Quantification and statistical analysis of HA cleavage from the blot is shown on the right. Error bars represent 1 standard deviation (S.D.) from at least 3 independent experiments. Data were analyzed by one-tailed Student's t-test where * indicate $p<0.05$, ** $p<0.01$ and *** $p<0.005$. (D) Representation western blots and quantification of ∆Glyco13 and 321S ∆Glyco13 cleavage of transiently co-transfecting HAs and plasmids expressing h-furin and cf-furin into 293T cells. Error bars represent 1 S.D. from at least 3 independent experiments. Statistical analysis and notations were same as Fig. 3.2A.

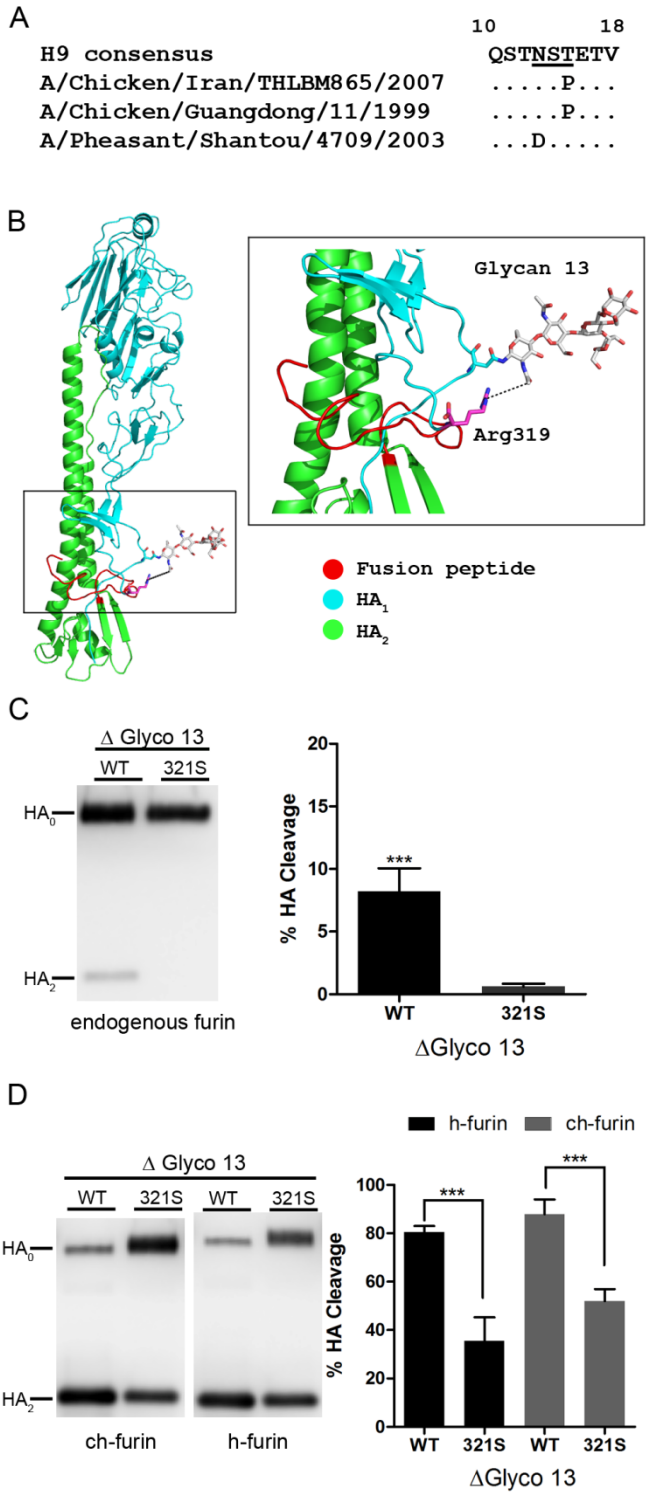
A
10 18
H9 consensus QSTNSTETV
A/Chicken/Iran/THLBM865/2007 .....P...
A/Chicken/Guangdong/11/1999 .....P...
A/Pheasant/Shantou/4709/2003 ...D.....
B
Glycan 13
Arg319
Fusion peptide
HA1
HA2
C
Δ Glyco 13
WT
321S
HA0
HA2
endogenous furin
% HA Cleavage
20
15
10
5
0
***
WT
321S
ΔGlyco 13
D
h-furin
ch-furin
Δ Glyco 13
WT
321S
WT
321S
HA0
HA2
ch-furin
h-furin
% HA Cleavage
100
80
60
40
20
0
***
***
WT
321S
WT
321S
ΔGlyco 13

3.2.6 Furin is responsible for cleavage of Israel810 HA

To confirm that the endogenous protease cleaving HA in 293T cells is furin, an siRNA knockdown assay was performed by co-transfecting WT ΔGlyco13 with siRNA targeting h-furin (sih-furin). Western blot data showed that sih-furin decreased the cleavage level from 13% (mock transfected) and 10% (non-targeting siRNA) to 2%, suggesting furin is the cellular factor that is responsible for HA cleavage in 293T cells (Figs. 3.4A, 3.4B). 321S ΔGlyco13 was used as a negative control of HA cleavage and showed no detectable HA cleavage in all three siRNA treatments (Figs. 3.4A, B). Control of knockdown was also examined by Q-RTPCR. The knockdown efficiency was ca. 50% when compared to the mock transfected control (Fig. 3.4C). Specificity of Q-RTPCR products were monitored in dissociation curves (data not shown) and the PCR products were run on 1% agarose gel for confirmation (Fig. 3.4C).

Figure 3.4. HA cleavage of WT ΔGlyco13 by endogenous furin in 293T cell. (A) Representative western blot image of HA cleavage by surface biotinylation in 293T cells. Pools of siRNA targeting h-furin (siFurin1-4), pools of non-targeting siRNA (siNon-target) and siRNA re-suspending buffer (simock) were co-transfected with WT ΔGlyco13 into 293T cells as described in Material and Methods. (B) Quantification and statistical analysis of HA cleavage from Fig. 3.4A. Error bars represent 1 S.D. from at least 3 independent experiments. (C) Verification of knockdown effect of furin after siRNA treatment. 2^{-DDCt} of human furin and h-GAPDH were determined by quantitative reverse transcript polymerase chain reaction (Q-RTPCR) normalized to mock treatment. On the right, the cDNAs of h-furin and h-GAPDH from qRT-OCR were evaluated on a 1% agarose gel. Error bars represent 1 S.D from 3 different experiments. Statistical analysis and notation are described as Fig. 3.2A.

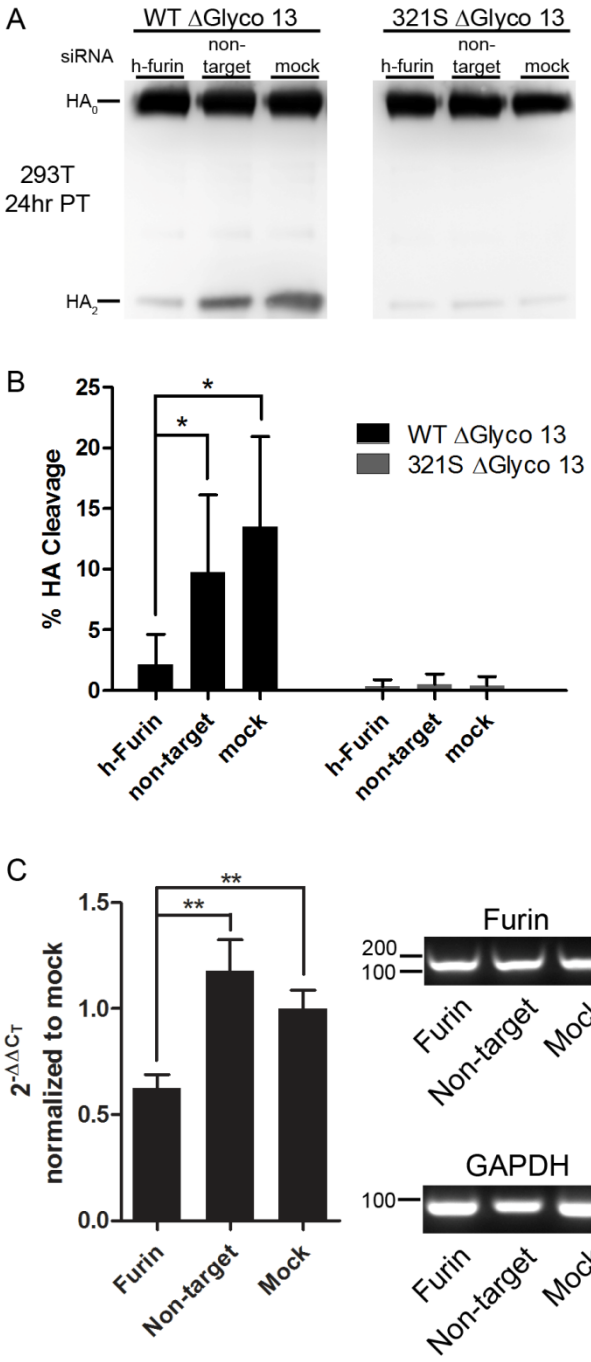
A
WT ΔGlyco 13
321S ΔGlyco 13
siRNA
h-furin
non-target
mock
HA0
HA2
293T
24hr PT
B
% HA Cleavage
WT ΔGlyco 13
321S ΔGlyco 13
h-Furin
non-target
mock
C
2-ΔΔCT
normalized to mock
Furin
Non-target
Mock
GAPDH
200
100

3.2.7 HA pseudovirus particles (PVs) are activated by endogenous furin

To confirm that HA cleavage results in a functional outcome for infection, a PV transduction assay was performed to indirectly quantify HA activation/fusion efficiency. PVs with influenza HA and NA on their surface were produced in 293T cells, and were used to infect MDCK cells. PV infectivity after different treatments is shown as relative light units (RLUs). Trypsin treatment, which activated all the PVs, was used as an internal control for the total amount of PV being produced. Fold differences between trypsin treatment and no treatment are indicated on top of each column pair in Fig. 3.5, and were used as an indirect measurement of HA activation efficiency. All the trypsin-treated PVs showed a high RLU value (10^7) indicating robust production and transduction of PVs of all the HAs tested. The no treatment group reveals a background level (10^3), which indicated no or very little activated particles. The fold difference of trypsin treated WT ΔGlyco13 is 4,400 times higher than no trypsin treatment. Although there is a 3 log difference for WT ΔGlyco13, it is slightly lower than the other 3 groups. The relatively low fold difference of WT ΔGlyco13 HA indicates it can be activated by endogenous furin slightly better than the other three HAs (Fig. 3.5A).

3.2.8 HA pseudovirus particles are activated by over-expression of h-furin and ch-furin

To test the functionality of HA activation under over-expression of h-furin and ch-furin, the PV infection assay was performed as described above, except that PVs were produced in 293T cells transiently transfected with either ch-furin or h-furin. Under both conditions, all four PVs are able to show high transduction level (10^5 – 10^7

RLU) after trypsin treatment, indicating successful production of PV (Figs. 3.5B, 3.5C). In general, the readings of PVs of the two ΔGlyco13 HAs are about 1 log lower than the WT HA. Of all the HAs we have tested, only 321S cannot be activated by overexpression of h-furin and ch-furin, reflected by low RLU values (10^3 – 10^4). WT ΔGlyco13 reveals 10^5 RLUs regardless of trypsin treatment, indicating all the PVs are activated before addition of trypsin. Furthermore, WT HA also shows a very little fold difference between trypsin treated or no trypsin treated conditions with 5.6-fold in h-furin and 14-fold in ch-furin. 321S ΔGlyco13 shows moderate level of activation by h-furin and ch-furin with 57-fold difference in h-furin and 510-fold in ch-furin.

Figure 3.5. Luciferase-based pseudoviral particles (PV) assay of Israel810HA and mutants produced in cells expressing either endogenous level or overexpressing ch or h-furin. (A) Quantitative HA mediated PV transduction assay in MDCK cells. Murine leukemia virus (MLV) based PV with HA and NA on the surface were produced in 293T cells described in material and methods. Harvested supernatant were either trypsin activated or mock activated before infecting MDCK cells. Infections were done in duplicates on MDCK cells for 2 days. Cells were lysed and relative light units (RLUs) were measured after addition of luciferin. Fold difference between trypsin and non trypsin treatments are shown on top of each column pair. Error bars represent 1 S.D. of 3 independent experiments. (B) Quantitative HA mediated PV infection assay in 293T cells expressing h-furin and (C) ch-furin. PV with HA and NA on the surface were produced in 293T cells overexpressing ch-furin and h-furin. Harvested PV was used to infect MDCK cells in duplicates and infection was monitored by RLU after addition of luciferin as described in Fig. 3.5A. Error bar represents 1 S.D. of 3 independent experiments. Statistical analysis was done as mentioned in Fig. 3.2A.

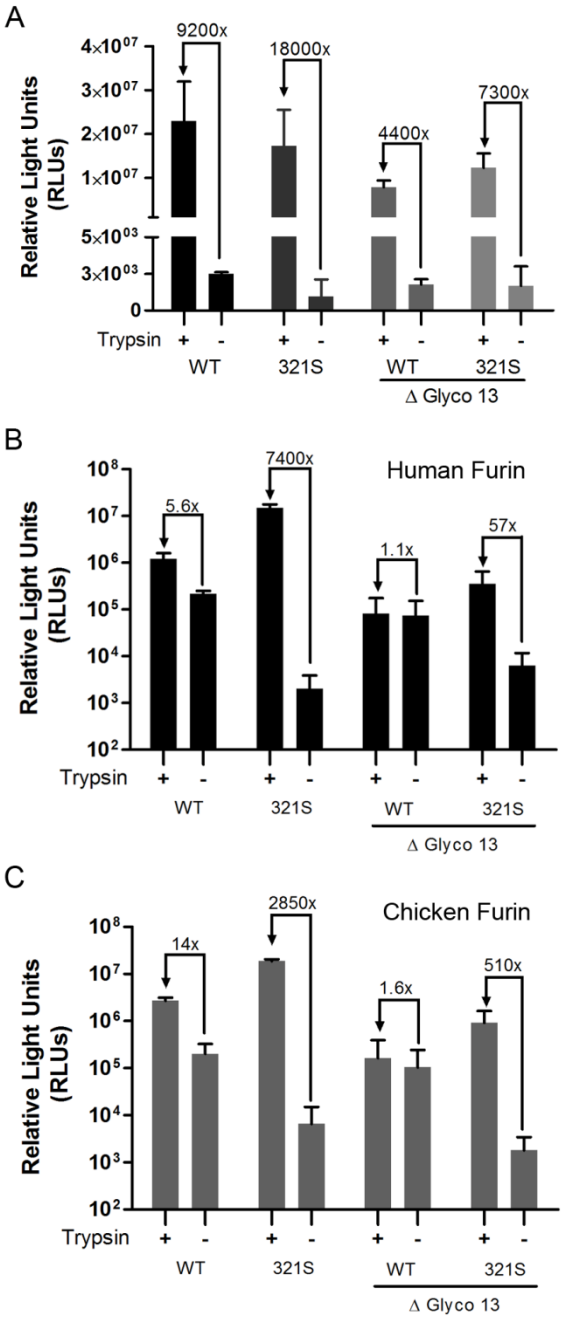
A
Relative Light Units (RLUs)
4×10^07
3×10^07
2×10^07
1×10^07
5×10^03
3×10^03
0
9200x
18000x
4400x
7300x
Trypsin + - + - + - + -
WT
321S
WT
321S
Δ Glyco 13
B
Human Furin
Relative Light Units (RLUs)
10^8
10^7
10^6
10^5
10^4
10^3
10^2
5.6x
7400x
1.1x
57x
Trypsin + - + - + - + -
WT
321S
WT
321S
Δ Glyco 13
C
Chicken Furin
Relative Light Units (RLUs)
10^8
10^7
10^6
10^5
10^4
10^3
10^2
14x
2850x
1.6x
510x
Trypsin + - + - + - + -
WT
321S
WT
321S
Δ Glyco 13

3.2.9 HA cleavage in avian cell lines correlates with furin expression level

H9N2 virus mainly infect avian species. Therefore to examine the cleavage of Israel810 HA in cell lines reflecting its natural tropism, we examined the HA activation pattern in different avian cell lines. We preformed surface biotinylation using chicken fibroblast (DF-1), quail fibroblast (QT-6) and chicken hepatocellular carcinoma (LMH) cells. Similar to 293T cells, all of the cell lines support HA cleavage of WT ΔGlyco13. QT-6, DF-1 and LMH allow 10%, 55% and 66% of HA cleavage respectively, as compared to 10% cleavage in 293T cells (Figs. 3.6A, 3.6B). None of the other three HAs were activated in these cell lines (Figs.3- 6A, 3.6B). The mRNA levels of furin relative to GAPDH of these avian cell lines were determined by quantitative-RTPCR (QRT-PCR) and were normalized to 293T cells. The reported 2^{-DDCt} values show that furin mRNA level of DF-1, QT-6 and LMH is 1-, 1.25- and 1.5-fold higher than 293T cells respectively (Fig. 3.6C). The cleavage efficiency correlates well with the relative mRNA level of furin in these cell lines.

Figure 3.6. HA cleavage by 3 different avian cell lines with various levels of furin expression. (A) Representative western blot image of HA cleavage by surface biotinylation of 3 different cell lines: Quail embryonic fibroblast (QT-6), chicken embryonic fibroblast (DF-1) and chicken primary hepatocellular carcinoma epithelial cell (LMH). (B) Quantification and statistic analysis of HA cleavage from Fig. 3.6A. Error bars represent 1 S.D. from at least 3 independent experiments. Statistical analysis and notations were described previously in Fig. 3.2A (C) Q-RTPCR analysis of relative expression of ch-furin mRNA to ch-GAPDH of the above cell lines. 2^{-DDCt} of ch-furin and ch-GAPDH were determined by Q-RTPCR and is normalized to 293T cells as references. Error bars represent 1 S.D from 3 different experiments starting from RNA extraction. Statistical analysis and notation are described as above.

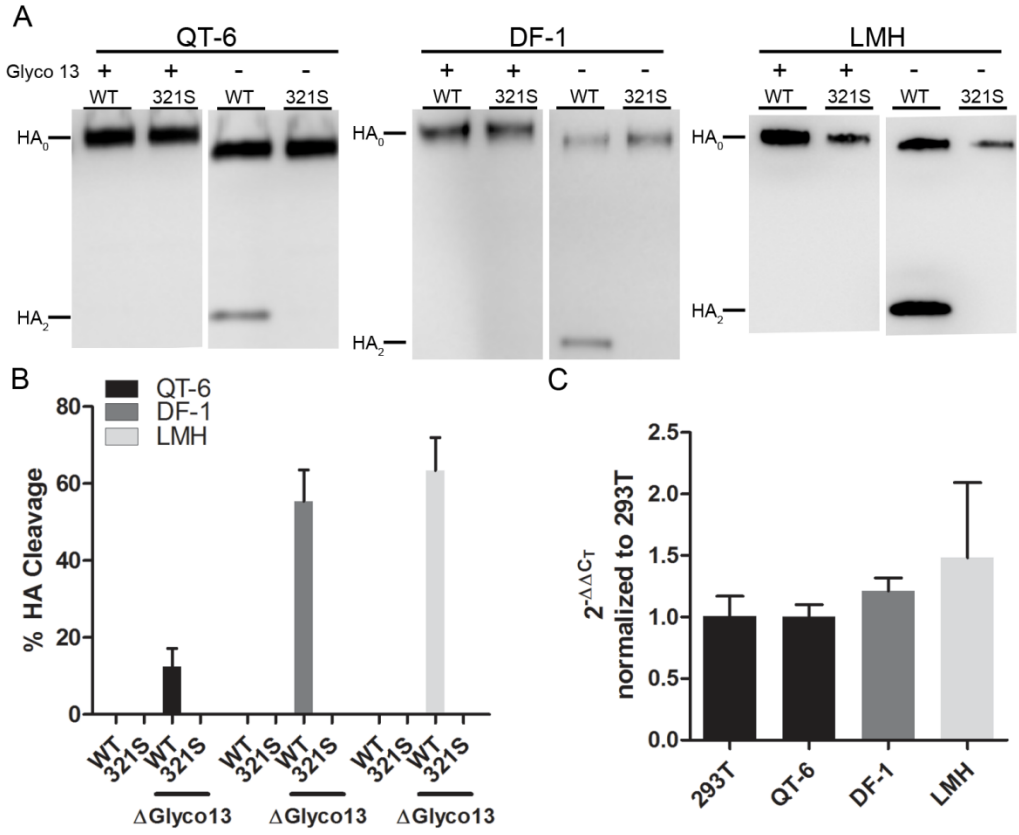

3.2.10 Substitution of the H9 cleavage site by HPAI H5 and H7 cleavage sites

Another possibility for increased HA cleavage is the insertion of additional basic residues in the cleavage site, as typified by H5N1 and H7N7 viruses. According to all the H9 HA sequences in the influenza database, H9 HAs have not been reported to contain any polybasic cleavage sites mimicking H5 or H7 HPAI. To test whether H9 HA is able to accommodate such modification, we substituted the original H9 cleavage site of Israel810 with H5 and H7 HPAI cleavage sites (Fig. 3.7A). Three constructs were made to mimic the H5N1 HPAI polybasic cleavage site (PB), the 11 amino acid insertion mimicking HPAI H7N3 isolated in British Columbia in 2004 (236) with a di-basic cleavage site (Insert+DB) or the same insertion with a tri-basic cleavage site (Insert+TB) (Fig. 3.7A).

Cell surface biotinylation and Western blot reveals that PB, Insert+DB and Insert+TB were all able to be cleaved by endogenous furin in 293T cells, in contrast to WT HA shown in earlier experiments (Fig. 3.7A). The cleavage efficiency varies on different constructs with Insert+TB with 85% being the highest HA cleavage efficiency. High efficiencies of HA cleavage, 58% and 56%, were also observed for PB and Insert-DB respectively (Figs. 3.7B, 3.7C). A Quantitative PV transduction assay was consistent with the biotinylation assays. In general, all constructs were able to incorporate into PV as shown in trypsin treated controls. PVs of PB and Insert+TB HA were completely activated with only 2.4x and 2.1x fold difference regardless of trypsin treatment. Insert+DB was activated by furin very well with only 180x fold difference between treatments. The small differences between treated and untreated sample for all the HAs indicated a trypsin independent activation mechanism similar to HPAI (Fig. 3.7D). Overall, the results of the PV assay

corresponded very well with the HA cleavage assay very well and demonstrates that H9 HA is able to accommodate all modifications found in HPAI.

3.2.11 H9 HAs with H5 and H7 HPAI cleavage sites affect PV infectivity

Multiple factors of the envelope glycoprotein including stability, expression level, rates of incorporation, receptor binding affinity and fusion activity affect PV transduction efficiency. Wild type Israel810 HA and ΔGlyco13 HA PV showed ~10^7 RLUs when transducing MDCK cells, indicating similar properties of both HAs at the level of virion (Fig. 7E). In contrast, all the PV with H5 and H7 HPAI mimicking HAs showed relatively lower readings of ~10^{4-5} RLUs when transducing MDCK cells. These drops in transduction efficiency suggest that such PVs infectivity is compromised (Fig. 7E) and indicate a decrease in viral fitness when compared to Israel810 HA and ΔGlyco13 HA.

Figure 3.7. Cleavage and activation of HPAI mimicking H9 mutants by endogenous furin. (A) Illustration of four Israel810HA mutants mimicking HPAI virus and their cleavage site sequences. Israel810HA WT sequence was illustrated in the two long boxes, below are the three HPAI mimicking HAs: Israel810HA-H5 polybasic (PB), Israel810HA-H7 insertion plus tre-basic site (Insert+TB) and Israel810HA-H7 insertion plus di-basic site (Insert+DB). (B) Representative western blot of the HPAI mimicking HA by surface biotinylation. (C) Quantification of HA cleavage in Fig. 3.7B. Error bars represent 1 S.D. from 3 independent experiments. (D) Quantitative HA mediated PV transduction assay of the HPAI mimicking HAs. PV with the HPAI mimicking HAs were produced as described in materials and methods. Harvested PVs were used to infect MDCK cells and luciferase activities were used as the indicator of transduction efficiency and HA mediated membrane fusion. Error bar represents 1 S.D. of 3 independent experiments. Statistical analyses and notations were done as mentioned in Fig. 3.5A. (E) Summary of RLUs of PV transduction in MDCK cells after trypsin treatment. Each value is deduced from their corresponding column from Fig. 3.5A and Fig. 3.7D and represents the mean of at least 3 independent experiments of PV transduction assay.

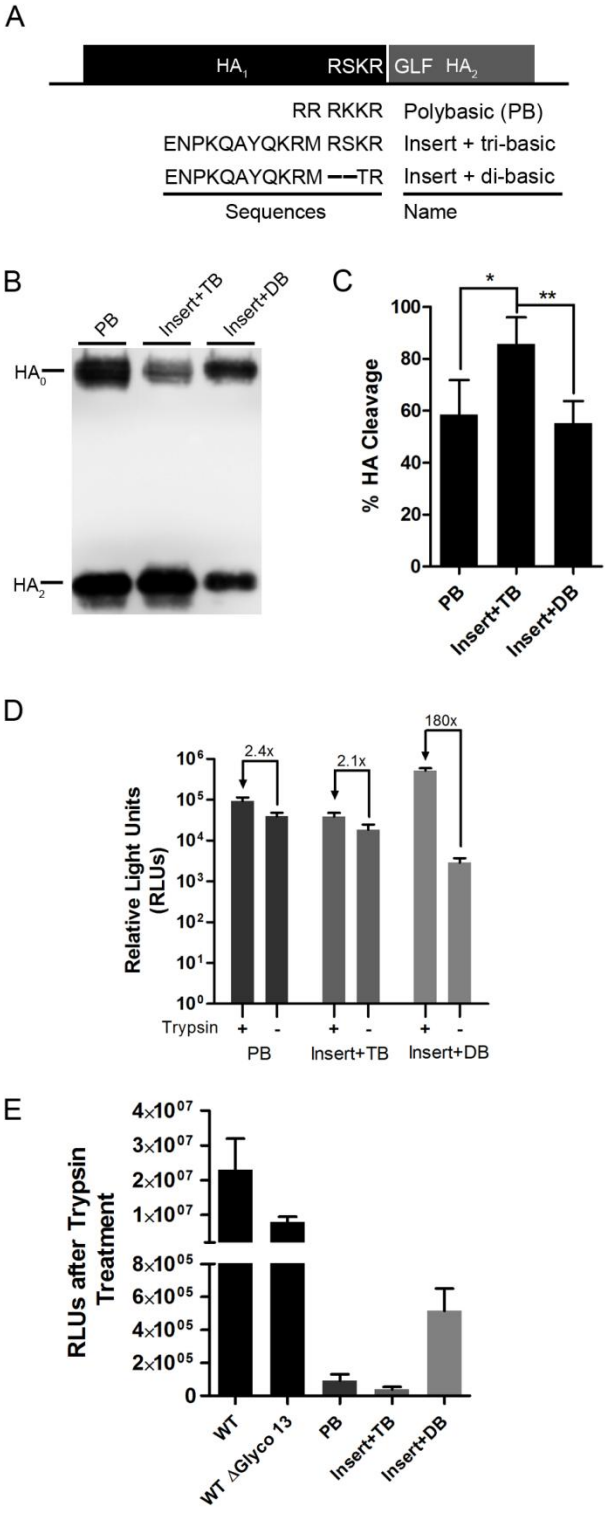
A
HA1
RSKR
GLF
HA2
RR RKKR
Polybasic (PB)
ENPKQAYQKRM RSKR
Insert + tri-basic
ENPKQAYQKRM --TR
Insert + di-basic
Sequences
Name
B
PB
Insert+TB
Insert+DB
HA0
HA2
C
% HA Cleavage
100
80
60
40
20
0
*
**
PB
Insert+TB
Insert+DB
D
Relative Light Units (RLUs)
2.4x
2.1x
180x
Trypsin
+
-
PB
Insert+TB
Insert+DB
E
RLUs after Trypsin Treatment
WT
WT ΔGlyco 13
PB
Insert+TB
Insert+DB

3.3 Discussion

In this manuscript, we focused on the cleavage activation of A/chicken/Israel/810/2001, an avian influenza with a distinct tri-basic cleavage site (R-S-K-R) that is predicted to be cleaved by furin, yet is not defined as highly pathogenic avian influenza (HPAI). A/chicken/Israel/810/2001 is representative of viruses with this cleavage site in an epizootic transmission of influenza in the poultry population of Israel between 2001 and 2005 (237). Other H9 viruses with tri-basic cleavage sites also meet a similar criteria for furin cleavability without classic HPAI definition (e.g. A/quail Shantou/2000 with a R-S-R-R cleavage site), however we chose to study A/chicken/Israel/810/2001 as it is representative of a distinct lineage of H9 viruses with an identical HA cleavage site (29 sequences isolated in Israel over the period 2001 - 2003). In contrast, quail/Shantou-like viruses with a R-S-R-R cleavage site have only been isolated very sporadically in the field (two isolations in China separated by more than ten years, in 2000 and 2011). In addition, an R-S-K-R sequence represents a slightly more optimized furin cleavage motif than R-S-R-R (Pitou scores of 9.14 and 8.97 respectively). We find that the HA of A/chicken/Israel/810/2001 can be cleaved by furin, with cleavage dependent on the Lys (K) residue adjacent to the cleavage site Arg (R). However, the efficiency of HA cleavage was only apparent under high furin expression conditions, with cleavage directly proportional to furin expression level in the cells. Notably, we find that removal of glycosylation site 13, a mutation already present in certain H9N2 field strains (e.g. A/chicken/Iran/THLBM865/2007), leads to the efficient activation of A/chicken/Israel/810/2001 by endogenous furin, showing the potential for a defined constellation of mutations that impact HA activation. Given the geographical proximity

in the source of these two virus strains in the Middle East, our data highlight the possibility of novel H9 viruses emerging in the field, with increased pathogenicity.

Previous studies have characterized the cleavage activation of H9 viruses with tri-basic vs di-basic cleavage sites (i.e. quail/Shantou) and have shown cleavage of HAs with both cleavage site types by human respiratory proteases (matriptase, TMPRSS2, HAT), but not by furin (226). It remains to be determined whether an R-S-R-R or R-S-K-R sequence is interchangeable from the perspective of furin cleavage under over-expression conditions and the ability to integrate with glycosylation site changes. The highly similar (although not identical) furin prediction scores for the two sequences indicate that both would behave in an equivalent manner. It is unclear why viruses with a R-S-K-R cleavage site, compared to R-S-R-R, have been found to circulate more widely in nature; this could be due to other changes in HA or other genes, or due to poultry production practices in different locations.

Despite the ubiquitous expression of furin, expression levels vary in different cell types, which can be an important determinant for viral infection. As shown for infectious bronchitis virus (IBV), the level of furin in cells can be a determining factor of their susceptibility to infection (238). Furin levels can also be altered by different triggers. Furin promoter can be up-regulated by 3-fold and 400-fold under hypoxia and iron depletion conditions, respectively (223, 239), which is similar if not higher to the level of expression produced in our experiments. Also, viral infection, including H5N1 HPAI, induces a transcription factor, hypoxia-inducible factor 1 (HIF-1), which positively regulates expression of multiple genes, including furin (240). Furthermore, bacterial infections, such as *Staphylococcus sp.* (241) and *Pseudomonas sp.* (242) which are prevalent in farmed poultry, can also induce HIF-1 and subsequent furin

expression. Such induction may allow an unusually high level of furin to activate HA containing R-S-K-R or R-S-S-R cleavage sites that are inert to furin cleavage under normal circumstances. This may also explain the higher mortality and morbidity rate of H9N2 in farmed poultry than in specific-pathogen-free chickens. The expression level of furin also varies among tissues, with kidneys being one of the tissues with relatively high expression of furin, and may account for the rare event of H9N2 being able to be nephrotropic (243-245).

Avian influenza viruses are grouped into two main categories: LPAI and HPAI. Transition from LPAI to HPAI is thought to be through series of mutations within the viral genome. Although some hallmark mutations of HPAI have been characterized including a polybasic cleavage site for H5 and a cleavage site insertion of H7, the evolution pathway of H9 viruses to become more pathogenic has yet to be fully determined. Over the past decade, several H9N2 outbreaks have shown some intermediate viruses that are certainly more pathogenic than generic LPAI but below the threshold of being HPAI (213-215, 219). These viruses may serve as intermediates of the H9 evolutionary pathway, allowing the virus to evolve and become more pathogenic. From our data, we show that constellation of mutations N15T and S321K, allows HA to be activated by endogenous furin. Our data and other previous reports suggest that H9 HA is able to accommodate a polybasic site or an 11 amino acid insertion and still be functionally cleaved by endogenous furin. However, such dramatic changes of H9 HA seem to be deleterious at the level of virion. From our pseudovirus transduction assays, we noticed big drops in PV infectivity (~ 1 to 2 logs in RLUs) of these HAs compared to the WT Israel810 HA which indicate a decrease in viral fitness. This observation may contribute to

explaining the puzzling observation that an insertion of a polybasic cleavage site in H9 HA that does not convert the virus to HPAI. Our study suggests that a better characterization at molecular level of influenza virus would help understand the broad spectrum of avian influenza virulence. For instance, introducing terms such as moderately pathogenic avian influenza (51) for viruses which are more pathogenic than LPAI and show biological features associated with high virulence, but do not meet the specific requirements of HPAI set by the OIE. Our studies illustrate that some MPAI, especially H9N2 influenza viruses, require a more thorough examination than just bioinformatics analysis.

HPAI is a generalized phenotype determined by series of complex genotypic changes in influenza virus. HPAI can arise through different combinations of mutations, therefore, it is predicted that a single mutation would not allow the virus to become HPAI. As shown by other groups, insertion of a polybasic site in H9 HA is not enough to convert the virus from LPAI to HPAI (227, 246). Our results indicate that efficient cleavage activation of an H9 HA by endogenous furin can be achieved by a combination of a tri-basic cleavage site (R-S-K-R) and a loss of a glycosylation site at HA1 residue 13. Each of these features are found individually in nature and our data show that the combined changes can be tolerated by the HA protein in terms of folding, stability and formation of particles. Whether this mutation combination translates into a highly pathogenic virus remains to be tested. Such studies should only be carried out under highly prescribed biosafety conditions and with appropriate administrative oversight. At present, our work is of importance in the context of influenza pandemic planning.

3.4 Acknowledgments

The authors thank Jean K. Millet, Xiangjie Sun and all the members in the Whittaker Lab for helpful discussions. We would also like to thank the Collins Lab for helpful suggestions throughout the study.

These studies were funded by the United States Department of Health and Human Services contract HHSN266200700008C (NIAID Centers of Excellence for Influenza Research and Surveillance). Work in the author's laboratory is also supported by a research grant from the National Institutes of Health (R01 AI48678).

CHAPTER 4

MODIFICATION OF THE HEMAGGLUTININ CLEAVAGE SITE ALLOWS INDIRECT ACTIVATION OF AVIAN INFLUENZA VIRUS H9N2 BY BACTERIAL STAPHYLOKINASE

Abstract

Influenza H9N2 is considered to be a low pathogenicity avian influenza (LPAI) virus that is found to infect both chickens and, to a lesser extent, humans. In 1996, the influenza virus, A/chicken/Korea/MS96-CE6/1996/H9N2 (MS96) was isolated from an outbreak in multiple farms in South Korea that resulted in upwards of 30% mortality in infected chickens. Furthermore, the virus was found in a number of organ tissues, indicating internal spread of the virus. However, complete recovery of specific pathogen free (SPF) chickens occurred after 3 days post infection with the MS96 virus. We hypothesize that bacterial co-infection may play a significant role in the drastic difference in disease progression between farmed and SPF chickens. A key determinant of influenza pathogenesis is the susceptibility of the viral hemagglutinin (HA) to proteolytic cleavage/activation. Here, we identified that an amino acid substitution, Ser to Tyr at the P2 position of the HA cleavage site optimizes cleavage by the protease plasmin (Pm). We also identified that certain *Staphylococcus sp.* are able to cleave/activate MS96 HA by activating plasminogen (Plg) to Pm by use of a virulence factor, staphylokinase (sak). Overall, these studies provided insight into the bacterial mediated enhancement of influenza virus infection and pathogenesis.

4.1 Introduction

Each year, influenza related illnesses cause 250,000 to 500,000 deaths and economical loss equivalent to 27 to 87 billion US dollars (9). In rare situations, two or more influenza viruses exchange their RNA genomes by antigenic switching and lead to emerge of novel pandemic influenza virus (41). For instance, the 2009 pandemic virus arose from quadruple reassortment between birds, pigs and humans influenza viruses and caused 71 to 167 billion USD of economical loss (18, 19). Zoonotic transmission of animal influenza to humans is also an important public health concern. Avian influenza virus (AIV) is on the top of the zoonotic transmission lists as modern human practices in the poultry industry provide an efficient way for close contact between humans and poultry. Indeed, increasing cases of humans infected by AIV have been reported, including transmission of both highly pathogenic avian influenza (HPAI) H5N1 and low pathogenic avian influenza (LPAI) H9N2. Furthermore, AIVs were involved in three out of four pandemic influenza outbreaks from the last century, indicating the tight link between pandemic and avian influenza viruses (67).

Influenza virus requires activation before infection and activation efficiency is an important determinant of viral virulence. The process of virus activation involves proteolytic cleavage on the viral envelope protein, hemagglutinin (HA) by host proteases. After cleavage, the precursor protein HA_0 is separated into HA_1 and HA_2 which is a required for successful viral entry. HA_1 binds to sialic acid on the surface glycoprotein receptor on host cells. After the virus binds to the host surface, it is internalized by receptor mediated endocytosis and deposited into the endosomal compartment (65). During endosomal maturation, the pH drops inside the endosomal lumen, which triggers HA to undergo a conformational change. After the

conformational change, the fusion peptide on HA_2 extends out and inserts into the endosomal membrane. After a series of conformational changes on HA, the endosomal and viral membranes merge and allow pore formation to release the viral ribonucleoprotein (vRNP) into cytoplasm. The strict requirement of HA cleavage restricts influenza infection to the upper respiratory tracts of humans and chickens as well as the intestinal tracts of waterfowl whereas specific proteases for HA activation are available. Therefore, protease usage for HA activation can also determines influenza tropism.

Proteases for HA activation are not limited to eukaryotic proteases, bacterial proteases are also involved in this process. For instance, *Staphylococcus sp.* and *Aerococcus viridians* secrete soluble proteases that are able to activate HA (173). *Pseudomonas aeruginosa* also indirectly activates HA by activating host proteases (173). Furthermore, bacterial streptokinase (skc) and staphylokinase (sak) are also able to activate eukaryotic plasminogen into plasmin which can then activate HA (194, 247).

Here, we study the HA cleavage properties of a LPAI AIV A/Korea/MS96-CE6/1996/H9N2 (MS96), which caused a high mortality rate in farmed chickens. MS96 has a Ser to Tyr mutation at the P2 position of the HA cleavage site, an equivalent mutation that is found in a neurotropic influenza A/WSN/1933/H1N1 (WSN). Such a mutation allows WSN to use cellular plasmin for activation. Similarly, MS96 HA allows plasmin-mediated HA cleavage, however, different from WSN, the activation mechanism of MS96 HA is independent of viral neuramindase (NA). We were able to show that MS96 virus uses a different activation mechanism by using bacterial sak to indirectly activate HA in the presence of chicken plasminogen (ch-Plg). A three way interactions between bacteria, the virus and the host potentially

explains the discrepancy in clinical outcome between farmed and SPF chickens during MS96 infection.

4.2 Results

4.2.1 Variation of P2 position of HA cleavage site in H9 HA

A multiple sequence alignment of full length influenza H9 HA from the NCBI database reveal a consensus HA cleavage site R-S-S-R of H9 HA. (Fig. 4.1A) The cleavage site sequence and the first 22 amino acid of the fusion peptide of several representative strains of H9N2 viruses are also shown. (Fig. 4.1A) The cleavage site of H9HA is highly conserved except the P2 position showing a high variability as depicted by Weblogo. (Fig. 4.1B) Viruses containing a P2 substitution are summarized, where glycine (Gly, G), aspartic acid (Asp, D) and asparagines (Asn, N) are the top three amino acids which replace the consensus P2 serine. (Fig. 4.1C) Three particularly interesting strains, chicken/Korea/MS96-CE6/1996 (MS96), chicken/Korea/GH2/2007 and ostrich/South Africa/9508103/1995 have a equivalent P2 Ser to Tyr mutation resembling the neuro-replicative mouse adapted strain A/WSN/1933.

Figure 4.1. Bioinformatic analysis of influenza H9N2 HA cleavage site. (A) Multiple sequence alignment of full length H9N2 HA from NCBI influenza database (http://www.ncbi.nlm.nih.gov/genomes/FLU/FLU.html). A total of 1057 sequences were aligned by MUSCLE alignment program. HA Consensus sequence from the P6 residue of the cleavage site through the first 22 amino acids sequence of the fusion peptide are shown in bold. Representative strains are shown underneath the consensus whereas differences are shown in single letter amino acid code. Accession numbers of the representative strains are as follows: A/duck/Hong Kong/W213/1997 (BAG72217), A/chicken/Hong Kong/G9/1997 (AAF00701), A/turkey/Wisconsin/1/1966 (BAA14335), A/chicken/South Korea/MS96-CE6/1996 (ACZ48628), A/chicken/South Korea/GH2/2007 (ADV36582) and A/ostrich/South Africa/9508103/1995 (AAQ04843). (B) Amino acids frequency at HA cleavage site. Frequencies of each position, from P6 to P3' of the H9 HA cleavage site are illustrated using WebLogo 3.0 (http://weblogo.threeplusone.com/). (C) Summary of P2 position variation of H9 HA. A numerical summary of the variation in the P2 position from 1057 H9N2 strains.

A

	Cleavage site P2P1 P1′	Fusion peptide
H9 consensus	**-PARSSR**	**GLFGAIAGFIEGGWSGLVAGWYG-**
A/Turkey/Wisconsin/1/1966	..V...	.....
A/Duck/Hong Kong/W213/1997	.....	.....
A/Chicken/Hong Kong/G9/1997	.....	.....
A/Chicken/South Korea/MS96-CE6/1996	..A.Y.	.....P.....
A/Chicken/South Korea/GH2/2007	..A.Y.	.....P.....
A/Ostrich/South Africa/9508103/1995	..A.Y.	.....P.....

B

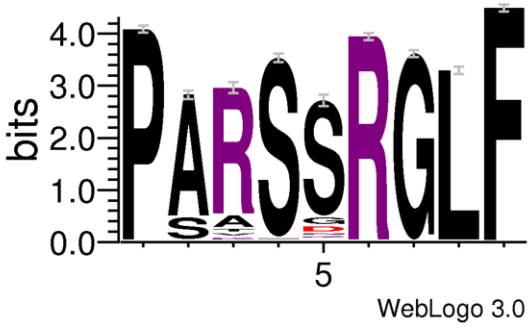

C

P2 Position	
Serine (S)	982
Glycine (G)	76
Aspartic acid (D)	59
Asparagine (N)	28
Lysine (K)	25
Tyrosine (Y)	8
Alanine (A)	7
Others	5

4.2.2 Chicken plasmin (ch-Pm) mediated cleavage of MS96 HA

To determine whether the MS96 HA tyrosine mutation optimizes HA for plasmin cleavability, MS96 HA was cloned into a mammalian expression vector and a mutant with a single substitution at the P2 position back to consensus serine was constructed. Cells expressing MS96 HA or MS96 HA-337S mutant were treated with increasing concentration of ch-Pm (100 mU/ml) for 30 min (Materials and Methods). Cell surface HA was detected by biotinylation and western blot. Western blot analysis reveals that MS96 HA is efficiently cleaved in a time dependent manner by ch-Pm. After 60 min of treatment with ch-Pm, about 15% of MS96HA WT is cleaved. In contrast, MS96 HA-337S does not show any significant cleavage with the highest being 5% after 60 min of ch-Pm treatment (Figs. 4.3a, b). MS96 HA cleavage by trypsin (3 μg/ml) is decreased from 50% to 40% compared to MS96 HA-337S indicating that a tyrosine residue at position 337Y selects for an alternative protease and slightly comprises the use of original protease for activation (Fig. 4.3b).

Figure 4.2. Chicken plasmin mediated A/Chicken/MS96-CE6/19966 (MS96) HA cleavage is dependent on 337Y. (A) HA cleavage of MS96 HA and MS96 HA-337S by ch-Pm. Surface biotinylation was performed on 293T cells expressing each HA. Transfected cells were treated with human ch-Pm (5 μg/ml) at the indicated time and cleavage product(s) were detected by western blot using anti-C9 antibody. (B) Quantification of the time-dependent ch-Pm mediated HA cleavage efficiency MS96 HA and MS96 HA-337S. The error bars represent the standard deviation of three independent experiments. Statistics were performed using a Student's t-test (unpaired, one-tail) by GraphPad Prism, comparing each individual treatment time (* $p<0.05$, ** $p<0.005$, *** $p<0.0001$).

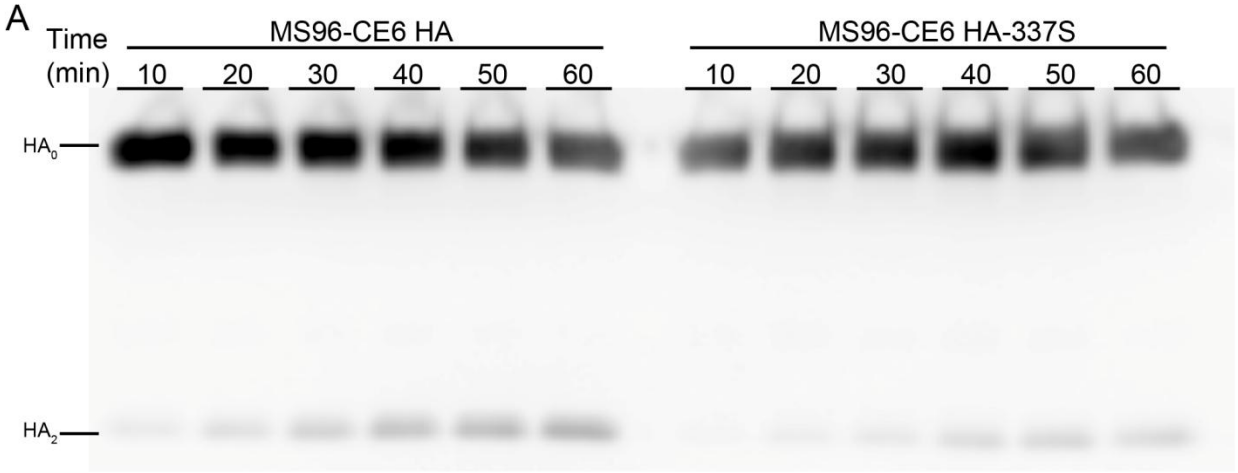

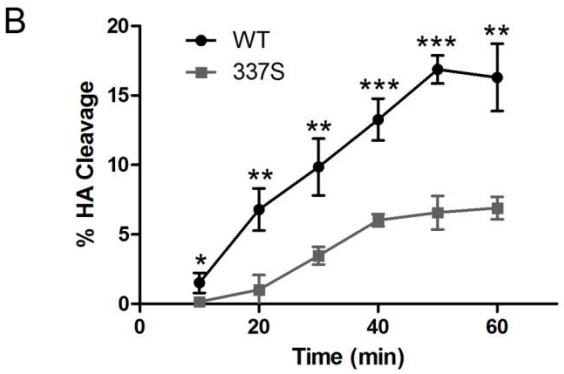

4.2.3 Plasminogen mediated cleavage of MS96HA requires plasminogen activators

A hallmark of the WSN virus is the additional NA-N146R mutation on the viral neuraminidase, which destroys a glycosylation site and allows plasminogen recruitment to the viral surface. The recruited plasminogen is then activated into plasmin and cleaves HA subsequently with an unknown mechanism which likely to involve tissue plasminogen activator (tPA) on the cell surface. To determine if MS96 NA performs a similar function as WSN NA in recuiting plasminogen and activating its cognate HA, cells expressing both MS96 HA and either MS96 NA or WSN NA were treated with ch-Plg (5μg/ml) for 18h. Biotinylation and western blot analysis shows HA cleavage of MS96HA WT only in the presence of WSNNA with about 40% of HA cleavage (Figs. 4.3a, b). This result suggests both a P2 tyrosine and a plasminogen recruiter are required for HA activation, which is independent of MS96 NA.

Figure 4.3. HA cleavage of MS96 HA by chicken plasminogen (ch-Plg) independent from its cognate neuraminidase. (A) Representative western blot picture of surface biotinylation after co-transfecting MS96 HA with MS96 NA or WSN NA in the presence or absence of ch-Plg (5 μg/ml) for 18h.

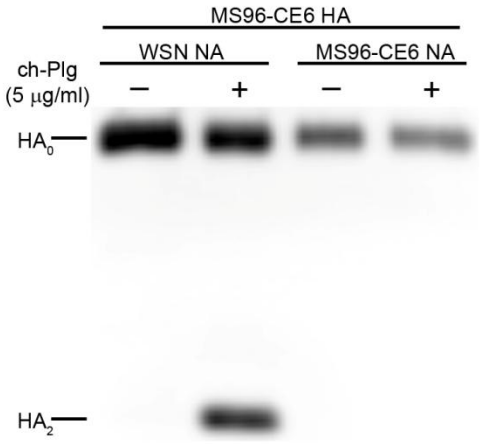

4.2.4 The bacterial co-factor staphylokinase (sak) indirectly cleaves MS96HA

In search of plasminogen recruiter and activator for MS96 HA, we hypothesized that an alternative source of activated plasminogen could be produced from co-infecting bacteria, either staphylokinase (sak) from *Staphylococcus sp*. or streptokinase (skc) from *Streptococcus sp*.. Both WT and mutant MS96 HA were transfected into 293T cells for surface biotinylation. Ch-Plg (5 μg/ml) was incubated with sak (10 μg/ml) or skc (5 μg/ml) for 1 hr at 37^{o}C for activation prior to treatment. Transfected cells underwent different treatments as indicated, western blot analysis reveals HA cleavage, ~ 35% when MS96 HA is incubated with both ch-Plg and sak. No significant HA cleavage was detected from any other treatments. Another bacterial plasminogen activator, skc, shows very weak activity on ch-Plg mediated HA cleavage. (Data not shown)

Figure 4.4. **Staphylokinase (sak) from *Streptococcus aureus* allows ch-Plg mediated HA cleavage of MS96 HA.** (A) Surface biotinylation was performed as mentioned above. 293T cells were transfected with MS96 HA and MS96 HA-337S and treated with different proteases as indicated for 1h. Cleavage products were detected by western blot using anti C9 antibody. (B) Quantification of the Staphylokinase/plasminogen (Skc-Plg)-dependent HA cleavage efficiency. Cleavage efficiencies were calculated. The error bars represent the standard deviation of three independent experiments, and statistics were performed as in Fig. 4.2.

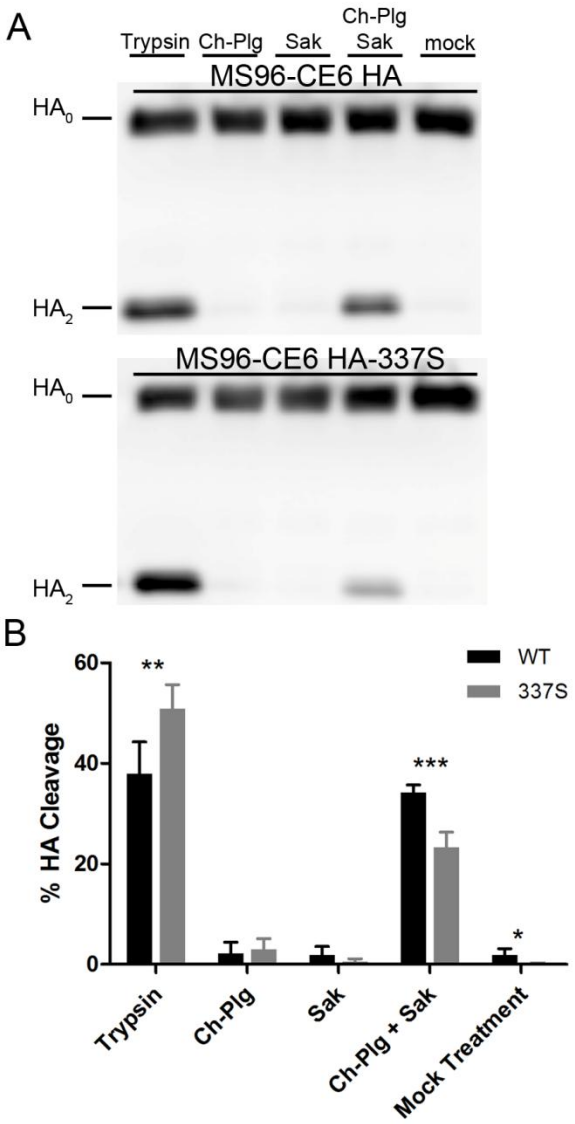

4.2.5 Ch-Pm and Plg mediated HA cleavage is functional and activates the virus

From western blot analysis, it clearly showed that MS96 HA is cleaved by ch-Pm. Nevertheless, a functional assay was needed to confirm that the cleavage is at the correct position and activates the virus. We used a surrogate pseudovirus system from mouse leukemia virus (MLV) to produce influenza pseudoviral particles (PV). MS96 HA, NA along with MLV-Gag-pol, pTG-Luc are co-transfected into 293T cells for 48 hr (Materials and Methods). The harvested PVs were treated differently as indicated and the treated PVs were used to infect MDCK cells. Luciferase activities were assayed after 2 days post-transduction by lysing the MDCK cells with cell lysis buffer. PVs infection is measured by reading of luciferase activities monitoring as an indirect method to assay functional HA activation. The data agree with HA cleavage results by western blot analysis whereas PV is activated after incubation with ch-Plg and sak. HA cleavage is also dependence on P2 tyrosine as MS96 HA-337S PV did not show significant activation. We also tested another bacterial co-factor streptokinase (ska) and showed very little HA cleavage or activation suggesting a bacterial specific HA activation mechanism in MS96 virus (Data not shown).

Figure 4.5. Luciferase-based pseudoviral particles (PV) assay of MS96 HA and MS96 HA-337S produced in 293T cells. Quantitative HA mediated PV transduction assay in MDCK cells. Murine leukemia virus (MLV) based PV with HA and NA on the surface were produced in 293T cells described in material and methods. Harvested supernatant were underwent different treatments as indicated before infecting MDCK cells. Infections were done in duplicates on MDCK cells for 2 days. Cells were lysed and relative light units (RLUs) were measured after addition of luciferin. Error bars represent 1 S.D. of 3 independent experiments.

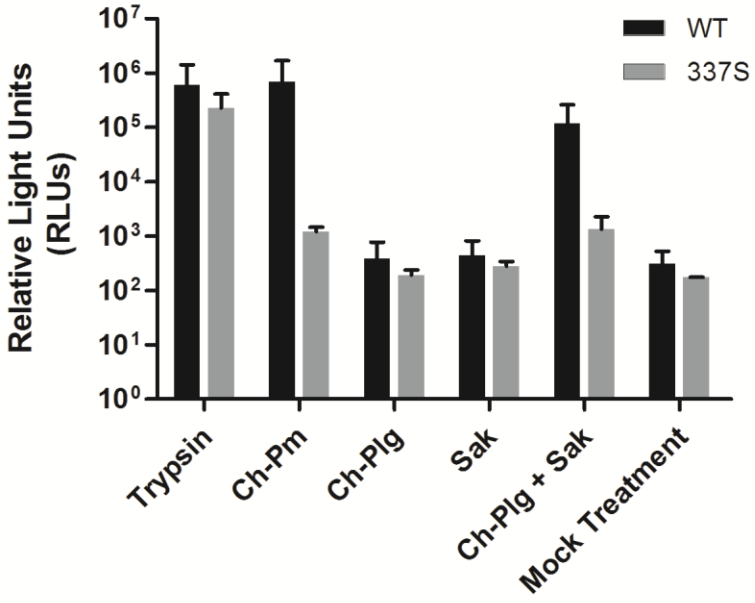

4.3 Discussion

The MS96 virus was first isolated in poultry farms in an outbreak in South Korea in 1996 (213). MS96 virus was able to spread into four local farms and infecting mainly the pullets in these farms. Mortality of chickens infected with MS96 is moderately high with a rate of 30%. Clinical symptoms of MS96 infected chickens include diarrhea, facial edema and drop in egg production to 0% (248). Necropsy of dead chickens revealed swollen kidney with urate deposit and atrophic and ruptured ova (249). The MS96 virus was found inside lung, kidney and feces from infected chicken, an indication of internal spread of the virus. However standard pathogenicity testing of MS96 in 6 weeks old specific-pathogens-free (SPF) chicken in a laboratory setting revealed no mortality and MS96 was hence characterized as an LPAI (248). The discrepancy between farmed chickens and SPF chickens is unclear. Our data suggested that bacterial co-infection may play a significant role in the dramatic increase in virulence of MS96 in farmed chickens compared to SPF chickens.

The MS96 HA is activated by ch-Pm efficiently activated and the process is dose dependent and required the S337Y mutation. Differing from WSN, the MS96 HA used a totally different mechanism for its HA activation independent of the viral NA. MS96 HA hijacks sak, a co-factor from *Staphylococcus sp.* to activate ch-Plg to ch-Pm and allow HA activation. This process between MS96 and *Staphylococcus sp.* is species specific as a similar bacterial co-factor skc from *Streptococcus sp.* shows a very weak activity. Such species specificity of MS96 virus and *Staphylococcus sp.* could possibly be explained by the inability of skc in activating ch-Plg. Results from the pseudovirus (PV) assay agree with the western blot findings by showing sak-dependent ch-Plg mediated PV activation. Together, out findings provide evidence for *Staphylococcus sp.* and MS96 synergy in the actual infection in South Korea in 1996.

In most cases, influenza viruses overcome the tropism restrictions by mutating the HA cleavage site to utilize other unconventional proteases for activation without interacting with other pathogens. For instance, highly pathogenic avian influenza (HPAI) is able to replicate systemically in animals by acquiring mutations at the cleavage site which allow a ubiquitous protease (furin) for activation (151). Furthermore, WSN, the neurovirulent mouse-adapted strain of influenza, gains its tropism in brain tissue by alteration of HA cleavability by using plasmin (148). In our study, we show that MS96 not only interacts with the host, but also with other pathogens to setup a unique activation mechanism. Furthermore, we reported AVI presumably co-evolves with bacteria and acquires help from bacteria to activate its own HA.

Ideally, challenge experiments in chickens need to be performed to support our hypothesis of the influenza-bacteria synergism via interaction between viral HA, bacterial sak and ch-Plg. These experiments would also allow us to determine the internal spreading of virus inside of infected chicken by determining whether viruses can disseminate throughout the body with the help of bacteria. Co-inoculation of MS96 and *Staphylococcus aureus* with an isogenic control of *Staphylococcus aureus ⊿sak* in chicken could also be performed.

4.4 Acknowledgments

The authors thank Xiangjie Sun, Sandrine Belouzard, Brian S. Hamilton, Tama Friling, Jean K Millet and all the members in the Whittaker Lab for helpful discussions. We would also like to thank the Collins Lab for helpful suggestions throughout the study. These studies were funded by the United States Department of Health and Human Services contract HHSN266200700008C (NIAID Centers of Excellence for Influenza Research and Surveillance). Work in the author's laboratory

is also supported by a research grant from the National Institutes of Health (R01 AI48678).

CHAPTER 5

DISCUSSION, FUTURE DIRECTION AND CONCLUSION

5.1 Discussion

In the 1970s, Dr. Lazarowitz and colleagues discovered that influenza viruses require proteolytic cleavage by cellular proteases to initiate successful infection (194). The finding was followed by the identification of multiple host and bacterial proteases involved in HA activation. However, the localization of many of these proteases does not match the natural tropism of influenza viruses. After almost 40 years, in 2006, the discoveries of tryptase Clara, TMPRSS2 and HAT have shed light on a group of physiologically relevant proteases involved in HA activation (156, 157, 161). Instead of searching for other protease candidates involved in HA activation, my studies focus on the mechanism of proteolytic activation by these proteases to activate HA in a clinically relevant setting. Through a series of experiments, I was able to dissect out three distinct mechanisms of HA activation that requires interplay between virus, bacteria and host.

Since influenza activation is the first step to initiate successful viral infection, it is tightly associated with viral pathogenesis and is an important determinant of viral tropism and growth kinetics. A single mutation at the HA cleavage site is sufficient to alter protease usage or expand the repertoire of protease usage. Using cell surface biotinylation, I was able to accurately determine the activation status of HAs on cell surface after protease treatments. Such technique allowed me to characterize a Ser to Tyr mutation at the P2 position of the HA cleavage site on a human pandemic virus that allows Pm to become an alternative protease for activation. After the initial characterization, I decided to study the underlying mechanism of Pm usage by this HA. Knowing that Plg is the physiologically relevant form of the protease, I focused

my study on how Plg gets activated and how it is used by the virus. By employing flow cytometry in my study, a technology applied extensively in immunology, I discovered that influenza HA can recruit Plg on the cell surface. Since tPA is a membrane bound protein, the recruited Plg gets activated into Pm allowing HA activation to occur. To my surprise, recruitment of Plg is a general property of influenza HAs suggesting a broad usage of such mechanism for other influenza viruses. To my knowledge, this is the first reported case of influenza HA actively recruiting a protease to facilitate its own activation.

Similarly to most of biological processes, other pathways may also be involved in Plg-mediated HA cleavage. Instead of searching for other eukaryotic proteins, I turned my focus to bacterial proteins and found that skc, a co-factor produced by *Streptococcus sp.* is involved in this process by directly activating Plg.

Bacterial co-infection with influenza has always been associated with complications of influenza related illness. The synergistic effects between two the pathogens are under active research. For instance, lung samples from patients who died from the 1918 “Spanish flu“ show signs of extensive bacterial pneumonia suggesting that bacterial co-infection was the main cause of death during that pandemic. As bacterial co-infection with influenza virus is a complex, multifaceted process, and my findings showed a tight link between bacteria co-infection with natural influenza infection. As a side project, I was able to show that a cysteine protease clostripain, produced by the Gram-positive bacteria *Clostridium histolyticum,* is able to activate H1, H2, H3, H7 and H9 HAs. This is the first example of a non-serine protease cleaving influenza HA (Data not shown).

In order to study the HA Ser to Tyr mutation on an actual virus, I used the CA0409 reverse genetic system to create two isogenic recombinant viruses with a

single polymorphism at the HA cleavage site and tested them in a mouse infection model. Although the mouse model did not show any phenotypic difference between rCA0409 HA-328Y and rCA0409 WT in both intranasal and intracranial infections, the clinical consequence of humans infected by the virus that harbor the mutation Bei718, is still undetermined.

Ser to Tyr mutation is not only limited to human influenza virus, after extensive bioinformatic analysis I identified a group of H9N2 AIV harboring an equivalent mutation. One virus with well documented clinical data MS96, is of particular interest. MS96 shows more severe clinical presentations in chickens found in farm setting than specific-pathogen-free (SPF) chickens, suggesting a possible bacterial synergy with the virus. By employing similar techniques from the Bei718 research, I discovered that MS96 use ch-Pm for HA activation. In contrast to Bei718, MS96 virus completely depends on the bacterial mechanism to activate ch-Plg. The hijacking of the *S. aureus* co-factor sak by the MS96 leads to activation of ch-Plg to ch-Pm and consequently to HA activation. Interestingly, other bacterial plasminogen activator (PA), such as skc from *S. pyogenes* shows a preference for h-Plg over ch-Plg. Such species specificity indicates unique interactions between *Staphylococcus sp.* and AIV as well as *Streptococcus sp.* and human influenza virus.

Since the Ser to Tyr mutation at the HA cleavage site clearly showed its importance in viral pathogenesis, I decided to determine the crystal structure of an uncleaved MS96 HA trimer. In Appendix I, I describe an optimized protocol for producing influenza HA trimer using a baculovirus expression system and a Drosophila S2 expression system (Data not shown). The optimized system allowed production of 2 mg/L of high quality influenza HA trimer after an easy but highly specific strep-tactin based affinity purification step which doubled the typical yield of

influenza HA production (250). The optimized system was also modified to produce influenza NA tetramers (Data not shown) for surface Plasmon resonance (SPR) to study the binding kinetics between HA, NA and h-Plg.

From the H9N2 AIV study, I uncovered an interesting fact that there are no indentified HPAI in the H9 subtype. Despite the fact that all H9 viruses are defined as LPAI, number of cases of H9N2 outbreaks showed moderate mortality rate in infected chickens, indicating an upward trend in virulence for H9 viruses. This observation gave rise to an interesting question: whether H9 influenza is able to convert into HPAI. Two groups of researchers took an extreme approach to answer this question by creating a chimeric H9N2 virus with a polybasic cleavage site using influenza reverse genetics (227, 246). In their chicken infection model, the chimeric virus remained LPAI and the authors concluded that the addition of polybasic cleavage site does not convert H9N2 to HPAI. However, by heavily depending on the data from a single chicken infection model, they overlooked some important details, such as the stability of the mutated HA and the mechanism of furin mediated HA cleavage. Furthermore, such dramatic change in the cleavage site is not likely to happen in nature, a fact that argues against the relevance of their study. With that in mind, I took an alternative approach which reflects the natural infection setting to provide some answers of this question.

By bioinformatic analysis, I found a group of H9 viruses in the Middle East harboring a tri-basic cleavage site on the HA. Analysis by athe furin cleavage site algorithm Pitou 2.0 predicted that such HA can be cleaved by furin (231). Taking Israel810 as a prototypic HA for my study, I showed that HA is not cleaved in 293T cells by human furin (h-furin) without addition of exogenous proteases. As HA is a protein folded into a complex tertiary structure, the discrepancies between predictions

and actual experimental data were well anticipated. To test whether expression levels and species specificity play a role in furin mediated cleavage, I decided to clone out both h-furin and chicken furin (ch-furin) for further testing. Both ch-furin and h-furin are able to cleave Israel810 HA when overexpressed, indicating expression levels of the protease is important. However, testing species specific HA cleavage by furin is not straightforward since expression levels cannot be easily controlled in transfection.

I introduced the ProteoTuner Shield System (ppTuner) for transient transfection to answer the species specific question. In contrast to the tetracycline on/off (Tet-on/off) system which allows analogue control of protein expression, ppTuner controls protein expression digitally. The technique is based upon the destabilization domain (DD) of FKBP protein which by default is targeted to the proteasomes for degradation. By fusing furin to the DD, the fusion protein becomes unstable and is constitutively targeted for degradation. A 0.75 kDa membrane permeable ligand, shield 1, binds to DD and protects the fusion protein from degradation. Therefore, DD-tagged furin levels can be post-translational controlled by the amount of shield 1 and are hence, tunable. Using the technique, I was able to show that ch-furin is more processive than h-furin in cleaving Israel810 HA and that HA cleavage is dose dependent for both furins.

Although furin levels can be up-regulated by multiple environmental and host factors, such processes during an actual influenza infection are still elusive. I decided to focus on viral aspects and test if additional mutation would enhance HA activation by endogenous furin. A natural occurring mutation, T15R which eliminates a bulky sugar moiety found in close proximity to the HA cleavage site, regulates Israel810 HA cleavage positively. The two mutations together allow HA activation by endogenous furin, a hallmark property of HPAI. After a series of confirmation experiments that

include siRNA knockdown and RT-PCR analysis, I was able to show that endogenous furin was responsible for Israel810 HA activation in multiple human and avian cells.

Although generation of recombinant viruses with these HA mutations could help bolster these findings, the biosafety concerns were not justified for me to produce such a potentially highly pathogenic virus. Influenza pseudoviruses (PVs) were generated as an alternative approach to study these mutations at the virus level. The PV data was coherent with the HA cleavage results indicating that PV was activated by endogenous furin. The PV data also suggests that the mutated HA is relatively stable compared to HA with a ploybasic cleavage site. Since HA stability is an important parameter for viral fitness, my observations might possibly explain why polybasic H9 viruses tend to stay lowly pathogenic. The study also suggests that H9 HA evolved on a different pathway than the one used by H5 and H7, a hypothesis that may also explain the absence of HPAI in H9, but multiple moderately pathogenic H9 viruses in nature.

5.2 Future Directions

The three mechanisms described above clearly show that the primary and tertiary structure of HA tightly controls viral activation and result in modulation of viral virulence. For future work, ferret and chicken influenza inflection models should be use to determine the possible outcome of Bei718, MS96 and Israel810 virus in natural infection setting. Bacterial co-infection model should be preferred to consolidate the mechanism of bacteria-influenza synergy in actual infection *in vivo*.

HA activation is an attractive target for therapeutic drug development. Indeed, the broad-spectrum serine protease inhibitors aprotinin, leupeptin and camostat have been used as treatment for influenza infections (251). However, use of aprotinin is

associated with an increased risk of renal dysfunction (252). The research on protease preferences of individual HAs I have conducted opens up the possibility of using a targeted protease inhibitor approach in treating influenza infection. Such targeted approach would be beneficial by minimizing potential side effects of inhibiting a broad range of serine proteases without massively diminishing the antiviral activity of the drug.

Prevention from influenza infections by vaccination is a critical aspect for controlling influenza. Studies on universal influenza antibodies that are able to neutralize a broad spectrum of viruses recently generated a lot of exciting results. However, some difficulties will be needed to overcome before clinical administration can start, including finding an efficient way to elicit universal antibody production *in vivo* and addressing the potential antibody-dependent enhancement (5) problem. Moreover, viruses that mutate conserved epitopes targeted by universal antibodies will very likely arise after wide administration of such vaccine. Because of some limitation of current vaccine production methods, an alternative strategy for vaccine production may be needed for the next pandemic. Using knowledge from HA activation, we could potentially engineer a fast growing vaccine seed by optimizing the HA cleavage site to the corresponding protease for HA activation. For example, changing the primary sequence of HA cleavage site to Ala-Asn-Gly-Arg would allow efficient viral activation by factor Xa, the protease responsible for HA activation in ECE. Furthermore, as our study suggested, Ser to Tyr at the P2 position of HA cleavage site may allow faster growth rate of influenza virus in tissue culture.

Studying sequence and structure of HA cleavage site has no doubt shed light on important aspects of the influenza life cycle and the knowledge gained may facilitate antiviral drug development that target virus entry into cells. However,

transmission of influenza virus is also an important aspect of influenza pathogenesis. Knowledge gained from the transmission process can lead to methods alleviating influenza transmission in the human population. Similarly to all viruses, influenza virus requires environmental cues to initiate different processes during infection. For instance, the low pH dependence of HA_2 conformational change allows the virus to deposit its genome at a precise time inside cells. Although always regarded solely as a priming step for influenza viruses, HA activation is possibly time-sensitive and needs to be occuring at the correct time and place. Activated HA is less stable than its non-activated form due to the exposure of the fusion peptide to exopeptidases digestion (253). Therefore, HA activated too early may negatively affect overall viral fitness due to protein degradation. In contrast, the limited time from attachment to endocytosis (~300 sec) agues in favor of the need for influenza virus to activate just prior to reaching the cell surface (254). Therefore, understanding the activation status of influenza virus in environment is maybe invaluable in learning more about viral transmission.

Since HA activation controls the infectivity of influenza virus, the activation status of the virus in environment prior to entering the host may play a critical role in transmission. Therefore, for future work, I hypothesize that the activation status of influenza virus affects viral infectivity. And by forcing premature activation and conformational changes of HA by modulating the environmental pH for example, we can reduce transmissibility of influenza viruses in the environment.

5.3 Conclusion

Influenza infection is still a major public health issue globally. In particular, during the occasional emergence of a pandemic virus, the field is racing against time to better understand the virus. A tremendous amount of time and effort spent by

researchers that allowed pushing forward the knowledge on different aspects of influenza infections. Thanks to the development of various new sequencing technologies, large libraries of influenza sequences can be easily generated. I took advantage of the power of bioinformatics combined it with traditional molecular biology and biochemistry to elucidate a small yet critical part of the influenza life cycle. The knowledge gained from my studies on the primary and tertiary structures of influenza cleavage sites and their modulation on viral pathogenesis can potentially lead to better treatment options and characterization of influenza virus in general. For instance, data from my studies would recommend use of antibiotic as a prophylactic treatment for influenza bacterial co-infections to diminish possible synergistic effects and disease severity. Another part of my study identified two pathogenic determinants of influenza HA and advocates close monitoring for such viruses. Last but not least, the mechanisms of protease usage by influenza viruses provide a more thorough understanding of this conventional yet critical HA cleavage activation process.

CHAPTER 6

MATERIALS AND METHODS

6.1 Cells, viruses, plasmids and reagents

293T/17 (CRL-11268), MDCK.1, MDCK.2 and MDCK (CCL-34) cells (American Type Culture Collection, ATCC) were maintained in Dulbecco's modified Eagle's medium (DMEM) supplemented with 10% heat-inactivated fetal bovine serum (Gibco), 100 units/ml of penicillin and 10 μg/ml of streptomycin (Cellgro), and 25 mM HEPES (Cellgro) at 37^{o}C in a 5% CO_2 incubator. DF-1 (CRL-12203), QT-6 (CRL-1708), Duck Embryo (CCL-141), CGBQ (CCL-169) and LMH (CRL-2117) were maintained according to ATCC recommended conditions. The Bei718 HA gene was synthesized by GeneArt/Life Technologies based on the sequence in NBCI Genebank (accession # ACZ98546), Israel810 HA gene (accession # ABS50802), MS96 HA gene (accession# AAF69255) and MS96 NA gene (accession#AZC45243). All the hemagglutinin genes were sub-cloned into the pEF4 vector (Invitrogen) whereas all H9HAs have an addition of C9-tag at the C-terminus, while neuraminidase genes were sub-cloned into the pCAGGS vector unless specified. Point mutations were introduced by QuickChange site-directed mutagenesis kit (Aglient) following the manufacturer guideline. Human furin and chicken furin were cloned from A549 cells and DF-1 cells respectively into pCMV-tag1 (Agilent). TPCK-trypsin was obtained from Themo Scientific, human plasmin (h-Pm) and plasminogen (h-Plg) was obtained from CalBiochem, streptokinase (group C) was obtained from Sigma, staphylokinase was obtain form BioVendor Laboratory Medicine, Inc., chicken plasminogen (ch-Plg) and chicken-plasmin (ch-Pm) were obtained from Innovative Research and 6-aminohexanoic acid was obtained from Alfa Aesar.

6.2 Influenza reverses genetic

The CA0409 reverse genetic system was a generous gift from Dr. Toru Takimoto (University of Rochester). Recombinant influenza viruses, rCA0409 WT and rCA0409 HA-328Y were produced as described previously (255). Briefly, 12 plasmids were co-transfected in 293T/MDCK cells for 48h using Lipofectamine 2000 (Invitrogen). The viruses were then plaque purified and amplified on MDCK cells grown in DMEM + 0.2% BSA + Hepes (25 mM) + Pen/Strep (10 μg/ml) in the presence of 3 μg/ml of TPCK-trypsin. The HA and NA genes were sequenced and confirmed to be free of unwanted mutations.

6.3 Surface biotinylation and western blot

293T cells were grown on poly-D-lysine-treated 24 well plates to 60-70% confluence and transfected with 500ng of plasmid using Lipofectamine 2000 for 18h. Transfected cells were washed with PBS and underwent different treatments in DMEM + 0.2% BSA as specified in each experiment. After the treatment, the plates were kept at 4^{o}C on ice and were washed with PBS and incubated with Sulfo-NHS-SS-biotin (250 μg/ml, Sigma) for 30 min. Excess biotin was quenched with glycine (50 mM) for 10 min. Cells were washed with PBS and then lysed by 1x RIPA buffer (Millipore) with Complete^{TM} protease inhibitor cocktail tablets (Roche) for 10 min. Lysed cells were centrifuged at 18,000 g for 20 min at 4^{o}C, supernatant was collected and added to 30 μl of a 50% suspension of streptavidin agarose beads (Thermo) and incubated at 4^{o}C on a rotating shaker for 18h to pull down all the biotinylated proteins. The beads were washed 3 times with RIPA buffer and resuspended in 30 μl of 2x Laemmli sample buffer + 10% beta-mercaptoethanol for western blotting. HA bands were detected by primary goat α-PR8 H_0 antibody (BEI Resources, NR-3148) and secondary rabbit α-goat conjugated to horseradish peroxidase (Thermo) or HA_0 and

HA_2 bands were detected by primary mouse α-C9 (ID4) antibody (BEI Resources, NR-3148) and secondary goat α-mouse conjugated to horseradish peroxidase (Thermo).

6.4 Quantification of HA cleavage

Western blot images were taken by FujiFilm LAS-3000. The pixel intensity of individual band was measured by Image J, and relative cleavage efficiencies were calculated by the following equation: $[(HA_1/HA_0+HA_1)]$ x100 or $[(HA_2/(HA_0+HA_2)]$ x100.

6.5 Immuno-plaque assay

MDCK cells were grown on 12 well plates to 90-100% confluence. Viruses were serially diluted in RPMI and incubated on MDCK cells for 1h at 37^{o}C. MDCK cells were washed 2 times with PBS before and after inoculation. Plaque assay medium (DMEM + 0.2% BSA + Hepes + Pen/Strep + 1% SeaPlaque Agarose (Lonza)) was added along with proteases and/or inhibitors as specified in each experiment. Plates were incubated at room temperature for 10 min for the agarose to solidify and incubated inversely at 37^{o}C, 5% CO_2 incubator for 3 days. Cells were fixed in 10% formalin for 1hr and permeabilized with 0.5% Triton X-100 for 3 min. Virally-infected cells were detected using primary mouse α-nuceloprotein (NP) and secondary goat α-mouse conjugated to alkaline phosphatase (JacksonImmuno Research). Individual plaque was visualized by adding BCIP/NBT substrate (Vector lab). Plaques were counted and viral titers were calculated.

6.6 Live cell plasminogen binding assay and flow cytometry

293T cells were grown on 12 well plates to 60-70% confluence and transfected with 1 μg of plasmid DNA using Lipofectamine 2000 for 18h. Cells were washed with PBS gently and incubated in DMEM + 0.2% BSA + Hepes for 30 min at 37^{o}C to remove any trace plasminogen in FBS. The plates were chilled on ice and

cells were detached in 10 mM EDTA for 10 min. Cell pellets were collected by low speed centrifugation at 4^{o}C and resuspended in 100 μl of 2 μM human-plasminogen in DMEM + 0.2% BSA + Hepes for 30 min at 4^{o}C on a rotating shaker. Non-bound plasminogen was removed by washing 3 times with DPBS. H-Plg was labeled using primary mouse α-plasminogen (GeneTex) and secondary chicken α-mouse Alexa-647 (Invitrogen). Labeled cells were chilled on ice and immediately analyzed by FACS on a LSRII system (BD Biosciences, San Diego, CA). FACS data were further analyzed using FlowJo software (Tree Star, Ashland, OR).

6.7 Viral pathogenesis in mouse model

For intranasal inoculation, twenty 8-week-old male BALB/c mice, eight for each experimental group and four for the PBS control, were inoculated intranasally with 10^5 pfu of virus diluted in 50 µl of PBS. Mouse body weights were measured daily for 6 days. Half of the mice were euthanized on day 3 and the other half on day 6. Indicated tissues were harvested, weighed and stored at -80^{o}C. Immuno-plaque assay was performed on 20% tissue homogenate in PBS. For intracranial inoculation, thirteen 5 week-old male BALC/c mice were used; four for each experimental group, three for the WSN control and two for an artificial cerebral spinal fluid (ACSF, from Tocris) control. Each mouse was inoculated intracranially with 10^3 pfu of virus diluted in 5 µl of ACSF, using a Hamilton syringe. Mouse body weight was measured every 12 h for 3 days. All mice were euthanized on day 3. Brain tissues were collected and viral titer determination was performed as described for intransal inoculation. All work with animals was carried out according to the Cornell University Animal Care and Use program under Animal Welfare Assurance A3347-01, and complied with the Public Health Service Policy on Humane Care and Use of Laboratory Animals.

6.8 Bacterial secondary infection mouse model

Sixteen 7-week-old male BALB/c mice, three for each experimental group and one for the mock infected control were inoculated intranasally with 10^5 pfu of virus diluted in 50 μl of DMEM on Day 0. 10^6 cfu of bacteria, *Streptococcus pyogenes* NZ131 were diluted in 50 μl of THY medium and inoculated intranasally on Day 3 post-infection. Mouse body weights were measured daily for 7 days. All the mice were euthanized on Day 7.

6.9 Tunable expression of chicken (ch) furin and human (h) furin

Ch-furin and h-furin were cloned into pPtunerC from Clontech using EcoRI and SalI restriction site. pPtunerC-ch-furin-DD or pPtunerC-h-furin-DD (200 ng) were co-transfeced with pEF4-Israel810HA (300 ng) into 293T cells. Shield 1 (Clontech) was added at 6h post-transfection and surface biotinylation and western blot were done as described above.

6.10 siRNA knockdown assay

293T cells were grown on poly-D-lysine-treated 24 well plates to 60-70% confluence and co-transfected with pEF4-HA plasmids and either ON-TARGETplus Non-Targeting siRNA or ON-TARGETplus Furin siRNA (Thermo) using DharmaFECT Duo (Thermo) for 24 hr following the user manual. Half of the cells were used to perform surface biotinylation to determine HA cleavage. The other half of the cells was harvested for Q-RTPCR to determine knockdown efficiency.

6.11 Quantitative reverse transcribed polymerase chain reaction (Q-RTPCR)

Approximately $1x10^6$ -$1x10^7$ cells were harvested and spun down at 300g for 5 min at 4^{o}C. Total RNA from the cell pellet was purified by RNeasy mini kit (Qiagen)

following the manufacturer guideline. RNA concentration was measured by a UV Spectrophotometer Q3000 (Quawell) and the quality was confirmed by 260/280 ratio, with the values ranging between 2.1-2.2. One-step Q-RTPCR was performed using QuantiTect SYBR Green RT-PCR Kit (Qiagen) following the user manual with 50 ng of RNA input. Human furin primers were acquired from PrimerBank (http://pga.mgh.harvard.edu/primerbank/) (256-258). Primer pairs for h-furin (PrimerBank ID: 20336193c1), primers for h-GAPDH, chicken-furin and ch-GAPDH were ordered from QuantiTect Primer Assays (Qiagen). Reactions were setup on ice on a 96-well plate and were run immediately using an Applied Biosystems (AP) 7500 Fast Real-time PCR system. The amplification plot and dissociation curves were analyzed by the 7500 Fast Real-time PCR software to determine the threshold cycles and dissociation of the each sample. Furin expression level was compared relatively to GAPDH expression and normalized to either 293T cells alone (Fig. 6C) or no siRNA treatment (Fig. 4C). 2^{-DDCt} was calculated as described previously (259).

6.12 MLV-based influenza pseudoviral particles (PV) transduction assay

To produce MLV based PV, 293T cells were grown on 12 well plates to 50 – 60 % confluence and transfected with MLV-gag-pol (350 ng), pTG-luc (500 ng), A/chicken/Korea/MS96/1996 (H9N2), Accession # AAF10404) neuramindase (NA) (350 ng), HAs (350 ng) and furin plasmids (350 ng, specified in individual experiment) for 48h using Lipofectamine 2000. Supernatants were harvested and filtered through 0.45 μm filter to remove any cell debris. The filtered supernatants containing PV were treated with or without trypsin (3 μg/ml) as specified in each experiment for 15 min at 37^{o}C to allow HA activation. After activation, excess trypsin activity was neutralized by addition of a 1:1 ratio of RPMI containing trypsin inhibitor from *Glycine max* (soybean) (Sigma-Aldrich). MDCK cells were grown on 24 well plates to 60 – 70 %

confluence and infected in duplicate by 200 μl of PV-RPMI mixture for 1h. 500 μl of DMEM + 2%FBS + Hepes + P/S was added to each well and incubated for 48h for transduction. Cells were lysed by 1x cell culture lysis reagent (Promega) for 1h at room temperature on a rocker. Transduction efficiency is measured as RLUs using a GloMax-20/20 luminometer (Promega) by mixing 10 μl of lysate and 20 μl of luciferase assay reagent (Promega).

6.13 Ch-Plg activation by Staphylokinase (sak)

Staphylokinase (100 μg/ml) and ch-Plg (50 μg/ml) were pre-incubated in 20 mM Tris pH 7.5 for 1.5h at 37^{o}C before treatment and use as a 10x solution

APPENDIX 1

PRODUCTION OF INFLUENZA HA BY THE BACULOVIRUS EXPRESSION SYSTEM

A1.1 Introduction

As fundamental building blocks of living organism, proteins play an important role in any biological processes. In order to study protein in great detail, a large amount of purified protein is often required. However, the quantity of proteins varies and could be very low in physiological conditions, which impose a big challenge to study. The invention of cloning and recombinant expression of protein in the 80s allows the field to move forward (260). The concept behind recombinant proteins is simple; protein of interest is cloned and mass-produced in a surrogate system, which allow efficient production of any proteins. Bacterial and yeast expression system are the two common systems for protein expression due to the rapid grow rate of the two organisms. Although the two systems cover protein production for prokaryotes and eukaryotes, some proteins are not optimal for the systems intrinsically.

Viral envelope proteins are of great interest not only because of their importance for viral life cycle, but also because they are the major antigenic determined for their host. Most of the viral envelope proteins are folded in complex structure and are highly glycosylated, which is not ideal for the generic expression system. Alternative expression systems were used to product recombinant viral envelope protein; including insect and mammalian cell expression systems. After a series of intensive optimization, both of them are able to produce a reliable amount of proteins. In here, we were able to modify the existing baculovirus system in our laboratory to produce large quantity and high quality of influenza hemagglutinin trimer (HA) for crystallography. The modified system allows efficient secretion of the HA and

a small affinity tag for one step purification. This system is already optimized and will require minimum effort to apply to other viral envelope proteins.

Figure A1.1. Construct designs of influenza HA trimer and NA tetramer production by the baculovirus expression system. (A) Construct of recombinant MS96 HA trimer for crystallography. The ecto-domain of influenza HA is fused with the melittin secretion peptide from honeybee at the N-terminus for efficient secretion (261). T4 fibrintin foldon from T4 bacterial phage is fused to the c-terminus of the HA to facilitate HA trimerization. The constructs use a nine amino acid long strep-tagII at the c-terminus for affinity purification. A prescission cleavage site is introduced between the HA and T4 foldon for removal of all the heterogeneous sequence from the HA after purification. From our design, the final product is just the ectodomain of HA trimer. (B) Construct of recombinant influenza HA trimer and (C) NA tetramer for surface plasmon resonance experiment (SPR). Tetramerization domain synthesized based on human vasodilator – stimulated phosphoprotein.

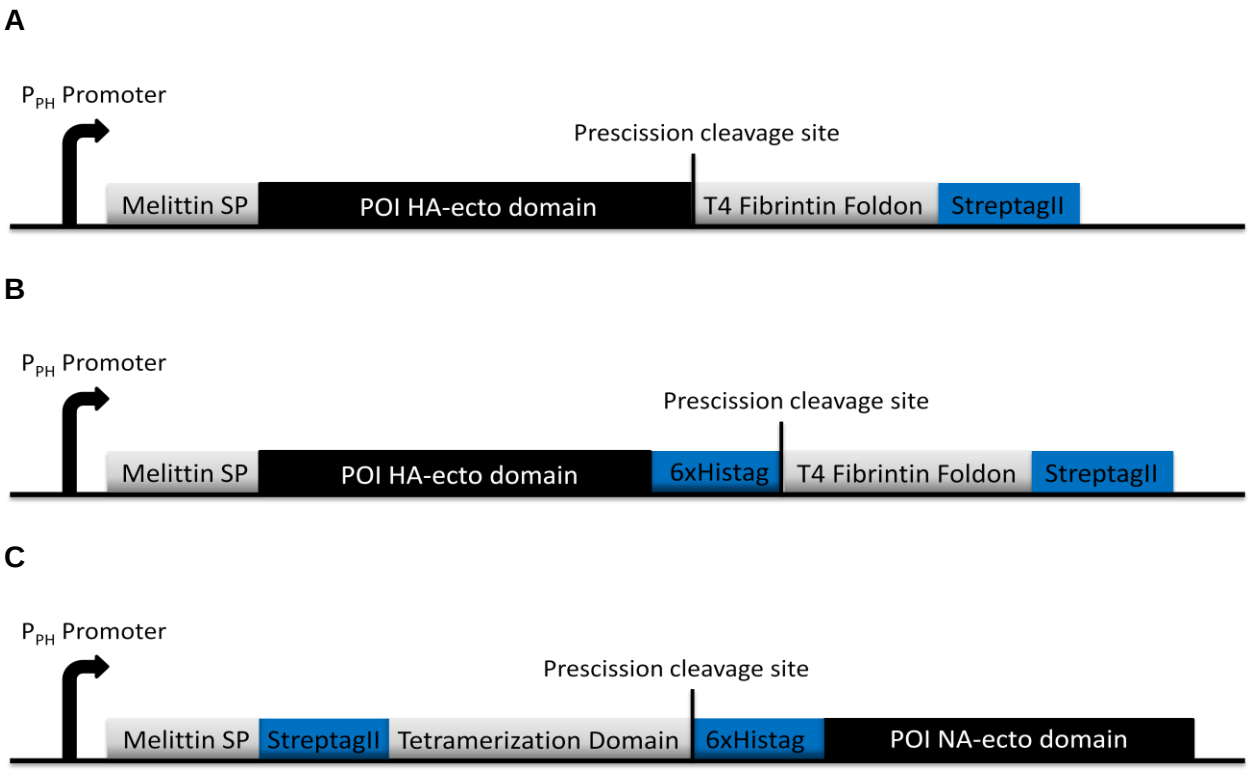

Figure A1.2. Schematic of MS96ce6 trimer production by the baculovirus expression system.

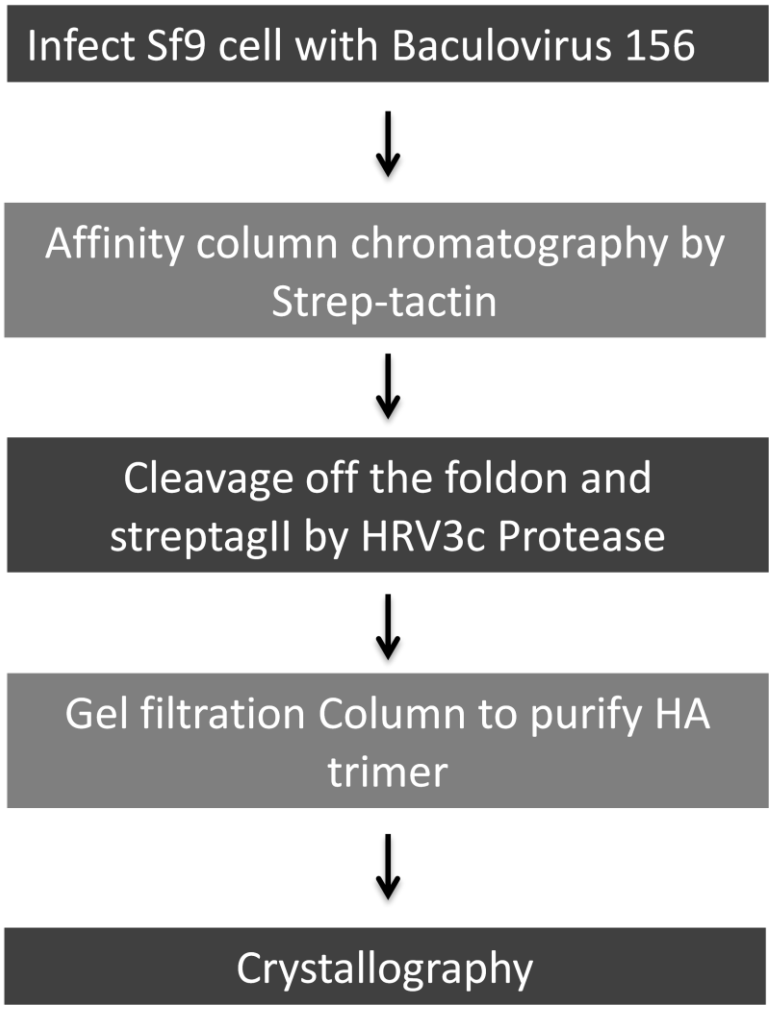

Figure A1.3. Conditions of MS96ce6HA trimer production.

Cell	Sf9 adopted in Sf900 III SFM ($5x10^6$ cell/ml, 95% viability)
Virus	Baculovirus-156 P3 ($3x10^7$pfu/ml)
MOI	~0.5
Medium	Sf900III SFM
Volume	500 ml (400 ml cells + 50 ml virus + 50 ml fresh medium)
Flask	2000 ml Erlenmeyer flask
Duration	4 days
Temperature	27 – 29^{o}C
Rpm	120

Figure A1.4. Purification of recombination MS96ce6 HA by affinity chromatography. (A) Conditions of affinity chromatography using strep-tactin bead. (B) SDS-PAGE of purified MS96ce6 HA from supernatant, Elute 1 – 10.

A

ASupernatant	Spin @ 4000 rpm for 40 min, @ 4oC Add to 10% glycerol
Affinity Bead	**10 ml Strep-tactin Incubate O/N on rocker and roller**
Elution Buffer	**100 nM Tris-HCl, 200 mM NaCl, 1 mM EDTA, 10% glycerol pH 8.0**
Elution Volume	**10 times, 5 ml each**

B

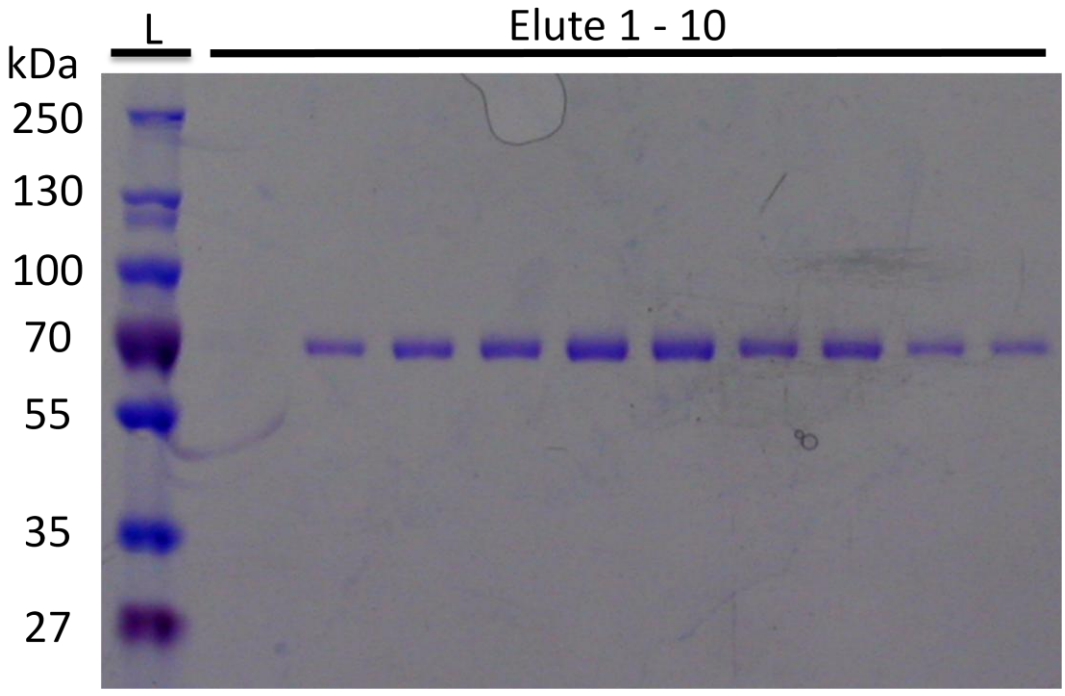

Figure A1.5. Purified MS96ce6HA ecto domain after HRV3c cleavage. (A) Conditions of HRV3c treatment. (B) SDS-PAGE of recombinant MS96 HA after HRV3c treatment.

A

Rxn Buffer	**500 mM Tris-HCl, 150 mM NaCl, 1 mM DTT, pH 7.55**
Enzyme	**0.2 mg HRV3c from A.G. Scientific**
Temperature	**4^{o}C**
Duration	**16 h**

B

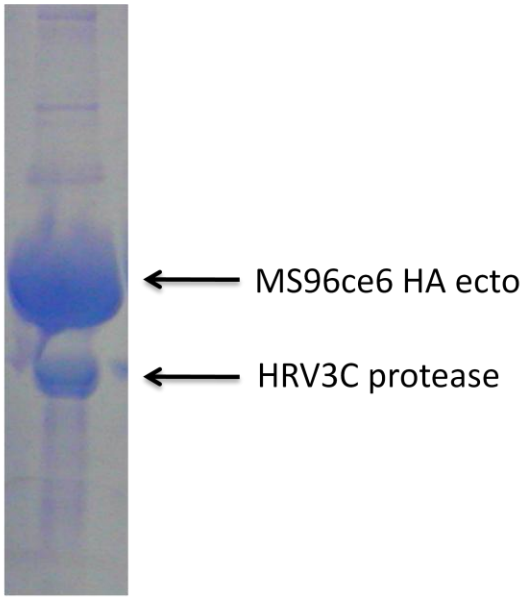

Total Purified Protein: 5 – 10mg

APPENDIX 2

IMMUNOPLAQUE ASSAY (INFLUENZA VIRUS)

Abstract

Despite developed a long time ago, plaque assay is still the gold standard for viral titer quantification in modern virology. The standard crystal violet-based plaque assay relies on virus' ability to induce cytopathic effect (CPE) which limits the assay to lytic viruses. Alternative viral quantification assays such as 50% tissue culture infectious assay ($TCID_{50}$) and genetic material quantification by Q-PCR provide a different way of viral quantification with their own shortcoming. In here, we modified the fluorescent focus assay and developed an antibody-based immunoplaque assay which provides a reliable and reproducible viral quantification independent of CPE. Our assay not only allows accurate determination of viral titer, but also provides information on viral kinetics, genetic stability and purity of the virus population.

A2.1 Materials and Reagents

1. MDCK cells*. Please note that there are multiple variants of MDCK on American Type Culture Collection (ATCC). This protocol has been tested for MDCK (CCL-34), MDCK.1 (CRL-2935) and MDCK.2 (CRL-2936)*
2. Recombinant A/California/04/2009 virus produced from 12 plasmids reverse genetic system (Generous gift from Professor Toru Takimoto from University of Rochester, New York, USA) (255)
3. Trypsin/EDTA (Cellgro, catalog number: 25-053-CI)
4. 2% SeaPlaque Agarose in ddH_2O (Lonza, catalog number: 50100)
5. TPCK-Trypsin (Thermo, catalog number: 20233)
6. PBS without Ca^{2+} and Mg^{2+} (Cellgro, catalog number: 21-030-CV)
7. DPBS with Ca^{2+} and Mg^{2+} (Cellgro, catalog number: 21-040-CV)

8. 10% formalin (Sigma-Aldrich, catalog number: HT501128-4L)
9. TritonX-100 (Sigma-Aldrich, catalog number: T9284)
10. 5% goat serum in DPBS (Gibco, catalog number: 16210-072)
11. Mouse anti-NP antibody from hybridoma: H16-L10-4R5 (ATCC, catalog number: HB-65)
12. Alkaline phosphatase conjugated Donkey anti-mouse antibody (Jackson Immuno Research, catalog number: 715-056-150)
13. Alexa Fluor 488 conjugated Goat anti-mouse antibody (Invitrogen, catalog number: A11001)
14. BCIP/NBT substrate (Vector Laboratories, catalog number: SK-5400)
15. DMEM (Cellgro, catalog number: 10-017-CV)
16. DMEM powder (Cellgro, catalog number: 50-003-PB)
17. Heat-inactivated fetal bovine serum (Gibco, catalog number: 26140079)
18. HEPES (Cellgro, catalog number: 25-060-CI)
19. Penicillin/Streptomycin (Cellgro 30-002-CI)
20. 7.5% BSA Fraction V (Gibco, catalog number: 15260)
21. RPMI 1640 powder (Cellgro, catalog number: 50-020-PB)
22. Tris base (US Biological, catalog number: T8600)
23. Sodium chloride (NaCl)
24. Magnesium chloride ($MgCl_2$)
25. Sodium hydroxide (NaOH)
26. Complete DMEM (cDMEM) (see Recipes)
27. 2x DMEM (see Recipes)
28. RPMI (see Recipes)
29. Alkaline phosphatase (AP) reaction buffer (see Recipes)

A2.2 Equipment

1. Standard tissue culture equipment
2. 12-well tissue culture plate
3. 37 °C 5% CO_2 cell culture incubator
4. Inverted fluorescence microscope (Optional)
5. Rocker
6. Laboratory spatula
7. Heated stir plate
8. Vortex
9. Axiovert 200 microscope

A2.3 Software

1. IPlab3.6.5 software

A2.4 Procedure

Day1

1. Each well on a 12-well-plate is seeded with 5 x 10^5 MDCK cells suspended in 1 ml of cDMEM.
2. The plate is incubated in the 5% CO_2 incubator at 37 °C overnight.

Day2 (or until cells reach 95% - 100% confluence)

3. Viruses are serially diluted (10-fold) in RPMI, vortex each dilutions and keep on ice before use.
4. MDCK cells are rinsed with 1 ml of DPBS twice.
5. MDCK cells are inoculated with 500 µl of viruses prepared from step 3.
6. The plate is incubated in 5% CO_2 incubator at 37 °C for 45 min.
7. Prepare SeaPlaque DMEM (pDMEM)

a. 2x DMEM is warmed at 37 °C water bath and 2% SeqPlaque agarose is melted on a hot plate at about 45 – 50 °C with stirring (*The cap should be slightly released to prevent pressure buildup).
b. To obtain pDMEM, pre-warm 2x DMEM and 2% agarose are mixed in 1:1 ratio in a sterile container and sit at room temperature for 5–10 min to cool down.
c. TPCK-trypsin (final concentration: 1 µg/ml) is added to the pDMEM.

8. Viral inoculums are aspirated and MDCK cells are rinsed with 1 ml of DPBS once.
9. 1.5 ml pDMEM + TPCK-trypsin from step 7-c is added to each well.
10. The plate is sat at room temperature (RT) for 10–15 min until pDMEM solidify.
11. The plate is incubated at 5% CO2 at 37 °C in the invert orientation (lid at the bottom) for 3 days.

Day 5 (or until visualization of plaque)

12. MDCK cells are fixed by adding 1.5 ml of 10% formalin directly on top of the agarose and incubated at RT for 2 h.
13. Extra formalin is aspirated and agarose from the well is removed and trashed carefully without disturbing the monolayer of cell using a laboratory spatula or equivalent tools.

Note: Experiment can be stopped after this step by adding PBS to cover the cells and store at 4 °C.

14. MDCK cells are permeabilized by 300 µl of 0.5% Triton-X100 in DPBS for 5 min on bench without agitation.
15. Cells are rinsed with 1 ml of PBS twice.

16. Cells are blocked by 300 µl of 5% goat serum in DPBS for 30 min at RT with agitation on rocker.
17. Cells are incubated with H16-L10-4R5 antibody (1:40) in 300 µl of 5% goat serum for 1 h at RT with agitation on a rocker.
18. Cells are rinsed with 1 ml of PBS twice.
19. Cells are incubated with alkaline phosphatase conjugated donkey anti-mouse (1:1,000) in 300 µl of 5% goat serum for 45 min at RT with agitation on a rocker.
20. Cells are rinsed with 1 ml of PBS twice and AP reaction buffer once.
21. Prepare the BCIP/NBT solution
    a. Added 2 drops of solution A, B and C into every 5 ml of AP reaction buffer.
    b. Mix by inverting the tube for 4–6 times.
22. 300 µl of BCIP/NBT solution is added to each well. The plate is put on a rocker in dark for 30 min or until the development of color.
23. The reaction is stopped by rinsing the plate with ddH2O.
24. The plate is air-dried at RT.
25. Count the number of plaques, check the plaque morphology and measure the size of plaques.

Alternative visualization method by fluorescence, fluorescent focus assay (FFA)

(Continuous from step 18)

19.1 Cells are incubated with goat anti-mouse Alexa Fluor 488 antibody (1:1,000) in 300 µl of 5% goat serum for 45 min at RT in dark.

20.1 Cells are rinsed with 1 ml of PBS twice.

21.1 Cells are covered with 500 µl of DPBS and store at 4 °C.

22.1 Check the plaque morphology and measure the size of plaques using an inverted fluorescence microscope.

Note: The protocol is optimized for influenza viruses. Modifications may be required for use in other viruses. For instance, factors required for multiple rounds of replication of the virus should be added in the pDMEM.

Figure A2.1. Diameter of Individual Plaque of A/California/04/2009/H1N1 Recombinatant Viruses (rCA0409). (A) Quantification of the diameter (μm) of 100 individual plaques of two different CA0409 viruses, wild type (WT) and HA-S328Y mutants (HA328Y). Images are taken by Axiovert 200 microscope using a 5x objective and diameters of each plaque are measured by IPlab3.6.5 software. Statistics are done by one-tail Student's t-test. (B) Representative image of plaques of CA0409 viruses stained with Alexa Fluor 488, scale bar = 200 μm. Images are taken by Sensicam using IPlab 3.6.5.

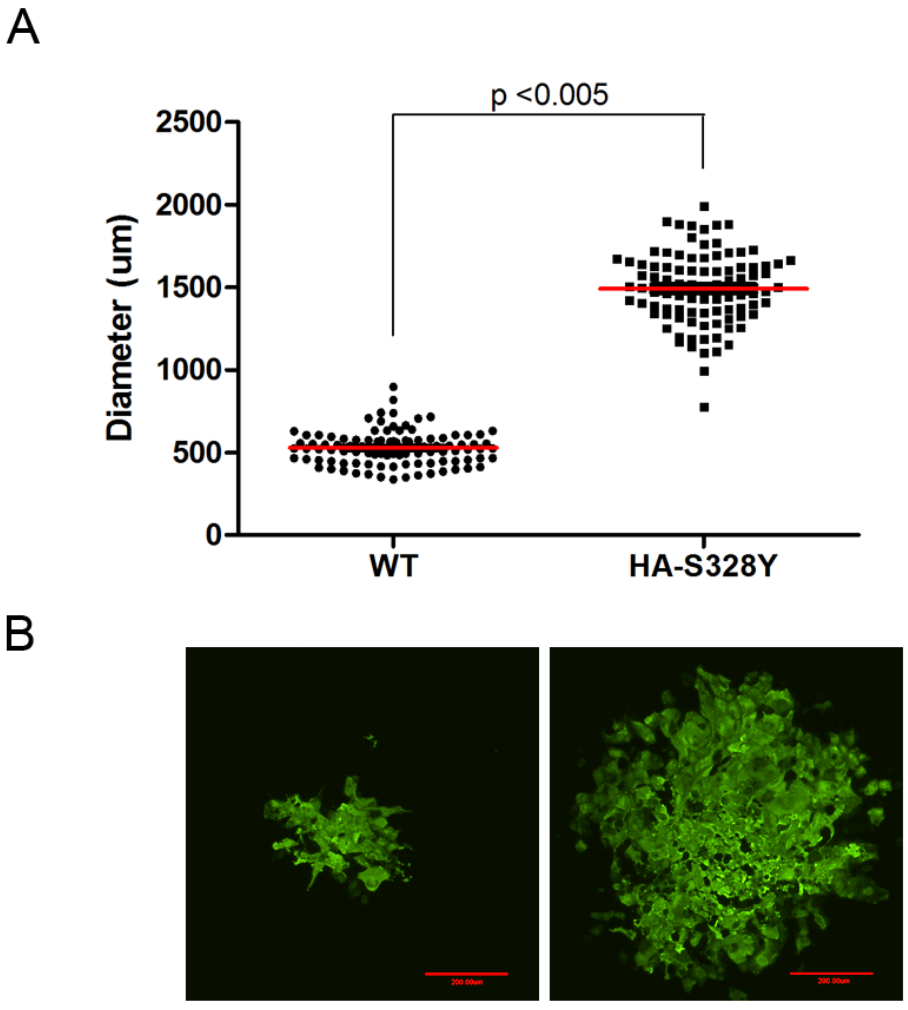

References

1. **Martin PM, Martin-Granel E.** 2006. 2,500-year evolution of the term epidemic. Emerg Infect Dis **12:**976-980.
2. **Smith W, Andrewes, C.H., Laidlaw, P.P.** 1933. A virus obtained from influenza patients. Lancet **2:**66-68.
3. **Webster RG, Yakhno M, Hinshaw VS, Bean WJ, Murti KG.** 1978. Intestinal influenza: replication and characterization of influenza viruses in ducks. Virology **84:**268-278.
4. **Hinshaw VS, Bean WJ, Geraci J, Fiorelli P, Early G, Webster RG.** 1986. Characterization of two influenza A viruses from a pilot whale. J Virol **58:**655-656.
5. **Tong S, Li Y, Rivailler P, Conrardy C, Castillo DA, Chen LM, Recuenco S, Ellison JA, Davis CT, York IA, Turmelle AS, Moran D, Rogers S, Shi M, Tao Y, Weil MR, Tang K, Rowe LA, Sammons S, Xu X, Frace M, Lindblade KA, Cox NJ, Anderson LJ, Rupprecht CE, Donis RO.** 2012. A distinct lineage of influenza A virus from bats. Proc Natl Acad Sci U S A **109:**4269-4274.
6. **Cox NJ, Subbarao K.** 2000. Global epidemiology of influenza: past and present. Annu Rev Med **51:**407-421.
7. **Webster RG, Bean WJ, Gorman OT, Chambers TM, Kawaoka Y.** 1992. Evolution and ecology of influenza A viruses. Microbiol Rev **56:**152-179.
8. **Tong S, Zhu X, Li Y, Shi M, Zhang J, Bourgeois M, Yang H, Chen X, Recuenco S, Gomez J, Chen LM, Johnson A, Tao Y, Dreyfus C, Yu W, McBride R, Carney PJ, Gilbert AT, Chang J, Guo Z, Davis CT, Paulson JC, Stevens J, Rupprecht CE, Holmes EC, Wilson IA, Donis RO.** 2013. New world bats harbor diverse influenza a viruses. PLoS Pathog **9:**e1003657.
9. **World-Health-Organization.** 2009. Influenza (Seasonal).
10. **Monto AS, Gravenstein S, Elliott M, Colopy M, Schweinle J.** 2000. Clinical signs and symptoms predicting influenza infection. Arch Intern Med **160:**3243-3247.
11. **CDC CfDCaP.** 2009. Bacterial coinfections in lung tissue specimens from fatal cases of 2009 pandemic influenza A (H1N1) - United States, May-August 2009. MMWR Morb Mortal Wkly Rep **58:**1071-1074.
12. **Mao L, Yang Y, Qiu Y.** 2012. Annual economic impacts of seasonal influenza on US counties: spatial heterogeneity and patterns. Int J Health Geogr **11:**16.
13. **Molinari NA, Ortega-Sanchez IR, Messonnier ML, Thompson WW, Wortley PM, Weintraub E, Bridges CB.** 2007. The annual impact of seasonal influenza in the US: measuring disease burden and costs. Vaccine **25:**5086-5096.
14. **Jamieson DJ, Honein MA, Rasmussen SA, Williams JL, Swerdlow DL, Biggerstaff MS, Lindstrom S, Louie JK, Christ CM, Bohm SR, Fonseca VP, Ritger KA, Kuhles DJ, Eggers P, Bruce H, Davidson HA, Lutterloh E, Harris ML, Burke C, Cocoros N, Finelli L, MacFarlane KF, Shu B, Olsen SJ.** 2009. H1N1 2009 influenza virus infection during pregnancy in the USA. Lancet **374:**451-458.
15. **Vaillant L, La Ruche G, Tarantola A, Barboza P.** 2009. Epidemiology of fatal cases associated with pandemic H1N1 influenza 2009. Euro Surveill **14**.

16. **Simonsen L, Clarke MJ, Schonberger LB, Arden NH, Cox NJ, Fukuda K.** 1998. Pandemic versus epidemic influenza mortality: a pattern of changing age distribution. J Infect Dis **178:**53-60.
17. **Taubenberger JK, Reid AH, Janczewski TA, Fanning TG.** 2001. Integrating historical, clinical and molecular genetic data in order to explain the origin and virulence of the 1918 Spanish influenza virus. Philos Trans R Soc Lond B Biol Sci **356:**1829-1839.
18. **Smith GJ, Vijaykrishna D, Bahl J, Lycett SJ, Worobey M, Pybus OG, Ma SK, Cheung CL, Raghwani J, Bhatt S, Peiris JS, Guan Y, Rambaut A.** 2009. Origins and evolutionary genomics of the 2009 swine-origin H1N1 influenza A epidemic. Nature **459:**1122-1125.
19. **World-Health-Organization.** 2009. Global alert and response, pandemic (H1N1) 2009, frequrently asked questions: what is phase 6? http://www.who.int/csr/disease/swineflu/frequently_asked_questions/levels_pandemic_alert/en/index.html. Accessed October 8, 2009.
20. **Meltzer MI, Cox NJ, Fukuda K.** 1999. The economic impact of pandemic influenza in the United States: priorities for intervention. Emerg Infect Dis **5:**659-671.
21. **Butt KM, Smith GJ, Chen H, Zhang LJ, Leung YH, Xu KM, Lim W, Webster RG, Yuen KY, Peiris JS, Guan Y.** 2005. Human infection with an avian H9N2 influenza A virus in Hong Kong in 2003. J Clin Microbiol **43:**5760-5767.
22. **Lin YP, Shaw M, Gregory V, Cameron K, Lim W, Klimov A, Subbarao K, Guan Y, Krauss S, Shortridge K, Webster R, Cox N, Hay A.** 2000. Avian-to-human transmission of H9N2 subtype influenza A viruses: relationship between H9N2 and H5N1 human isolates. Proc Natl Acad Sci U S A **97:**9654-9658.
23. **Mounts AW, Kwong H, Izurieta HS, Ho Y, Au T, Lee M, Buxton Bridges C, Williams SW, Mak KH, Katz JM, Thompson WW, Cox NJ, Fukuda K.** 1999. Case-control study of risk factors for avian influenza A (H5N1) disease, Hong Kong, 1997. J Infect Dis **180:**505-508.
24. **Yuen KY, Chan PK, Peiris M, Tsang DN, Que TL, Shortridge KF, Cheung PT, To WK, Ho ET, Sung R, Cheng AF.** 1998. Clinical features and rapid viral diagnosis of human disease associated with avian influenza A H5N1 virus. Lancet **351:**467-471.
25. **Gilbert M, Xiao X, Pfeiffer DU, Epprecht M, Boles S, Czarnecki C, Chaitaweesub P, Kalpravidh W, Minh PQ, Otte MJ, Martin V, Slingenbergh J.** 2008. Mapping H5N1 highly pathogenic avian influenza risk in Southeast Asia. Proc Natl Acad Sci U S A **105:**4769-4774.
26. **Imai M, Watanabe T, Hatta M, Das SC, Ozawa M, Shinya K, Zhong G, Hanson A, Katsura H, Watanabe S, Li C, Kawakami E, Yamada S, Kiso M, Suzuki Y, Maher EA, Neumann G, Kawaoka Y.** 2012. Experimental adaptation of an influenza H5 HA confers respiratory droplet transmission to a reassortant H5 HA/H1N1 virus in ferrets. Nature **486:**420-428.
27. **Herfst S, Schrauwen EJ, Linster M, Chutinimitkul S, de Wit E, Munster VJ, Sorrell EM, Bestebroer TM, Burke DF, Smith DJ, Rimmelzwaan GF, Osterhaus AD, Fouchier RA.** 2012. Airborne transmission of influenza A/H5N1 virus between ferrets. Science **336:**1534-1541.
28. **Smith H, Sweet C.** 1988. Lessons for human influenza from pathogenicity studies with ferrets. Rev Infect Dis **10:**56-75.

29. **Krug RM.** 2003. The potential use of influenza virus as an agent for bioterrorism. Antiviral Res **57:**147-150.
30. **Sui J, Hwang WC, Perez S, Wei G, Aird D, Chen LM, Santelli E, Stec B, Cadwell G, Ali M, Wan H, Murakami A, Yammanuru A, Han T, Cox NJ, Bankston LA, Donis RO, Liddington RC, Marasco WA.** 2009. Structural and functional bases for broad-spectrum neutralization of avian and human influenza A viruses. Nat Struct Mol Biol **16:**265-273.
31. **Steel J, Lowen AC, Wang TT, Yondola M, Gao Q, Haye K, Garcia-Sastre A, Palese P.** 2010. Influenza virus vaccine based on the conserved hemagglutinin stalk domain. MBio **1**.
32. **Neirynck S, Deroo T, Saelens X, Vanlandschoot P, Jou WM, Fiers W.** 1999. A universal influenza A vaccine based on the extracellular domain of the M2 protein. Nat Med **5:**1157-1163.
33. **Khurana S, Loving CL, Manischewitz J, King LR, Gauger PC, Henningson J, Vincent AL, Golding H.** 2013. Vaccine-Induced Anti-HA2 Antibodies Promote Virus Fusion and Enhance Influenza Virus Respiratory Disease. Sci Transl Med **5:**200ra114.
34. **Crowe JE, Jr.** 2013. Universal Flu Vaccines: Primum non nocere. Sci Transl Med **5:**200fs234.
35. **von Itzstein M, Wu WY, Kok GB, Pegg MS, Dyason JC, Jin B, Van Phan T, Smythe ML, White HF, Oliver SW, et al.** 1993. Rational design of potent sialidase-based inhibitors of influenza virus replication. Nature **363:**418-423.
36. **Kim CU, Lew W, Williams MA, Liu H, Zhang L, Swaminathan S, Bischofberger N, Chen MS, Mendel DB, Tai CY, Laver WG, Stevens RC.** 1997. Influenza neuraminidase inhibitors possessing a novel hydrophobic interaction in the enzyme active site: design, synthesis, and structural analysis of carbocyclic sialic acid analogues with potent anti-influenza activity. J Am Chem Soc **119:**681-690.
37. **De Clercq E.** 2004. Antivirals and antiviral strategies. Nat Rev Microbiol **2:**704-720.
38. **O'Donoghue JM, Ray CG, Terry DW, Jr., Beaty HN.** 1973. Prevention of nosocomial influenza infection with Amantadine. Am J Epidemiol **97:**276-282.
39. **Bright RA, Shay DK, Shu B, Cox NJ, Klimov AI.** 2006. Adamantane resistance among influenza A viruses isolated early during the 2005-2006 influenza season in the United States. JAMA **295:**891-894.
40. **Moscona A.** 2009. Global transmission of oseltamivir-resistant influenza. N Engl J Med **360:**953-956.
41. **Palses PS, M.L. .** 2013. Orthomyxoviridae In Knipe DM, Howley PM (ed), Fields Virology 6th. Lippincott Williams & Wilkins, Philadelphia, PA. **1**.
42. **Kilbourne ED, Murphy JS.** 1960. Genetic studies of influenza viruses. I. Viral morphology and growth capacity as exchangeable genetic traits. Rapid in ovo adaptation of early passage Asian strain isolates by combination with PR8. J Exp Med **111:**387-406.
43. **Morgan C, Rose HM, Moore DH.** 1956. Structure and development of viruses observed in the electron microscope. III. Influenza virus. J Exp Med **104:**171-182.
44. **Rossman JS, Jing X, Leser GP, Balannik V, Pinto LH, Lamb RA.** 2010. Influenza virus m2 ion channel protein is necessary for filamentous virion formation. J Virol **84:**5078-5088.

45. **Zebedee SL, Lamb RA.** 1989. Growth restriction of influenza A virus by M2 protein antibody is genetically linked to the M1 protein. Proc Natl Acad Sci U S A **86:**1061-1065.
46. **Seladi-Schulman J, Steel J, Lowen AC.** 2013. Spherical influenza viruses have a fitness advantage in embryonated eggs, while filament-producing strains are selected in vivo. J Virol.
47. **Roberts PC, Lamb RA, Compans RW.** 1998. The M1 and M2 proteins of influenza A virus are important determinants in filamentous particle formation. Virology **240:**127-137.
48. **Rossman JS, Lamb RA.** 2011. Influenza virus assembly and budding. Virology **411:**229-236.
49. **Bialas KM, Desmet EA, Takimoto T.** 2012. Specific residues in the 2009 H1N1 swine-origin influenza matrix protein influence virion morphology and efficiency of viral spread in vitro. PLoS One **7:**e50595.
50. **Zheng W, Olson J, Vakharia V, Tao YJ.** 2013. The Crystal Structure and RNA-Binding of an Orthomyxovirus Nucleoprotein. PLoS Pathog **9:**e1003624.
51. **Gerl MJ, Sampaio JL, Urban S, Kalvodova L, Verbavatz JM, Binnington B, Lindemann D, Lingwood CA, Shevchenko A, Schroeder C, Simons K.** 2012. Quantitative analysis of the lipidomes of the influenza virus envelope and MDCK cell apical membrane. J Cell Biol **196:**213-221.
52. **Zebedee SL, Lamb RA.** 1988. Influenza A virus M2 protein: monoclonal antibody restriction of virus growth and detection of M2 in virions. J Virol **62:**2762-2772.
53. **Ruigrok RWH.** 1998. Structure of influenza A, B and C viruses. . KG Nicholson, RG Webster, AJ Hay (Eds.) Textbook of influenza (Blackwell Science)**:**54-64.
54. **Shaw ML, Stone KL, Colangelo CM, Gulcicek EE, Palese P.** 2008. Cellular proteins in influenza virus particles. PLoS Pathog **4:**e1000085.
55. **Sun X, Whittaker GR.** 2007. Role of the actin cytoskeleton during influenza virus internalization into polarized epithelial cells. Cell Microbiol **9:**1672-1682.
56. **LeBouder F, Morello E, Rimmelzwaan GF, Bosse F, Pechoux C, Delmas B, Riteau B.** 2008. Annexin II incorporated into influenza virus particles supports virus replication by converting plasminogen into plasmin. J Virol **82:**6820-6828.
57. **He X, Zhou J, Bartlam M, Zhang R, Ma J, Lou Z, Li X, Li J, Joachimiak A, Zeng Z, Ge R, Rao Z, Liu Y.** 2008. Crystal structure of the polymerase PA(C)-PB1(N) complex from an avian influenza H5N1 virus. Nature **454:**1123-1126.
58. **Sugiyama K, Obayashi E, Kawaguchi A, Suzuki Y, Tame JR, Nagata K, Park SY.** 2009. Structural insight into the essential PB1-PB2 subunit contact of the influenza virus RNA polymerase. EMBO J **28:**1803-1811.
59. **Poch O, Sauvaget I, Delarue M, Tordo N.** 1989. Identification of four conserved motifs among the RNA-dependent polymerase encoding elements. EMBO J **8:**3867-3874.
60. **Guilligay D, Tarendeau F, Resa-Infante P, Coloma R, Crepin T, Sehr P, Lewis J, Ruigrok RW, Ortin J, Hart DJ, Cusack S.** 2008. The structural basis for cap binding by influenza virus polymerase subunit PB2. Nat Struct Mol Biol **15:**500-506.
61. **Dias A, Bouvier D, Crepin T, McCarthy AA, Hart DJ, Baudin F, Cusack S, Ruigrok RW.** 2009. The cap-snatching endonuclease of influenza virus polymerase resides in the PA subunit. Nature **458:**914-918.

62. **Hara K, Shiota M, Kido H, Ohtsu Y, Kashiwagi T, Iwahashi J, Hamada N, Mizoue K, Tsumura N, Kato H, Toyoda T.** 2001. Influenza virus RNA polymerase PA subunit is a novel serine protease with Ser624 at the active site. Genes Cells **6:**87-97.
63. **Horimoto T, Kawaoka Y.** 2005. Influenza: lessons from past pandemics, warnings from current incidents. Nat Rev Microbiol **3:**591-600.
64. **Schibli DJ, Weissenhorn W.** 2004. Class I and class II viral fusion protein structures reveal similar principles in membrane fusion. Mol Membr Biol **21:**361-371.
65. **Skehel JJ, Wiley DC.** 2000. Receptor binding and membrane fusion in virus entry: the influenza hemagglutinin. Annu Rev Biochem **69:**531-569.
66. **Nicholls JM, Bourne AJ, Chen H, Guan Y, Peiris JS.** 2007. Sialic acid receptor detection in the human respiratory tract: evidence for widespread distribution of potential binding sites for human and avian influenza viruses. Respir Res **8:**73.
67. **Wright PF, Neumann, G., Kawaoka, Y. .** 2013. Orthomyxoviridae In Knipe DM, Howley PM (ed), Fields Virology 6th. Lippincott Williams & Wilkins, Philadelphia, PA. **1**.
68. **Cox NJ, Kawaoka, Y.** 1998. Orthomyxoviruses: influenza. In Topley and Wilson's Microbiology and Microbial Infections, ed. BWJ Mahy, L Collier **1:**385-433.
69. **Ito T, Couceiro JN, Kelm S, Baum LG, Krauss S, Castrucci MR, Donatelli I, Kida H, Paulson JC, Webster RG, Kawaoka Y.** 1998. Molecular basis for the generation in pigs of influenza A viruses with pandemic potential. J Virol **72:**7367-7373.
70. **Matrosovich M, Tuzikov A, Bovin N, Gambaryan A, Klimov A, Castrucci MR, Donatelli I, Kawaoka Y.** 2000. Early alterations of the receptor-binding properties of H1, H2, and H3 avian influenza virus hemagglutinins after their introduction into mammals. J Virol **74:**8502-8512.
71. **Cross KJ, Wharton SA, Skehel JJ, Wiley DC, Steinhauer DA.** 2001. Studies on influenza haemagglutinin fusion peptide mutants generated by reverse genetics. EMBO J **20:**4432-4442.
72. **Carr CM, Chaudhry C, Kim PS.** 1997. Influenza hemagglutinin is spring-loaded by a metastable native conformation. Proc Natl Acad Sci U S A **94:**14306-14313.
73. **Floyd DL, Ragains JR, Skehel JJ, Harrison SC, van Oijen AM.** 2008. Single-particle kinetics of influenza virus membrane fusion. Proc Natl Acad Sci U S A **105:**15382-15387.
74. **Brownlee GG, Fodor E.** 2001. The predicted antigenicity of the haemagglutinin of the 1918 Spanish influenza pandemic suggests an avian origin. Philos Trans R Soc Lond B Biol Sci **356:**1871-1876.
75. **Ekiert DC, Friesen RH, Bhabha G, Kwaks T, Jongeneelen M, Yu W, Ophorst C, Cox F, Korse HJ, Brandenburg B, Vogels R, Brakenhoff JP, Kompier R, Koldijk MH, Cornelissen LA, Poon LL, Peiris M, Koudstaal W, Wilson IA, Goudsmit J.** 2011. A highly conserved neutralizing epitope on group 2 influenza A viruses. Science **333:**843-850.
76. **Kornfeld R, Kornfeld S.** 1985. Assembly of asparagine-linked oligosaccharides. Annu Rev Biochem **54:**631-664.

77. **Sun S, Wang Q, Zhao F, Chen W, Li Z.** 2012. Prediction of biological functions on glycosylation site migrations in human influenza H1N1 viruses. PLoS One **7:**e32119.
78. **Belser JA, Jayaraman A, Raman R, Pappas C, Zeng H, Cox NJ, Katz JM, Sasisekharan R, Tumpey TM.** Effect of D222G mutation in the hemagglutinin protein on receptor binding, pathogenesis and transmissibility of the 2009 pandemic H1N1 influenza virus. PLoS One **6:**e25091.
79. **Caton AJ, Brownlee GG, Yewdell JW, Gerhard W.** 1982. The antigenic structure of the influenza virus A/PR/8/34 hemagglutinin (H1 subtype). Cell **31:**417-427.
80. **Amorij JP, Huckriede A, Wilschut J, Frijlink HW, Hinrichs WL.** 2008. Development of stable influenza vaccine powder formulations: challenges and possibilities. Pharm Res **25:**1256-1273.
81. **Portela A, Digard P.** 2002. The influenza virus nucleoprotein: a multifunctional RNA-binding protein pivotal to virus replication. J Gen Virol **83:**723-734.
82. **Lin BC, Lai CJ.** 1983. The influenza virus nucleoprotein synthesized from cloned DNA in a simian virus 40 vector is detected in the nucleus. J Virol **45:**434-438.
83. **Honda A, Ueda K, Nagata K, Ishihama A.** 1988. RNA polymerase of influenza virus: role of NP in RNA chain elongation. J Biochem **104:**1021-1026.
84. **Shapiro GI, Krug RM.** 1988. Influenza virus RNA replication in vitro: synthesis of viral template RNAs and virion RNAs in the absence of an added primer. J Virol **62:**2285-2290.
85. **Whittaker G, Kemler I, Helenius A.** 1995. Hyperphosphorylation of mutant influenza virus matrix protein, M1, causes its retention in the nucleus. J Virol **69:**439-445.
86. **Whittaker G, Bui M, Helenius A.** 1996. Nuclear trafficking of influenza virus ribonuleoproteins in heterokaryons. J Virol **70:**2743-2756.
87. **Gerritz SW, Cianci C, Kim S, Pearce BC, Deminie C, Discotto L, McAuliffe B, Minassian BF, Shi S, Zhu S, Zhai W, Pendri A, Li G, Poss MA, Edavettal S, McDonnell PA, Lewis HA, Maskos K, Mortl M, Kiefersauer R, Steinbacher S, Baldwin ET, Metzler W, Bryson J, Healy MD, Philip T, Zoeckler M, Schartman R, Sinz M, Leyva-Grado VH, Hoffmann HH, Langley DR, Meanwell NA, Krystal M.** 2011. Inhibition of influenza virus replication via small molecules that induce the formation of higher-order nucleoprotein oligomers. Proc Natl Acad Sci U S A **108:**15366-15371.
88. **Colman PM.** 1994. Influenza virus neuraminidase: structure, antibodies, and inhibitors. Protein Sci **3:**1687-1696.
89. **Mitnaul LJ, Matrosovich MN, Castrucci MR, Tuzikov AB, Bovin NV, Kobasa D, Kawaoka Y.** 2000. Balanced hemagglutinin and neuraminidase activities are critical for efficient replication of influenza A virus. J Virol **74:**6015-6020.
90. **Rosenthal PB, Zhang X, Formanowski F, Fitz W, Wong CH, Meier-Ewert H, Skehel JJ, Wiley DC.** 1998. Structure of the haemagglutinin-esterase-fusion glycoprotein of influenza C virus. Nature **396:**92-96.
91. **Matrosovich MN, Matrosovich TY, Gray T, Roberts NA, Klenk HD.** 2004. Neuraminidase is important for the initiation of influenza virus infection in human airway epithelium. J Virol **78:**12665-12667.

92. **Goto H, Wells K, Takada A, Kawaoka Y.** 2001. Plasminogen-binding activity of neuraminidase determines the pathogenicity of influenza A virus. J Virol **75:**9297-9301.
93. **Goto H, Kawaoka Y.** 1998. A novel mechanism for the acquisition of virulence by a human influenza A virus. Proc Natl Acad Sci U S A **95:**10224-10228.
94. **Li S, Schulman J, Itamura S, Palese P.** 1993. Glycosylation of neuraminidase determines the neurovirulence of influenza A/WSN/33 virus. J Virol **67:**6667-6673.
95. **Sugrue RJ, Belshe RB, Hay AJ.** 1990. Palmitoylation of the influenza A virus M2 protein. Virology **179:**51-56.
96. **Holsinger LJ, Nichani D, Pinto LH, Lamb RA.** 1994. Influenza A virus M2 ion channel protein: a structure-function analysis. J Virol **68:**1551-1563.
97. **Takeda M, Pekosz A, Shuck K, Pinto LH, Lamb RA.** 2002. Influenza a virus M2 ion channel activity is essential for efficient replication in tissue culture. J Virol **76:**1391-1399.
98. **Stouffer AL, Acharya R, Salom D, Levine AS, Di Costanzo L, Soto CS, Tereshko V, Nanda V, Stayrook S, DeGrado WF.** 2008. Structural basis for the function and inhibition of an influenza virus proton channel. Nature **451:**596-599.
99. **Weinheimer VK, Becher A, Tonnies M, Holland G, Knepper J, Bauer TT, Schneider P, Neudecker J, Ruckert JC, Szymanski K, Temmesfeld-Wollbrueck B, Gruber AD, Bannert N, Suttorp N, Hippenstiel S, Wolff T, Hocke AC.** 2012. Influenza A viruses target type II pneumocytes in the human lung. J Infect Dis **206:**1685-1694.
100. **Elton D, Simpson-Holley M, Archer K, Medcalf L, Hallam R, McCauley J, Digard P.** 2001. Interaction of the influenza virus nucleoprotein with the cellular CRM1-mediated nuclear export pathway. J Virol **75:**408-419.
101. **Watanabe K, Takizawa N, Katoh M, Hoshida K, Kobayashi N, Nagata K.** 2001. Inhibition of nuclear export of ribonucleoprotein complexes of influenza virus by leptomycin B. Virus Res **77:**31-42.
102. **Iwatsuki-Horimoto K, Horimoto T, Fujii Y, Kawaoka Y.** 2004. Generation of influenza A virus NS2 (NEP) mutants with an altered nuclear export signal sequence. J Virol **78:**10149-10155.
103. **Noton SL, Medcalf E, Fisher D, Mullin AE, Elton D, Digard P.** 2007. Identification of the domains of the influenza A virus M1 matrix protein required for NP binding, oligomerization and incorporation into virions. J Gen Virol **88:**2280-2290.
104. **Hale BG, Randall RE, Ortin J, Jackson D.** 2008. The multifunctional NS1 protein of influenza A viruses. J Gen Virol **89:**2359-2376.
105. **Chien CY, Tejero R, Huang Y, Zimmerman DE, Rios CB, Krug RM, Montelione GT.** 1997. A novel RNA-binding motif in influenza A virus non-structural protein 1. Nat Struct Biol **4:**891-895.
106. **Liu J, Lynch PA, Chien CY, Montelione GT, Krug RM, Berman HM.** 1997. Crystal structure of the unique RNA-binding domain of the influenza virus NS1 protein. Nat Struct Biol **4:**896-899.
107. **Talon J, Horvath CM, Polley R, Basler CF, Muster T, Palese P, Garcia-Sastre A.** 2000. Activation of interferon regulatory factor 3 is inhibited by the influenza A virus NS1 protein. J Virol **74:**7989-7996.

108. **Wang X, Li M, Zheng H, Muster T, Palese P, Beg AA, Garcia-Sastre A.** 2000. Influenza A virus NS1 protein prevents activation of NF-kappaB and induction of alpha/beta interferon. J Virol **74:**11566-11573.
109. **Pichlmair A, Schulz O, Tan CP, Naslund TI, Liljestrom P, Weber F, Reis e Sousa C.** 2006. RIG-I-mediated antiviral responses to single-stranded RNA bearing 5'-phosphates. Science **314:**997-1001.
110. **Gack MU, Albrecht RA, Urano T, Inn KS, Huang IC, Carnero E, Farzan M, Inoue S, Jung JU, Garcia-Sastre A.** 2009. Influenza A virus NS1 targets the ubiquitin ligase TRIM25 to evade recognition by the host viral RNA sensor RIG-I. Cell Host Microbe **5:**439-449.
111. **Min JY, Li S, Sen GC, Krug RM.** 2007. A site on the influenza A virus NS1 protein mediates both inhibition of PKR activation and temporal regulation of viral RNA synthesis. Virology **363:**236-243.
112. **Min JY, Krug RM.** 2006. The primary function of RNA binding by the influenza A virus NS1 protein in infected cells: Inhibiting the 2'-5' oligo (A) synthetase/RNase L pathway. Proc Natl Acad Sci U S A **103:**7100-7105.
113. **Kochs G, Koerner I, Thiel L, Kothlow S, Kaspers B, Ruggli N, Summerfield A, Pavlovic J, Stech J, Staeheli P.** 2007. Properties of H7N7 influenza A virus strain SC35M lacking interferon antagonist NS1 in mice and chickens. J Gen Virol **88:**1403-1409.
114. **Noah DL, Twu KY, Krug RM.** 2003. Cellular antiviral responses against influenza A virus are countered at the posttranscriptional level by the viral NS1A protein via its binding to a cellular protein required for the 3' end processing of cellular pre-mRNAS. Virology **307:**386-395.
115. **Conenello GM, Zamarin D, Perrone LA, Tumpey T, Palese P.** 2007. A single mutation in the PB1-F2 of H5N1 (HK/97) and 1918 influenza A viruses contributes to increased virulence. PLoS Pathog **3:**1414-1421.
116. **Wise HM, Barbezange C, Jagger BW, Dalton RM, Gog JR, Curran MD, Taubenberger JK, Anderson EC, Digard P.** 2011. Overlapping signals for translational regulation and packaging of influenza A virus segment 2. Nucleic Acids Res **39:**7775-7790.
117. **Chen W, Calvo PA, Malide D, Gibbs J, Schubert U, Bacik I, Basta S, O'Neill R, Schickli J, Palese P, Henklein P, Bennink JR, Yewdell JW.** 2001. A novel influenza A virus mitochondrial protein that induces cell death. Nat Med **7:**1306-1312.
118. **McAuley JL, Chipuk JE, Boyd KL, Van De Velde N, Green DR, McCullers JA.** 2010. PB1-F2 proteins from H5N1 and 20 century pandemic influenza viruses cause immunopathology. PLoS Pathog **6:**e1001014.
119. **Zamarin D, Garcia-Sastre A, Xiao X, Wang R, Palese P.** 2005. Influenza virus PB1-F2 protein induces cell death through mitochondrial ANT3 and VDAC1. PLoS Pathog **1:**e4.
120. **Pena L, Vincent AL, Loving CL, Henningson JN, Lager KM, Li W, Perez DR.** 2012. Strain-dependent effects of PB1-F2 of triple-reassortant H3N2 influenza viruses in swine. J Gen Virol **93:**2204-2214.
121. **McAuley JL, Hornung F, Boyd KL, Smith AM, McKeon R, Bennink J, Yewdell JW, McCullers JA.** 2007. Expression of the 1918 influenza A virus PB1-F2 enhances the pathogenesis of viral and secondary bacterial pneumonia. Cell Host Microbe **2:**240-249.
122. **Wise HM, Foeglein A, Sun J, Dalton RM, Patel S, Howard W, Anderson EC, Barclay WS, Digard P.** 2009. A complicated message: Identification of a

novel PB1-related protein translated from influenza A virus segment 2 mRNA. J Virol **83:**8021-8031.
123. **Fodor E, Smith M.** 2004. The PA subunit is required for efficient nuclear accumulation of the PB1 subunit of the influenza A virus RNA polymerase complex. J Virol **78:**9144-9153.
124. **Jagger BW, Wise HM, Kash JC, Walters KA, Wills NM, Xiao YL, Dunfee RL, Schwartzman LM, Ozinsky A, Bell GL, Dalton RM, Lo A, Efstathiou S, Atkins JF, Firth AE, Taubenberger JK, Digard P.** 2012. An overlapping protein-coding region in influenza A virus segment 3 modulates the host response. Science **337:**199-204.
125. **Wise HM, Hutchinson EC, Jagger BW, Stuart AD, Kang ZH, Robb N, Schwartzman LM, Kash JC, Fodor E, Firth AE, Gog JR, Taubenberger JK, Digard P.** 2012. Identification of a novel splice variant form of the influenza A virus M2 ion channel with an antigenically distinct ectodomain. PLoS Pathog **8:**e1002998.
126. **Kuiken T, van den Brand J, van Riel D, Pantin-Jackwood M, Swayne DE.** 2010. Comparative pathology of select agent influenza a virus infections. Vet Pathol **47:**893-914.
127. **van Riel D, Munster VJ, de Wit E, Rimmelzwaan GF, Fouchier RA, Osterhaus AD, Kuiken T.** 2006. H5N1 Virus Attachment to Lower Respiratory Tract. Science **312:**399.
128. **Eierhoff T, Hrincius ER, Rescher U, Ludwig S, Ehrhardt C.** 2010. The epidermal growth factor receptor (EGFR) promotes uptake of influenza A viruses (IAV) into host cells. PLoS Pathog **6:**e1001099.
129. **Rust MJ, Lakadamyali M, Zhang F, Zhuang X.** 2004. Assembly of endocytic machinery around individual influenza viruses during viral entry. Nat Struct Mol Biol **11:**567-573.
130. **Chen C, Zhuang X.** 2008. Epsin 1 is a cargo-specific adaptor for the clathrin-mediated endocytosis of the influenza virus. Proc Natl Acad Sci U S A **105:**11790-11795.
131. **Nunes-Correia I, Eulalio A, Nir S, Pedroso de Lima MC.** 2004. Caveolae as an additional route for influenza virus endocytosis in MDCK cells. Cell Mol Biol Lett **9:**47-60.
132. **Sieczkarski SB, Whittaker GR.** 2002. Influenza virus can enter and infect cells in the absence of clathrin-mediated endocytosis. J Virol **76:**10455-10464.
133. **de Vries E, Tscherne DM, Wienholts MJ, Cobos-Jimenez V, Scholte F, Garcia-Sastre A, Rottier PJ, de Haan CA.** 2011. Dissection of the influenza A virus endocytic routes reveals macropinocytosis as an alternative entry pathway. PLoS Pathog **7:**e1001329.
134. **Rossman JS, Leser GP, Lamb RA.** 2012. Filamentous influenza virus enters cells via macropinocytosis. J Virol **86:**10950-10960.
135. **Karlsson Hedestam GB, Fouchier RA, Phogat S, Burton DR, Sodroski J, Wyatt RT.** 2008. The challenges of eliciting neutralizing antibodies to HIV-1 and to influenza virus. Nat Rev Microbiol **6:**143-155.
136. **Fischer JA, Eun SH, Doolan BT.** 2006. Endocytosis, endosome trafficking, and the regulation of Drosophila development. Annu Rev Cell Dev Biol **22:**181-206.
137. **Santiago-Tirado FH, Bretscher A.** 2011. Membrane-trafficking sorting hubs: cooperation between PI4P and small GTPases at the trans-Golgi network. Trends Cell Biol **21:**515-525.

138. **Lanzrein M, Schlegel A, Kempf C.** 1994. Entry and uncoating of enveloped viruses. Biochem J **302 (Pt 2):**313-320.
139. **Galloway SE, Reed ML, Russell CJ, Steinhauer DA.** 2012. Influenza HA subtypes demonstrate divergent phenotypes for cleavage activation and pH of fusion: implications for host range and adaptation. PLoS Pathog **9:**e1003151.
140. **Sugrue RJ, Hay AJ.** 1991. Structural characteristics of the M2 protein of influenza A viruses: evidence that it forms a tetrameric channel. Virology **180:**617-624.
141. **Bui M, Whittaker G, Helenius A.** 1996. Effect of M1 protein and low pH on nuclear transport of influenza virus ribonucleoproteins. J Virol **70:**8391-8401.
142. **Cross KJ, Burleigh LM, Steinhauer DA.** 2001. Mechanisms of cell entry by influenza virus. Expert Rev Mol Med **3:**1-18.
143. **Zhirnov OP, Ikizler MR, Wright PF.** 2002. Cleavage of influenza a virus hemagglutinin in human respiratory epithelium is cell associated and sensitive to exogenous antiproteases. J Virol **76:**8682-8689.
144. **Endo Y, Carroll KN, Ikizler MR, Wright PF.** 1996. Growth of influenza A virus in primary, differentiated epithelial cells derived from adenoids. J Virol **70:**2055-2058.
145. **de Curtis I, Simons K.** 1989. Isolation of exocytic carrier vesicles from BHK cells. Cell **58:**719-727.
146. **Garten W, Klenk HD.** 1999. Understanding influenza virus pathogenicity. Trends Microbiol **7:**99-100.
147. **Klenk HD, Garten W.** 1994. Host cell proteases controlling virus pathogenicity. Trends Microbiol **2:**39-43.
148. **Sun X, Tse LV, Ferguson AD, Whittaker GR.** 2010. Modifications to the hemagglutinin cleavage site control the virulence of a neurotropic H1N1 influenza virus. J Virol **84:**8683-8690.
149. **Perdue ML.** 2008. Molecular Determinants of Pathogenesis for Avain Influenza Viruses, p. 23-41. *In* Swayne DE (ed.), Avian Influenza. Blackwell, Ames, Iowa.
150. **Klenk H-D, Garten W.** 1994. Activation cleavage of viral spike proteins by host proteases, p. 241-280. *In* Wimmer E (ed.), Cellular Receptors for Animal Viruses. Cold Spring Harbor Press, Cold Spring Harbor, NY.
151. **Kawaoka Y, Webster RG.** 1988. Sequence requirements for cleavage activation of influenza virus hemagglutinin expressed in mammalian cells. Proc Natl Acad Sci U S A **85:**324-328.
152. **Hedstrom L.** 2002. Serine protease mechanism and specificity. Chem Rev **102:**4501-4524.
153. **Hartley BS, Kilby BA.** 1954. The reaction of p-nitrophenyl esters with chymotrypsin and insulin. Biochem J **56:**288-297.
154. **Kunitz M.** 1938. Formation of Trypsin from Trypsinogen by an Enzyme Produced by a Mold of the Genus Penicillium. J Gen Physiol **21:**601-620.
155. **Gotoh B, Yamauchi F, Ogasawara T, Nagai Y.** 1992. Isolation of factor Xa from chick embryo as the amniotic endoprotease responsible for paramyxovirus activation. FEBS Lett **296:**274-278.
156. **Kido H, Yokogoshi Y, Sakai K, Tashiro M, Kishino Y, Fukutomi A, Katunuma N.** 1992. Isolation and characterization of a novel trypsin-like protease found in rat bronchiolar epithelial Clara cells. A possible activator of the viral fusion glycoprotein. J Biol Chem **267:**13573-13579.

157. **Murakami M, Towatari T, Ohuchi M, Shiota M, Akao M, Okumura Y, Parry MA, Kido H.** 2001. Mini-plasmin found in the epithelial cells of bronchioles triggers infection by broad-spectrum influenza A viruses and Sendai virus. Eur J Biochem **268:**2847-2855.
158. **Kido H, Okumura Y, Yamada H, Le TQ, Yano M.** 2007. Proteases essential for human influenza virus entry into cells and their inhibitors as potential therapeutic agents. Curr Pharm Des **13:**405-414.
159. **Chaipan C, Kobasa D, Bertram S, Glowacka I, Steffen I, Tsegaye TS, Takeda M, Bugge TH, Kim S, Park Y, Marzi A, Pohlmann S.** 2009. Proteolytic activation of the 1918 influenza virus hemagglutinin. J Virol **83:**3200-3211.
160. **Wang W, Butler EN, Veguilla V, Vassell R, Thomas JT, Moos M, Jr., Ye Z, Hancock K, Weiss CD.** 2008. Establishment of retroviral pseudotypes with influenza hemagglutinins from H1, H3, and H5 subtypes for sensitive and specific detection of neutralizing antibodies. J Virol Methods **153:**111-119.
161. **Bottcher E, Matrosovich T, Beyerle M, Klenk HD, Garten W, Matrosovich M.** 2006. Proteolytic activation of influenza viruses by serine proteases TMPRSS2 and HAT from human airway epithelium. J Virol **80:**9896-9898.
162. **Kido H, Okumura Y, Takahashi E, Pan HY, Wang S, Chida J, Le TQ, Yano M.** 2008. Host envelope glycoprotein processing proteases are indispensable for entry into human cells by seasonal and highly pathogenic avian influenza viruses. J Mol Genet Med **3:**167-175.
163. **Cederholm-Williams SA.** 1981. Concentration of plasminogen and antiplasmin in plasma and serum. J Clin Pathol **34:**979-981.
164. **Ponting CP, Marshall JM, Cederholm-Williams SA.** 1992. Plasminogen: a structural review. Blood Coagul Fibrinolysis **3:**605-614.
165. **Nienaber VL, Young SL, Birktoft JJ, Higgins DL, Berliner LJ.** 1992. Conformational similarities between one-chain and two-chain tissue plasminogen activator (t-PA): implications to the activation mechanism on one-chain t-PA. Biochemistry **31:**3852-3861.
166. **Irigoyen JP, Munoz-Canoves P, Montero L, Koziczak M, Nagamine Y.** 1999. The plasminogen activator system: biology and regulation. Cell Mol Life Sci **56:**104-132.
167. **Kruithof EK.** 1988. Plasminogen activator inhibitors--a review. Enzyme **40:**113-121.
168. **Thomas G.** 2002. Furin at the cutting edge: from protein traffic to embryogenesis and disease. Nat Rev Mol Cell Biol **3:**753-766.
169. **Seidah NG, Mayer G, Zaid A, Rousselet E, Nassoury N, Poirier S, Essalmani R, Prat A.** 2008. The activation and physiological functions of the proprotein convertases. Int J Biochem Cell Biol **40:**1111-1125.
170. **Hamilton BS, Gludish DW, Whittaker GR.** 2013. Cleavage activation of the human-adapted influenza virus subtypes by matriptase reveals both subtype and strain specificities. J Virol **86:**10579-10586.
171. **Hamilton BS, Sun X, Chung C, Whittaker GR.** 2012. Acquisition of a novel eleven amino acid insertion directly N-terminal to a tetrabasic cleavage site confers intracellular cleavage of an H7N7 influenza virus hemagglutinin. Virology **434:**88-95.
172. **Tashiro M, Ciborowski P, Reinacher M, Pulverer G, Klenk HD, Rott R.** 1987. Synergistic role of staphylococcal proteases in the induction of influenza virus pathogenicity. Virology **157:**421-430.

173. **Scheiblauer H, Reinacher M, Tashiro M, Rott R.** 1992. Interactions between bacteria and influenza A virus in the development of influenza pneumonia. J Infect Dis **166:**783-791.
174. **Kishida N, Sakoda Y, Eto M, Sunaga Y, Kida H.** 2004. Co-infection of Staphylococcus aureus or Haemophilus paragallinarum exacerbates H9N2 influenza A virus infection in chickens. Arch Virol **149:**2095-2104.
175. **McCullers JA.** 2006. Insights into the interaction between influenza virus and pneumococcus. Clin Microbiol Rev **19:**571-582.
176. **Ratner AJ, Lysenko ES, Paul MN, Weiser JN.** 2005. Synergistic proinflammatory responses induced by polymicrobial colonization of epithelial surfaces. Proc Natl Acad Sci U S A **102:**3429-3434.
177. **Iverson AR, Boyd KL, McAuley JL, Plano LR, Hart ME, McCullers JA.** 2011. Influenza Virus Primes Mice for Pneumonia From Staphylococcus aureus. J Infect Dis.
178. **Park K, Bakaletz LO, Coticchia JM, Lim DJ.** 1993. Effect of influenza A virus on ciliary activity and dye transport function in the chinchilla eustachian tube. Ann Otol Rhinol Laryngol **102:**551-558.
179. **Plotkowski MC, Puchelle E, Beck G, Jacquot J, Hannoun C.** 1986. Adherence of type I Streptococcus pneumoniae to tracheal epithelium of mice infected with influenza A/PR8 virus. Am Rev Respir Dis **134:**1040-1044.
180. **McCullers JA, Bartmess KC.** 2003. Role of neuraminidase in lethal synergism between influenza virus and Streptococcus pneumoniae. J Infect Dis **187:**1000-1009.
181. **Okamoto S, Kawabata S, Nakagawa I, Okuno Y, Goto T, Sano K, Hamada S.** 2003. Influenza A virus-infected hosts boost an invasive type of Streptococcus pyogenes infection in mice. J Virol **77:**4104-4112.
182. **Sanford BA, Davison VE, Ramsay MA.** 1982. Fibrinogen-mediated adherence of group A Streptococcus to influenza A virus-infected cell cultures. Infect Immun **38:**513-520.
183. **McCullers JA, Rehg JE.** 2002. Lethal synergism between influenza virus and Streptococcus pneumoniae: characterization of a mouse model and the role of platelet-activating factor receptor. J Infect Dis **186:**341-350.
184. **Louria DB, Blumenfeld HL, Ellis JT, Kilbourne ED, Rogers DE.** 1959. Studies on influenza in the pandemic of 1957-1958. II. Pulmonary complications of influenza. J Clin Invest **38:**213-265.
185. **Bano S, Naeem K, Malik SA.** 2003. Evaluation of pathogenic potential of avian influenza virus serotype H9N2 in chickens. Avian Dis **47:**817-822.
186. **Tashiro M, Ciborowski P, Klenk HD, Pulverer G, Rott R.** 1987. Role of Staphylococcus protease in the development of influenza pneumonia. Nature **325:**536-537.
187. **Cox NJ, Subbarao K.** 2000. Global epidemiology of influenza: past and present. Annu. Rev. Med. **51:**407-421.
188. **Wiley DC, Skehel JJ.** 1987. The structure and function of the hemagglutinin membrane glycoprotein of influenza virus. Ann. Rev. Biochem. **56:**365-394.
189. **Choi SY, Bertram S, Glowacka I, Park YW, Pohlmann S.** 2009. Type II transmembrane serine proteases in cancer and viral infections. Trends Mol Med **15:**303-312.
190. **Steinhauer DA.** 1999. Role of hemagglutinin cleavage for the pathogenicity of influenza virus. Virology **258:**1-20.

191. **Neumann G, Noda T, Kawaoka Y.** 2009. Emergence and pandemic potential of swine-origin H1N1 influenza virus. Nature **459:**931-939.
192. **Stuart-Harris CH.** 1939. A neurotropic strain of human influenza virus. Lancet **233:**497-499.
193. **Stuart-Harris CH, Schild GC.** 1976. Influenza. The Viruses and the Disease. Edward Arnold, London.
194. **Lazarowitz SG, Goldberg AR, Choppin PW.** 1973. Proteolytic cleavage by plasmin of the HA polypeptide of influenza virus: host cell activation of serum plasminogen. Virology **56:**172-180.
195. **Schulman JL, Palese P.** 1977. Virulence factors of influenza A viruses: WSN virus neuraminidase required for plaque production in MDBK cells. J Virol **24:**170-176.
196. **Goto H, Kawaoka Y.** 1998. A novel mechanism for the acquisition of virulence by a human influenza A virus. Proc. Natl. Acad. Sci. USA **95:**10224-10228.
197. **Hiti AL, Davis AR, Nayak DP.** 1981. Complete sequence analysis shows that the hemagglutinins of the H0 and H2 subtypes of human influenza virus are closely related. Virology **111:**113-124.
198. **Weinstein MJ, Doolittle RF.** 1972. Differential specificities of the thrombin, plasmin and trypsin with regard to synthetic and natural substrates and inhibitors. Biochim Biophys Acta **258:**577-590.
199. **Robbins KC, Summaria L.** 1970. Human plasminogen and plasmin, p. 184-199. *In* Perlmann G, Lorand L (ed.), Methods in Enzymology, vol. 19. Academic Press, New York.
200. **Hervio LS, Coombs GS, Bergstrom RC, Trivedi K, Corey DR, Madison EL.** 2000. Negative selectivity and the evolution of protease cascades: the specificity of plasmin for peptide and protein substrates. Chem Biol **7:**443-453.
201. **Wang XY, Kilgore PE, Lim KA, Wang SM, Lee J, Deng W, Mo MQ, Nyambat B, Ma JC, Favorov MO, Clemens JD.** 2011. Influenza and bacterial pathogen coinfections in the 20th century. Interdiscip Perspect Infect Dis **2011:**146376.
202. **McArthur JD, Cook SM, Venturini C, Walker MJ.** 2012. The role of streptokinase as a virulence determinant of Streptococcus pyogenes--potential for therapeutic targeting. Curr Drug Targets **13:**297-307.
203. **Chen GW, Tsao KC, Huang CG, Gong YN, Chang SC, Liu YC, Wu HH, Yang SL, Lin TY, Huang YC, Shih SR.** 2012. Amino acids transitioning of 2009 H1N1pdm in Taiwan from 2009 to 2011. PLoS One **7:**e45946.
204. **Teijaro JR, Walsh KB, Cahalan S, Fremgen DM, Roberts E, Scott F, Martinborough E, Peach R, Oldstone MB, Rosen H.** 2011. Endothelial cells are central orchestrators of cytokine amplification during influenza virus infection. Cell **146:**980-991.
205. **Homme PJ, Easterday BC.** 1970. Avian influenza virus infections. I. Characteristics of influenza A-turkey-Wisconsin-1966 virus. Avian Dis **14:**66-74.
206. **Capua I, Alexander DJ.** 2009. Avian influenza infection in birds: a challenge and opportunity for the poultry veterinarian. Poult Sci **88:**842-846.
207. **Guo YJ, Krauss S, Senne DA, Mo IP, Lo KS, Xiong XP, Norwood M, Shortridge KF, Webster RG, Guan Y.** 2000. Characterization of the pathogenicity of members of the newly established H9N2 influenza virus lineages in Asia. Virology **267:**279-288.

208. **Negovetich NJ, Feeroz MM, Jones-Engel L, Walker D, Alam SM, Hasan K, Seiler P, Ferguson A, Friedman K, Barman S, Franks J, Turner J, Krauss S, Webby RJ, Webster RG.** 2011. Live bird markets of Bangladesh: H9N2 viruses and the near absence of highly pathogenic H5N1 influenza. PLoS One **6:**e19311.
209. **Alexander DJ.** 2003. Report on avian influenza in the Eastern Hemisphere during 1997-2002. Avian Dis **47:**792-797.
210. **Brown IH, Banks J, Manvell RJ, Essen SC, Shell W, Slomka M, Londt B, Alexander DJ.** 2006. Recent epidemiology and ecology of influenza A viruses in avian species in Europe and the Middle East. Dev Biol (Basel) **124:**45-50.
211. **Peiris M, Yuen KY, Leung CW, Chan KH, Ip PL, Lai RW, Orr WK, Shortridge KF.** 1999. Human infection with influenza H9N2. Lancet **354:**916-917.
212. **OIE WOfAH-.** 2008. Manual of Diagnostic Tests and Vaccines for Terrestrial Animals, 6 ed.
213. **Lee CW, Song CS, Lee YJ, Mo IP, Garcia M, Suarez DL, Kim SJ.** 2000. Sequence analysis of the hemagglutinin gene of H9N2 Korean avian influenza viruses and assessment of the pathogenic potential of isolate MS96. Avian Dis **44:**527-535.
214. **Banet-Noach C, Perk S, Simanov L, Grebenyuk N, Rozenblut E, Pokamunski S, Pirak M, Tendler Y, Panshin A.** 2007. H9N2 influenza viruses from Israeli poultry: a five-year outbreak. Avian Dis **51:**290-296.
215. **Nili H, Asasi K.** 2003. Avian influenza (H9N2) outbreak in Iran. Avian Dis **47:**828-831.
216. **Xu KM, Li KS, Smith GJ, Li JW, Tai H, Zhang JX, Webster RG, Peiris JS, Chen H, Guan Y.** 2007. Evolution and molecular epidemiology of H9N2 influenza A viruses from quail in southern China, 2000 to 2005. J Virol **81:**2635-2645.
217. **Zhang P, Tang Y, Liu X, Liu W, Zhang X, Liu H, Peng D, Gao S, Wu Y, Zhang L, Lu S.** 2009. A novel genotype H9N2 influenza virus possessing human H5N1 internal genomes has been circulating in poultry in eastern China since 1998. J Virol **83:**8428-8438.
218. **Matrosovich MN, Krauss S, Webster RG.** 2001. H9N2 influenza A viruses from poultry in Asia have human virus-like receptor specificity. Virology **281:**156-162.
219. **Abdel-Moneim AS, Afifi MA, El-Kady MF.** 2012. Isolation and mutation trend analysis of influenza A virus subtype H9N2 in Egypt. Virol J **9:**173.
220. **Shapiro J, Sciaky N, Lee J, Bosshart H, Angeletti RH, Bonifacino JS.** 1997. Localization of endogenous furin in cultured cell lines. J Histochem Cytochem **45:**3-12.
221. **Su AI, Wiltshire T, Batalov S, Lapp H, Ching KA, Block D, Zhang J, Soden R, Hayakawa M, Kreiman G, Cooke MP, Walker JR, Hogenesch JB.** 2004. A gene atlas of the mouse and human protein-encoding transcriptomes. Proc Natl Acad Sci U S A **101:**6062-6067.
222. **Werth N, Beerlage C, Rosenberger C, Yazdi AS, Edelmann M, Amr A, Bernhardt W, von Eiff C, Becker K, Schafer A, Peschel A, Kempf VA.** 2010. Activation of hypoxia inducible factor 1 is a general phenomenon in infections with human pathogens. PLoS One **5:**e11576.
223. **McMahon S, Grondin F, McDonald PP, Richard DE, Dubois CM.** 2005. Hypoxia-enhanced expression of the proprotein convertase furin is mediated

by hypoxia-inducible factor-1: impact on the bioactivation of proproteins. J Biol Chem **280:**6561-6569.

224. **Izidoro MA, Gouvea IE, Santos JA, Assis DM, Oliveira V, Judice WA, Juliano MA, Lindberg I, Juliano L.** 2009. A study of human furin specificity using synthetic peptides derived from natural substrates, and effects of potassium ions. Arch Biochem Biophys **487:**105-114.
225. **Krysan DJ, Rockwell NC, Fuller RS.** 1999. Quantitative characterization of furin specificity. Energetics of substrate discrimination using an internally consistent set of hexapeptidyl methylcoumarinamides. J Biol Chem **274:**23229-23234.
226. **Baron J, Tarnow C, Mayoli-Nussle D, Schilling E, Meyer D, Hammami M, Schwalm F, Steinmetzer T, Guan Y, Garten W, Klenk HD, Bottcher-Friebertshauser E.** 2012. Matriptase, HAT, and TMPRSS2 activate the hemagglutinin of H9N2 influenza A viruses. J Virol **87:**1811-1820.
227. **Gohrbandt S, Veits J, Breithaupt A, Hundt J, Teifke JP, Stech O, Mettenleiter TC, Stech J.** 2011. H9 avian influenza reassortant with engineered polybasic cleavage site displays a highly pathogenic phenotype in chicken. J Gen Virol **92:**1843-1853.
228. **Kawaoka Y, Naeve CW, Webster RG.** 1984. Is virulence of H5N2 influenza viruses in chickens associated with loss of carbohydrate from the hemagglutinin? Virology **139:**303-316.
229. **Lee CW, Lee YJ, Senne DA, Suarez DL.** 2006. Pathogenic potential of North American H7N2 avian influenza virus: a mutagenesis study using reverse genetics. Virology **353:**388-395.
230. **Gibson CA, Daniels RS, Oxford JS, McCauley JW.** 1992. Sequence analysis of the equine H7 influenza virus haemagglutinin gene. Virus Res **22:**93-106.
231. **Tian S, Huajun W, Wu J.** 2012. Computational prediction of furin cleavage sites by a hybrid method and understanding mechanism underlying diseases. Sci Rep **2:**261.
232. **Golender N, Panshin A, Banet-Noach C, Nagar S, Pokamunski S, Pirak M, Tendler Y, Davidson I, Garcia M, Perk S.** 2008. Genetic characterization of avian influenza viruses isolated in Israel during 2000-2006. Virus Genes **37:**289-297.
233. **Arnold K, Bordoli L, Kopp J, Schwede T.** 2006. The SWISS-MODEL workspace: a web-based environment for protein structure homology modelling. Bioinformatics **22:**195-201.
234. **Kiefer F, Arnold K, Kunzli M, Bordoli L, Schwede T.** 2009. The SWISS-MODEL Repository and associated resources. Nucleic Acids Res **37:**D387-392.
235. **Brown EG, Liu H, Kit LC, Baird S, Nesrallah M.** 2001. Pattern of mutation in the genome of influenza A virus on adaptation to increased virulence in the mouse lung: identification of functional themes. Proc Natl Acad Sci U S A **98:**6883-6888.
236. **Pasick J, Handel K, Robinson J, Copps J, Ridd D, Hills K, Kehler H, Cottam-Birt C, Neufeld J, Berhane Y, Czub S.** 2005. Intersegmental recombination between the haemagglutinin and matrix genes was responsible for the emergence of a highly pathogenic H7N3 avian influenza virus in British Columbia. J Gen Virol **86:**727-731.

237. **Perk S, Panshin A, Shihmanter E, Gissin I, Pokamunski S, Pirak M, Lipkind M.** 2006. Ecology and molecular epidemiology of H9N2 avian influenza viruses isolated in Israel during 2000-2004 epizootic. Dev Biol (Basel) **124:**201-209.
238. **Tay FP, Huang M, Wang L, Yamada Y, Liu DX.** 2012. Characterization of cellular furin content as a potential factor determining the susceptibility of cultured human and animal cells to coronavirus infectious bronchitis virus infection. Virology **433:**421-430.
239. **Silvestri L, Pagani A, Camaschella C.** 2008. Furin-mediated release of soluble hemojuvelin: a new link between hypoxia and iron homeostasis. Blood **111:**924-931.
240. **Tolnay AE, Baskin CR, Tumpey TM, Sabourin PJ, Sabourin CL, Long JP, Pyles JA, Albrecht RA, Garcia-Sastre A, Katze MG, Bielefeldt-Ohmann H.** 2010. Extrapulmonary tissue responses in cynomolgus macaques (Macaca fascicularis) infected with highly pathogenic avian influenza A (H5N1) virus. Arch Virol **155:**905-914.
241. **Beerlage C, Greb J, Kretschmer D, Assaggaf M, Trackman PC, Hansmann ML, Bonin M, Eble JA, Peschel A, Brune B, Kempf VA.** 2013. Hypoxia-inducible factor 1-regulated lysyl oxidase is involved in Staphylococcus aureus abscess formation. Infect Immun **81:**2562-2573.
242. **Kirienko NV, Kirienko DR, Larkins-Ford J, Wahlby C, Ruvkun G, Ausubel FM.** 2013. Pseudomonas aeruginosa disrupts Caenorhabditis elegans iron homeostasis, causing a hypoxic response and death. Cell Host Microbe **13:**406-416.
243. **Mosleh N, Dadras H, Mohammadi A.** 2009. Molecular quantitation of H9N2 avian influenza virus in various organs of broiler chickens using TaqMan real time PCR. J Mol Genet Med **3:**152-157.
244. **Hadipour MM, Farjadian SH, Azad F, Kamravan M, Dehghan A.** 2011. Nephropathogenicity of H9N2 Avian Influenza Virus in Commercial Broiler Chickens Following Intratracheal Inoculation. J. Anim. Vet. Adv. **10:**1706-1710.
245. **Pazani J, Marandi MV, Ashrafihelan J, Marjanmehr SH, Ghods F.** 2008. Pathological Studies of A / Chicken / Tehran / ZMT - 173/99 (H9N2) Influenza Virus in Commercial Broiler Chickens of Iran. Int. J. Poult. Sci. **5:**502-510.
246. **Soda K, Asakura S, Okamatsu M, Sakoda Y, Kida H.** 2011. H9N2 influenza virus acquires intravenous pathogenicity on the introduction of a pair of di-basic amino acid residues at the cleavage site of the hemagglutinin and consecutive passages in chickens. Virol J **8:**64.
247. **Tse LV, Marcano VC, Huang W, Pocwierz MS, Whittaker GR.** 2013. Plasmin-mediated activation of pandemic H1N1 influenza virus hemagglutinin is independent of the viral neuraminidase. J Virol **87:**5161-5169.
248. **Kim JA, Cho SH, Kim HS, Seo SH.** 2006. H9N2 influenza viruses isolated from poultry in Korean live bird markets continuously evolve and cause the severe clinical signs in layers. Vet Microbiol **118:**169-176.
249. **Mo IP, Song, S.C., Kim, K.S., Rhee, J.C.** 2003. An Occurrence of Non-Highly Pathogenic Avian Influenza in Korea. Avian Disease **47:**379-383.
250. **Stevens J, Corper AL, Basler CF, Taubenberger JK, Palese P, Wilson IA.** 2004. Structure of the uncleaved human H1 hemagglutinin from the extinct 1918 influenza virus. Science **303:**1866-1870.

251. **Zhirnov OP, Klenk HD, Wright PF.** 2011. Aprotinin and similar protease inhibitors as drugs against influenza. Antiviral Res **92:**27-36.
252. **Bosman M, Royston D.** 2008. Aprotinin and renal dysfunction. Expert Opin Drug Saf **7:**663-677.
253. **Doms RW, Helenius A, White J.** 1985. Membrane fusion activity of the influenza virus hemagglutinin. The low pH-induced conformational change. J Biol Chem **260:**2973-2981.
254. **Lakadamyali M, Rust MJ, Babcock HP, Zhuang X.** 2003. Visualizing infection of individual influenza viruses. Proc Natl Acad Sci U S A **100:**9280-9285.
255. **Bussey KA, Bousse TL, Desmet EA, Kim B, Takimoto T.** 2010. PB2 residue 271 plays a key role in enhanced polymerase activity of influenza A viruses in mammalian host cells. J Virol **84:**4395-4406.
256. **Spandidos A, Wang X, Wang H, Seed B.** 2010. PrimerBank: a resource of human and mouse PCR primer pairs for gene expression detection and quantification. Nucleic Acids Res **38:**D792-799.
257. **Spandidos A, Wang X, Wang H, Dragnev S, Thurber T, Seed B.** 2008. A comprehensive collection of experimentally validated primers for Polymerase Chain Reaction quantitation of murine transcript abundance. BMC Genomics **9:**633.
258. **Wang X, Seed B.** 2003. A PCR primer bank for quantitative gene expression analysis. Nucleic Acids Res **31:**e154.
259. **Livak KJ, Schmittgen TD.** 2001. Analysis of relative gene expression data using real-time quantitative PCR and the 2(-Delta Delta C(T)) Method. Methods **25:**402-408.
260. **Mulligan RC, Berg P.** 1980. Expression of a bacterial gene in mammalian cells. Science **209:**1422-1427.
261. **Tessier DC, Thomas DY, Khouri HE, Laliberte F, Vernet T.** 1991. Enhanced secretion from insect cells of a foreign protein fused to the honeybee melittin signal peptide. Gene **98:**177-183.